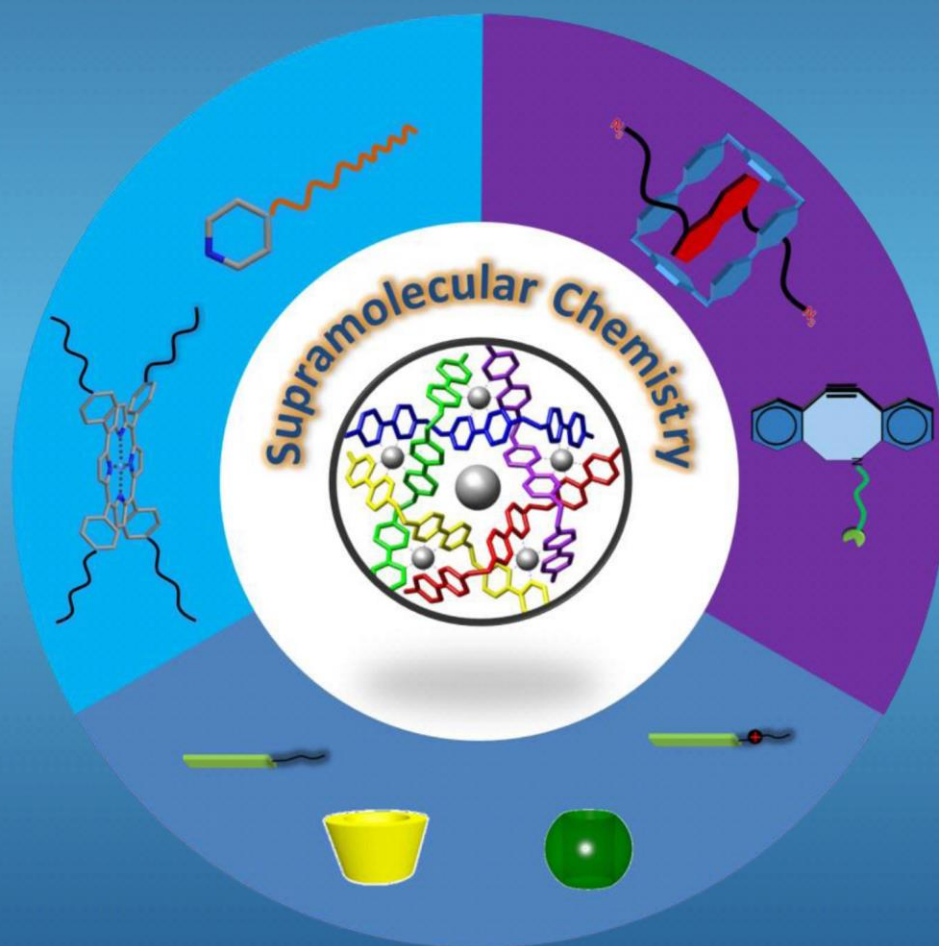


The Development of Rotaxanes, Dynamic Miktoarm Star Polymers and Photo-responsive Hydrogel Networks *via* Non-covalent Interactions



Zhanyao Hou

Promoter: Prof. Dr. Richard Hoogenboom

The Development of Rotaxanes, Dynamic Miktoarm
Star Polymers and Photo-responsive Hydrogel
Networks *via* Non-covalent Interactions

Zhanyao Hou

2018

Submitted in partial fulfillment of the requirements

For the degree of Doctor of Science

Promoter:

Prof. Richard Hoogenboom

Department of Organic and Macromolecular Chemistry, Ghent University

Zhanyao Hou

The Development of Rotaxanes, Dynamic Miktoarm Star Polymers and Photo-responsive Hydrogel
Networks *via* Non-covalent Interactions
Dissertation, Ghent University, Belgium

Zhanyao Hou was funded by the Chinese Scholarship Council (201407650003) and Special Research Fund (BOF) of Ghent University (BOF 01SC0415).

Members of the examination committee:

Prof. Dr. Richard Hoogenboom (Ghent University, BE)

Prof. Dr. Patrice Woisel (University of Lille, FR)

Prof. Dr. Wim Dehaen (KULeuven, BE)

Prof. Dr. Annemieke Madder (Ghent University, BE)

Prof. Dr. Bruno De Geest (Ghent University, BE)

Prof. Dr. Rik Van Deun (Ghent University, BE)

The author and the promoter give the authorisation to consult and copy parts of this work for personal use only. Every other use is subject to the copyright laws. Permission to reproduce any material contained in this work should be obtained from the author.

TABLE OF CONTENT

LIST OF ABBREVIATIONS AND SYMBOLS	1
OUTLINE AND AIMS OF THIS THESIS	1
CHAPTER 1 INTRODUCTION	5
1.1 SUPRAMOLECULAR CHEMISTRY	6
1.2 THE DEVELOPMENT OF SUPRAMOLECULAR STAR POLYMERS	17
1.3 SUPRAMOLECULAR HYDROGELS	25
1.4 ROTAXANES VIA CLICK CHEMISTRY	29
1.5 REVERSIBLE ADDITION-FRAGMENTATION CHAIN TRANSFER POLYMERIZATION	30
1.6 SUMMARY	33
1.7 REFERENCES	35
CHAPTER 2 A SUPRAMOLECULAR MIKTOARM STAR POLYMER BASED ON PORPHYRIN METAL COMPLEXATION IN WATER	41
2.1 INTRODUCTION	43
2.2 RESULTS AND DISCUSSION	44
2.3 CONCLUSIONS	54
2.4 EXPERIMENTAL SECTION	55
2.5 REFERENCES	61
CHAPTER 3 REVERSIBLE TRANSFORMATION FROM SUPRAMOLECULAR TO COVALENT CROSSLINKING OF AN ANTHRACENE-BASED HYDROGEL VIA UV IRRADIATION	63
3.1 INTRODUCTION	65
3.2 RESULTS AND DISCUSSION	66
3.3 CONCLUSIONS	81
3.4 EXPERIMENTAL SECTION	81
3.5 REFERENCES	87
CHAPTER 4 A DIBENZOAZACYCLOOCTYNE AS A REACTIVE CHAIN STOPPER FOR [2]ROTAXANES	89
4.1 INTRODUCTION	91
4.2 RESULTS AND DISCUSSION	92
4.3 CONCLUSIONS	100
4.4 EXPERIMENTAL SECTION	101
CHAPTER 5 GENERAL CONCLUSIONS AND OUTLOOK	107
NEDERLANDSE SAMENVATTING	110
ACKNOWLEDGEMENTS	112
SCIENTIFIC PUBLICATIONS	113

LIST OF ABBREVIATIONS AND SYMBOLS

A	Absorbance
An	Anthracene
ATRP	Atom transfer radical polymerization
BIPY ²⁺	4,4'-bipyridinium
CD	Cyclodextrin
CB[n]	Cucurbit[n]urils
CBPQT ⁴⁺	Cyclobis(paraquat- <i>p</i> -phenylene)
CTA	Chain transfer agent
CA	Cyanuric acid
CuAAC	Copper(I)-catalyzed azide-alkyne cycloaddition
DABCO	1,4-diazabicyclo[2.2.2]octane
DIBAC	Dibenzoazacyclooctyne
DMA	N,N-dimethylacetamide
DNP	1,5-dioxynaphthalene
Đ	Dispersity
DOSY	Diffusion ordered spectroscopy
DB	Dialkoxybenzene
DLS	Dynamic light scattering
ESI	Electrospray ionization
Im	Imidazole
HFIP	hexafluoro-2-propanol
I	Initiator
ITC	Isothermal titration calorimetry
G	Guest
GC	Gas chromatography
H	Host
HABA	2-(4-Hydroxyphenylazo)benzoic acid
HW	Hamilton wedge
k_{on}	The rate of host/guest complexation
k_{off}	The rate of dissociate of host/guest complex
K_a	Binding constant of complex
k_p	Propagation rate constant
Mn	Number average molecular weight
MALDI-TOF	Matrix assisted laser desorption/ionization-Time of flight
MIMs	Mechanically interlocked molecules
MBTTCP	Methyl-2-(<i>n</i> -butyltrithiocarbonyl)propanoate

List of abbreviations and symbols

NAM	N-acryloylmorpholine
NMP	Nitroxide-mediated polymerization
NMR	Nuclear magnetic resonance
NOESY	Nuclear overhauser effect spectroscopy
Py	Pyridine
PFPA	Pentafluorophenyl acrylate
PNIPAm	Poly(N-isopropylacrylamide)
PPG	Poly(propylene glycol)
PMPC	Poly(2-methacryloyloxyethyl phosphorylcholine)
PDMAAm	Poly(<i>N,N</i> -dimethylacrylamide)
PDEAAm	Poly(<i>N,N</i> -diethylacrylamide)
PDMA	Poly (<i>N, N</i> ,-dimethylacrylamide)
PEG	Poly(ethylene glycol)
PEGME	Poly(ethylene glycol) methyl ether
PmDEGA	Poly(methoxydiethylene glycol acrylate)
PMMA	Poly(methyl methacrylate)
RAFT	Reversible addition-fragmentation chain transfer polymerization
R _p	Polymerization rate
SEC	Size exclusion chromatography
SPAAC	Strain-promoted azide–alkyne cycloaddition
TFA	Trifluoroacetic acid
TTF	Tetrathiafulvalene
TPP	Tetra(4-acetylphenyl)porphyrin

Outline and aims of this thesis

Non-covalent interactions between molecules, also known as supramolecular interactions, widely exist in nature, such as the formation of the DNA double helix and the folding of proteins. Such non-covalent interactions play a crucial role in chemistry, physics and particularly in biodisciplines, and provide the flexibility, specificity and dynamics required in biological processes and advanced material science. As a result, the area of supramolecular chemistry not only attracts chemists and biochemists but also a wide variety of researchers in other disciplines, such as physics, mathematics and engineering. Polymer chemists have employed supramolecular interactions to build complex dynamic polymer architectures and supramolecular polymeric materials in recent years. Such supramolecular polymers and materials exhibit outstanding dynamic properties compared to their analogues that are constructed by covalent interaction. More specifically, the dynamic nature of the supramolecular interactions provides the ability of responding to external stimuli. Non-covalent interactions provide a platform for designing various next generation polymeric materials with adaptive behavior, reshapability (recycling), self-healing and low temperature processing. Apart from polymeric materials, non-covalent interactions have also been widely used in nanoscience, particularly for developing molecular machines.

In order to extend the application of non-covalent interactions as driving forces in the construction of supramolecular polymeric materials and molecular machines, this thesis focused on the development of dynamic polymer architectures, polymeric hydrogels and mechanically interlocked molecules. Within this thesis novel concepts of supramolecular star-polymers, switchable supramolecular hydrogels and straightforward synthesis of rotaxanes have been explored.

To achieve these research aims, this thesis is divided into 5 chapters.

The rationale for these three research topics will be given below while a broader introduction into the different areas will be provided in the introductory **Chapter 1**.

The properties of polymeric materials mainly depend on the chemical components and the topological structure. Branched polymers which are gaining interest due to their remarkable characteristics and properties arising from their condensed non-linear structure, and multiple chain ends. Branched polymers have widely been used in various fields, such as nanocontainers or drug delivery. The advent of supramolecular chemistry provides a novel approach to prepare branched polymers driven by non-covalent interactions that offer dynamic and potentially stimuli-responsive reversible formation of the branched polymer structure from the individual polymer precursors. Up to now, different non-covalent interactions, *e. g.* hydrogen bonding, metal-ligand coordination, and host-guest interactions were utilized for the preparation of supramolecular branched polymer. Star polymers represent a kind of rather defined branched polymers where all chains come together in

a core structure. Such star polymers were selected in this thesis as basis for the construction of dynamic branched polymeric architecture in which the association state of the arms to the core is controlled by the supramolecular interactions. In **Chapter 2**, the zinc porphyrin/pyridine (ZnTPP/Py) complexation based *metal-ligand interaction* was chosen to construct supramolecular miktoarm star polymers based on the complexation of a four-arm covalent star polymer having zinc porphyrin as core and a second linear polymer with a pyridine end-group. The synthesis of these building blocks and their supramolecular assembly into supramolecular mikto-arm star polymers, which are star-polymers that have different polymeric arms attached to the same core, in water is discussed in **Chapter 2**.

Hydrogels are (polymeric) networks extensively swollen with water and they have been widely employed in industrial and biological areas. Hydrogels can be sub-divided into chemical hydrogels (covalently crosslinked) and supramolecular hydrogels (physically crosslinked). Chemical hydrogels exhibit excellent mechanical properties and they have been widely employed for applications where tough and stable hydrogels are required, such as contact lenses. However, because of the nature of the covalent crosslinks, chemical hydrogels tend to be brittle, cannot be reshaped and do not provide possibilities for self-healing. In contrast, supramolecular hydrogels overcome these limitations of chemical hydrogels, and could undergo sol-gel transition depending on the environmental conditions. However, these improved dynamics come at the cost of being mechanically weaker systems. Polymer chemists have combined both covalent and non-covalent crosslinking in one system attempting to improve the properties of hydrogels and to combine the best of both worlds. Despite the beauty of this approach, some irreversible bond breaking will be unavoidable during damage. Inspired by this idea, we designed a novel hydrogel which can undergo a complete transition between physical crosslinking and chemical crosslinking, thereby taking advantage of the strong points of both chemical and physical hydrogels, namely excellent mechanical properties and reshapability, self-healing and low temperature processing abilities. Anthracene side-functionalized poly(*N*-acryloylmorpholine) were developed to form such switchable hydrogels. The polymers were physically crosslinked by the addition of a large macrocyclic host (γ -CD or CB[8]) that form ternary inclusion complexes with two anthracene molecules *via host-guest interaction* acting as physical crosslinks. The photodimerization of anthracene inside host cavity convert the hydrogel to chemical crosslinking, thereby locking in the system and switching off the dynamic supramolecular interactions. Conversely, the cycloreversion of the anthracene dimers leads to the transition of the covalently crosslinked hydrogel back to a physically crosslinked hydrogel as will be discussed in **Chapter 3**.

Rotaxanes are a subset of the family of mechanically interlocked molecules (MIMs), which have attracted increasing attention for over 50 years owing to their wide range of potential application in molecular devices such as molecular machines, muscles and elevators. Rotaxanes as rather simple MIMs constitute important building blocks for the preparation of functional artificial nanomachines. Therefore, more efficient synthetic strategies for the construction of rotaxanes is important as basis

for the future development of nanomachines. In **chapter 4**, we introduced a novel reactive stopper to straightforwardly construct [2]rotaxanes by strain-promoted azide–alkyne cycloaddition, in which the pseudorotaxane is consisted of cyclobis(paraquat-*p*-phenylene) and 1,5-dialkoxynaphthalene assembled *via donor-acceptor host-guest interactions*. The developed straightforward synthetic strategy provides the opportunity to prepare mechanically interlocked molecules efficiently.

Finally, the general conclusions and outlook of the thesis will be discussed in **Chapter 5**

Chapter 1 Introduction

As stated in the motivation and overview section, the present thesis focuses on non-covalent interactions, which are also called supramolecular interactions. Such interactions were employed in various research areas after its first application in the modern sense by Jean-Marie Lehn in 1978. Chemists have attained an astonishing degree of control over the non-covalent interactions and have used these techniques to construct a plethora of beautiful and functional structures. A feature of particular interest is the dynamic property of non-covalent interactions, which has been facilitating molecular chemistry and has led to the emergence of various adaptive materials, such as supramolecular polymer materials, or molecular devices. In this thesis, three different non-covalent interactions, metal-ligand interactions, host-guest interactions and charge transfer interactions, were employed to explore their applications in polymer materials and nanotechnology. More specifically, the complexation of metalloporphyrin and pyridine was used to construct a novel supramolecular star polymer; the host-guest interactions between anthracene with γ -cyclodextrin or cucurbit[8]urils act as cross-linkers for a switchable supramolecular hydrogel; and a pseudorotaxane based on charge transfer interactions between cyclobis(paraquat-*p*-phenylene) and 1,5-dialkoxynaphthalene, which was stoppered straightforwardly by strain-promoted azide-alkyne cycloaddition. The fundamental concepts and theoretical background about these three research topics are described in the following sections as well as an overview of these topics that have been published in recent years.

1.1 Supramolecular Chemistry

1.1.1 The overview of supramolecular chemistry

Supramolecular chemistry is often defined as being chemistry beyond the molecule that focuses on the chemical systems made up of assembled molecular subunits or components. The early innovator in this field, Jean-Marie Lehn, received the Nobel Prize shared with Donald Cram and Charles Pedersen in 1987 for their contribution in host-guest interactions with crown-ethers referring to their development and use of molecules with structure-specific interactions of high selectivity. More recently in 2016, a second Nobel Prize was awarded to Jean-Pierre Sauvage, Sir J. Fraser Stoddart, and Bernard L. Feringa for their introduction and advance of molecular machines, which are mostly based on supramolecular interactions. Supramolecular chemistry is different from the traditional chemistry that focuses on the covalent bond, as it investigates the weaker and reversible noncovalent interactions between molecules. The relationship between molecular and supramolecular chemistry regarding to structure and function is depicted in Figure 1.1.

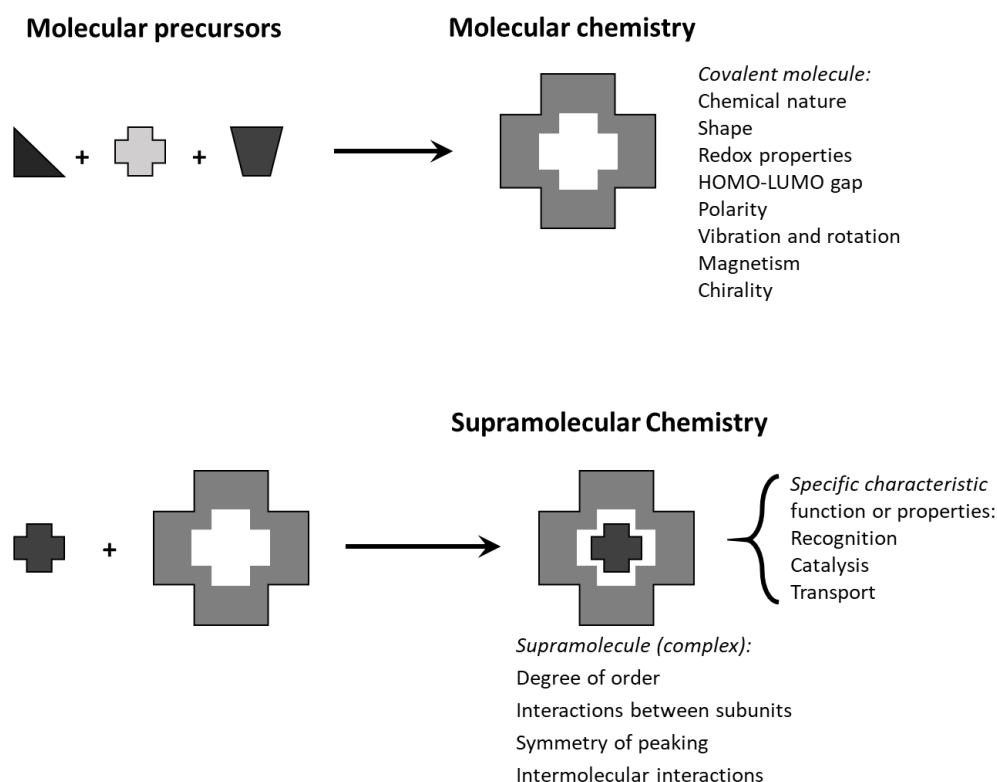


Figure 1.1 Comparison between the scope of molecular and supramolecular chemistry according to Lehn.¹

Supramolecular chemistry, comparing to the traditional chemistry, is a young discipline that stems from the late 1960s and early 1970s. However, its concepts and roots maybe traced back to 1810s, and the chronology of the field is illustrated in Table 1.1. Supramolecular chemistry has attracted the chemist's attention and gained rapidly growing interest based on the developments in macrocyclic chemistry in the 1960s, especially the development of macrocyclic ligands for alkali metal cation binding. After that, more and more chemists became interested in supramolecular

chemistry, often also inspired by the beauty of natural self-assembly processes. Nature employs a limited number of building blocks in combination with non-covalent interactions to construct complex functional assemblies. Some of the most well-known examples of supramolecular chemistry in nature include the assembly of double helical DNA, enzyme-substrate recognition, metal-ligand complexes, the folding and assembly of proteins and changes in protein assemblies such as focussing of the eye, healing processes and temperature regulation (Figure 1.2). Inspired by the impressive use of supramolecular assembly in nature, the supramolecular chemists aim to develop well-defined synthetic structures with controlled ordering and/or self assembly resulting in functional systems. Recently, the modern supramolecular chemistry was used in various fields, such as drug delivery,²⁻³ smart materials,⁴⁻¹² catalysis,¹³ data storage and processing,¹⁴⁻¹⁶ and nanotechnology¹⁷⁻¹⁸.

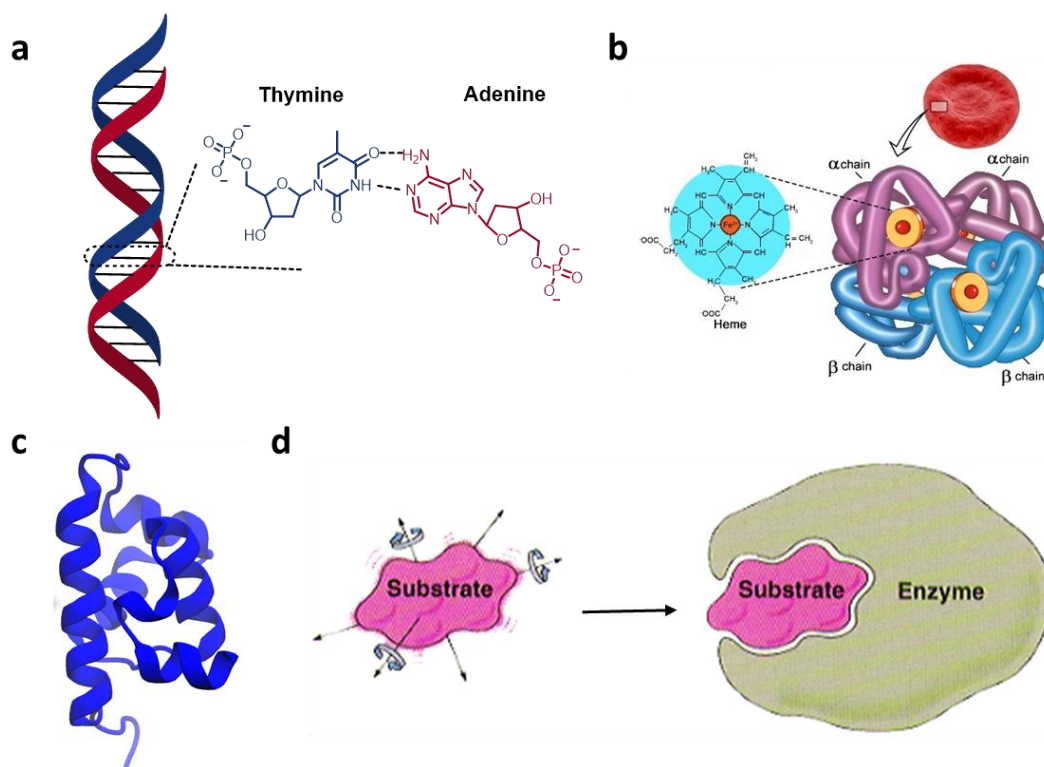


Figure 1.2 Some examples of natural assembly driven by non-covalent interactions (a): double helical DNA structure constructed by hydrogen bonding; (b) Hemoglobin molecule containing metal-ligand interaction; (c) the folding and assembly of protein reprinted from ref; (d) the recognition of enzyme-substrate.¹⁹

Table 1.1 Timeline of supramolecular chemistry adapted from ref.²⁰

1810-	S. H. Davy: discovery of chlorine hydrate
1841-	C. Schafhäütl: study of graphite intercalates
1849-	F. Wöhler: β -quinol H ₂ S clathrate
1891-	A. Villiers and C. R. Hebd: cyclodextrin inclusion compounds
1893	A. Werner: coordination chemistry
1894-	E. Fischer: <i>lock and key</i> concept
1906-	P. Ehrlich: introduction of the concept of a <i>receptor</i>
1937-	K. L. Wolf: the term <i>Übermoleküle</i> is coined to describe organised entities arising from the association of coordinatively saturated species (<i>e.g.</i> the acetic acid dimer)
1939-	L. Pauling: hydrogen bonds are included in the groundbreaking book <i>The Nature of the Chemical Bond</i>
1940-	M. F. Bengen: urea channel inclusion compounds
1945	H. M. Powell: X-ray crystal structures of β -quinol inclusion compounds; the term 'clathrate' is introduced to describe compounds where one component is enclosed within the framework of another
1949-	C. J. Brown and A. C. Farthing: synthesis of [2.2]paracyclophane
1953-	J. Watson and F. Crick: structure of DNA
1956-	D. C. Hodgkin: X-ray crystal structure of vitamin B ₁₂
1959-	D. Cram: attempted synthesis of cyclophane charge transfer complexes with (NC) ₂ C=C(CN) ₂
1961-	N. F. Curtis: first Schiff's base macrocycle from acetone and ethylene diamine
1964-	D. H. Busch and E. G. Jäger: Schiff's base macrocycles
1967-	C. Pedersen: crown ethers
1968-	C. H. Park and H. E. Simmons: <i>Katapinand</i> anion hosts
1969-	J. M. Lehn: synthesis of the first cryptands
1969-	R. Breslow: catalysis by cyclodextrins
1973-	D. Cram: spherand hosts produced to test the importance of preorganisation
1978-	J. M. Lehn: introduction of the term 'supramolecular chemistry', defined as the 'chemistry of molecular assemblies and of the intermolecular bond'
1979-	G. W. Gokel and M. Okahara: development of the lariat ethers as a subclass of host
1981-	F. Vögtle and M. E. Weber: podand hosts and development of nomenclature
1981-	W. A. Freeman, W. L. Mock and N. Y. Shih: The structure of cucurbit[n]urils was first elucidated
1986-	A. P. de Silva: Fluorescent sensing of alkali metal ions by crown ether derivatives
1987-	Award of the Nobel prize for Chemistry to D. J. Cram, J. M. Lehn and C. J. Pedersen for their work in supramolecular chemistry
1996-	J. L. Atwood, E. Davies, D. MacNicol & F. Vögtle: publication of <i>Comprehensive Supramolecular Chemistry</i> containing contributions from many key groups and summarising the development and state of the art
1996-	J. K. M. Sander: the first example of a dynamic combinatorial chemistry system
2003-	Award of the Nobel prize for Chemistry to P. Agre and R. MacKinnon for their discovery of water channels and the characterisation of cation and anion channels, respectively.
2004-	J. F. Stoddart: the first discrete Borromean-linked molecule, a landmark in topological synthesis.
2008-	Pillar[5]arenes as macrocyclic host was first reported by T. Ogoshi
2016	Award of the Nobel prize for Chemistry to J. P. Sauvage, J. F. Stoddart and B. L. Feringa for the design and synthesis of molecular machines.
2017-	J. Christian and R. Gwenaél: the world's first nanocar race on gold surface was taken place in the Centre for Materials Elaboration and Structural Studies in Toulouse.

Generally, supramolecular chemistry can be classified into two main categories: (i) the chemistry associated with a molecule recognizing a guest molecule (**host-guest chemistry**); (ii) the chemistry associated to molecules that assemble into larger structures by non-covalent interactions (**self-assembly**). The difference between the host-guest chemistry and self-assembly is illustrated schematically in Figure 1.3, whereby it should be noted that host-guest chemistry is also included in the more general term self-assembly. The term host-guest chemistry was first defined by Donald Cram in 1977 to depict the chemistry of complexes formed by two or more molecules or ions that are held together in certain structures through noncovalent interactions.²¹

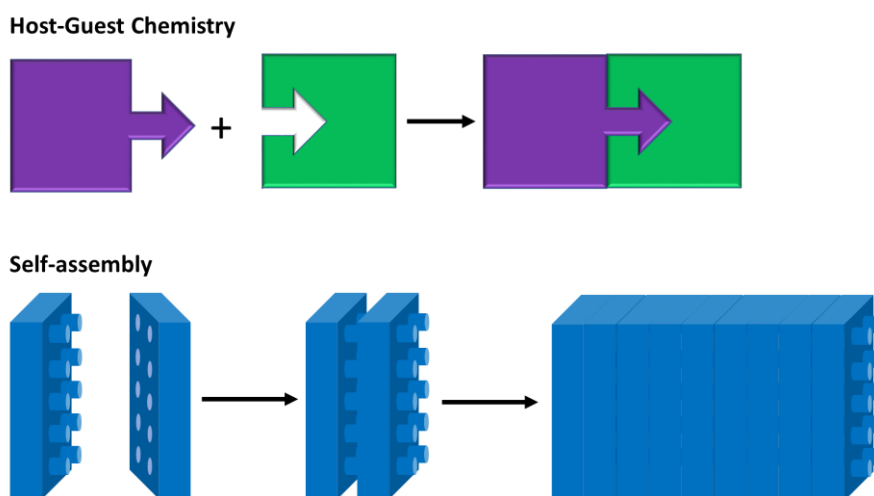


Figure 1.3 Schematic illustrating the difference between host-guest chemistry and self-assembly.

Supramolecular chemistry deals with weak and reversible non-covalent physical interactions between molecules. These weaker supramolecular interactions, include hydrogen bonding, metal-ligand interaction, host-guest interaction, van der Waals forces, π - π interaction and electrostatic effects, form the basis for molecular recognition, self-assembly,²² host-guest chemistry,²³ and mechanically interlocked molecular architectures^{3, 24-25}. The term “supramolecular interaction” includes a wide range of association strengths, which are summarized in Figure 1.4. Among these supramolecular interactions, metal-ligand coordination, host-guest interaction and electrostatic effects were employed in this thesis and these interactions will be highlighted further on.

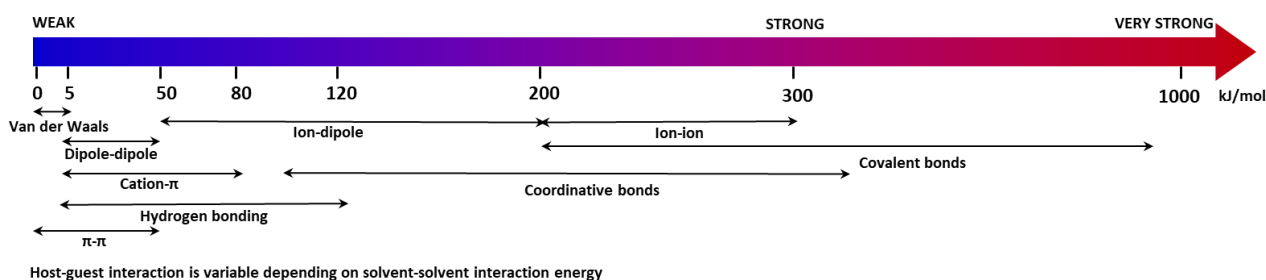


Figure 1.4 Overview of the strength of different (non)covalent interactions.

1.1.2 Binding constant of non-covalent interaction

1.1.2.1 Definition

In this part of the thesis, we will define the two building blocks that associate via non-covalent interactions as host (H) and guest (G), but the discussion can also be used to describe self-assembly of two molecules in general. The thermodynamic stability of the non-covalent interaction in a specific solvent at a given temperature is described by the binding constant, K_a , also called association constant. The binding constant is the inverse of the dissociation constant, and associated with the thermodynamically stable supramolecular equilibrium of association and dissociation of the host and guest molecules, which is formalized as:



Where m , n represent the stoichiometry of the formation of complex. The binding constant is often calculated using concentrations of host, guest and host-guest complex and thus has units of M^{-1} or M^{-2} for a 1:1 or 1:2 complex, respectively. The binding constant is also characterized by the on-rate constant k_{on} and off-rate constant k_{off} . In equilibrium, the forward binding transition $mH + nG \rightarrow H_mG_n$ should be balanced by the backward unbinding transition $H_mG_n \rightarrow mH + nG$. That is

$$k_{on} * [H]^m * [G]^n = k_{off} * [H_mG_n] \quad \text{Equation (2)}$$

Where $[H]$, $[G]$ and $[H_mG_n]$ represent the concentration of free host, the concentration of free guest and the concentration of complex. The binding constant K_a is defined by equation (3):

$$K_a = \frac{k_{on}}{k_{off}} = \frac{[H_mG_n]}{[H]^m[G]^n} \quad \text{Equation (3)}$$

1.1.2.2 Measurement of binding constants

An important aspect of the calculation of the binding constant is the use of the correct stoichiometry model. Even though in some cases the ratio of the host to guest is predictable, it must be determined and confirmed by experiment. A number of possible methods to determine the stoichiometry ratio of supramolecular association was listed by Connors in a previous review.²⁶ Among these methods, Job's method is the most popular method and was also applied in his work. In principle, the concentration of H_mG_n ($[H_mG_n]$) complex is at maximum when the ratio of host to guest is equal to m/n . To determine this, the mole fraction of the guest (f_G) is varied while keeping the total concentration of the host and guest constant. The concentration of the host-guest complex is then plotted against the mole fraction yielding a curve with a maxima when $f_G = n/(m+n)$. Practically, the concentration of the host/guest complex has to be determined by a change in characteristics of the host and/or guest upon binding, such as the 1H NMR chemical shift or UV/Vis band, which have linear dependence on the concentration of complex, is utilized and plotted against f_G . For a 1:1

complex, the Job plot should give a maximum when $f_G = 0.5$ while a maximum at $f_G = 0.66$ would correspond to a 1:2 stoichiometry (Figure 1.5).

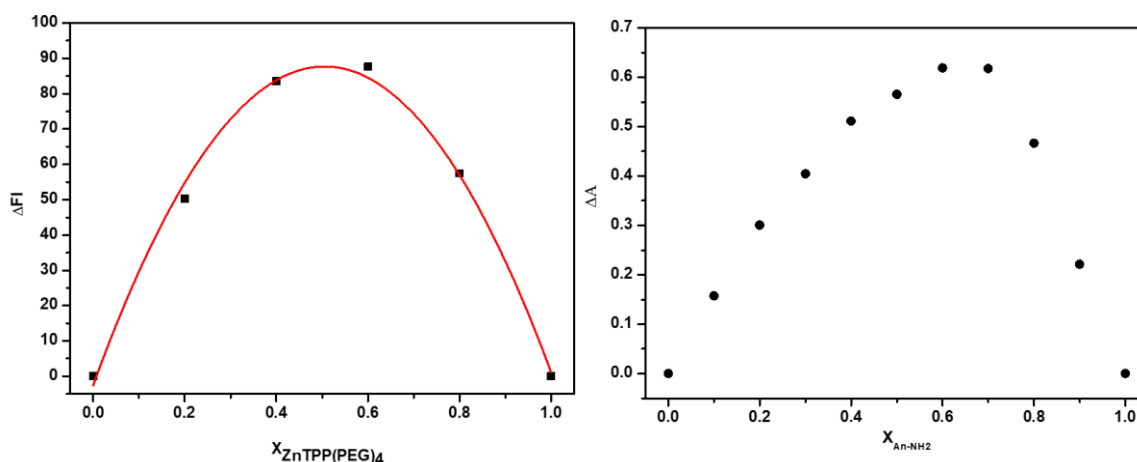


Figure 1.5 Two examples of Job plots for 1:1 (left) and 1:2 (right) host-guest complex. (from Chapters 2 and 3)

In principle, the binding constants can be determined by any experimental technique that can yield information about the concentration of the formed complex, $[H_mG_n]$, and the changing concentration of the host or guest. Practically, the most common approach to measure the binding constant is the supramolecular titration method. Here, one component is gradually added to the solution of the other binding partner while monitoring a physical property change, *e. g.* specific chemical resonance (NMR), absorption of UV-Vis/fluorescence band, or the heat formed or absorbed (isothermal titration calorimetry-ITC).

We take the UV-Vis spectrophotometric titration, which was used in this thesis, as an example to illustrate the titration method in general. UV-Vis spectroscopic titration, or spectrophotometric titration, refers to monitoring the intensity of an absorption band at a particular wavelength that is characteristic of either the complex or free host or guest upon stepwise addition of one of the binding partners. We define the absorption band coming from host in the following section. The absorbance intensity vs. concentration of added guest to a solution of constant host concentration can be plotted. For a 1:1 complex with the binding constant $K_a = [HG]/[H][G]$, the absorbance intensity A_{obs} at a certain wavelength is given by:

$$A_{obs} = \varepsilon_H l [H] + \varepsilon_{HG} l [HG] \quad \text{Equation (4)}$$

Where A_{obs} is the observed absorbance; ε is the molar absorption coefficient; l is the path length. If the concentration of the complex $[HG]$ is known, then the concentration of free host $[H]$ or guest $[G]$ can be determined by the equation:

$$[H]_0 = [H] + [HG] \quad \text{Equation (5)}$$

$$[G]_0 = [G] + [HG] \quad \text{Equation (6)}$$

We define the fraction of host complexed with guest as f_{HG} ($f_{HG}=[HG]/[H]_0$), Then after introducing equation (3) and (5), f_{HG} can be rewritten as:

$$f_{HG} = \frac{[HG]}{[H]+[HG]} = \frac{K_a[G]}{1+K_a[G]} \quad \text{Equation (7)}$$

Where $[H]_0$ is the initial concentration of host, which is a known constant. When equation (4) and (7) are combined, a new equation can be given:

$$A_{obs} = A_0 + (\varepsilon_{HG} - \varepsilon_H)l[H]_0 \times \frac{K_a[G]}{1+K_a[G]} \quad \text{Equation (8)}$$

Here, A_0 is the initial absorbance of the host solution without guest. When much more guest is added than the amount of host, then $[G]_0 \gg [HG]$. From equation (6), the unknown concentration of free guest will become close to the amount of the added guest, $[G]_0 \approx [G]$. Then, equation (8) can be rewritten as:

$$A_{obs} = A_0 + (\varepsilon_{HG} - \varepsilon_H)l[H]_0 \times \frac{K_a[G]_0}{1+K_a[G]_0} \quad \text{Equation (9)}$$

In equation (9), A_{obs} , A_0 , $[H]_0$ is a known and fixed parameter; ε_{HG} , ε_H , and K_a are unknown constants. The titration curve can be given by plotting the observed absorbance against the variable $[G]_0$. Finally, the binding constant can be given by a non-linear curve fitting of the data based on equation (9). A UV titration and data processing example is shown in Figure 1.6.

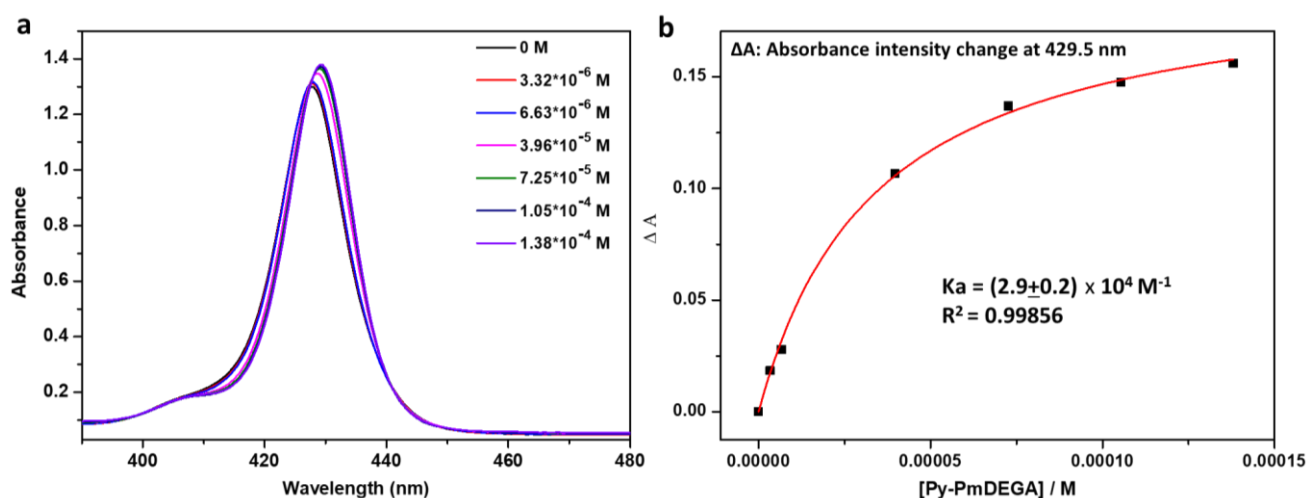


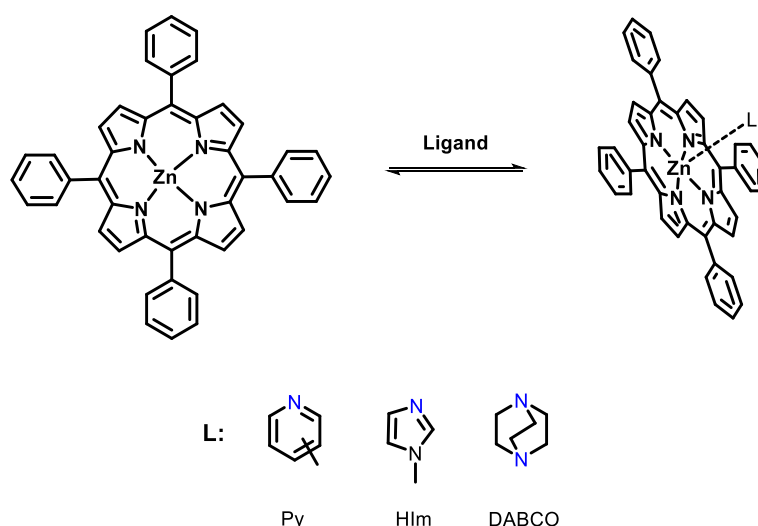
Figure 1.6 UV titration of 1:1 complexation and data processing based on equation (9). (from Chapter 2)

1.1.3 The non-covalent interactions that were employed in this thesis

As aforementioned, non-covalent interactions include hydrogen bonding, metal-ligand interactions, host-guest interactions, van der Waals forces, π - π interactions and electrostatic effects. In this thesis, metal-ligand interactions and host-guest interactions were employed to build supramolecular materials. These three non-covalent interactions and the corresponding building blocks will be described in further detail in the following sections.

1.1.3.1 Metal-ligand interaction based on metalloporphyrin complex

Porphyrins are a group of heterocyclic macrocyclic organic compounds, consisting of four (modified) pyrrole subunits interconnected at the α carbon positions by methine. The macrocyclic porphyrin is capable of binding different kinds of transition metal ions in its central cavity. After metal complexation, the positions on the metal ion axial to the plane of porphyrin ring are available to bind with other ligands.²⁷⁻⁴⁰ In the last few decades, the application of metalloporphyrins in biological systems has been reported in many papers, especially the effects of axial ligand binding on the metalloporphyrin structures.^{37, 41-44} Zinc porphyrin (ZnTPP) is one of the most accessible compounds among the metalloporphyrins and has, therefore, been chosen to study coordination with various electron-donor ligands. The structure of zinc porphyrin and the corresponding complex are depicted in Scheme 1.1. ZnTPP can be easily purified and is well soluble in organic solvents. Furthermore, in contrast to manganese-, copper-, and iron-containing porphyrins, ZnTPP does not participate in redox reactions. Up to date, ZnTPP was highly employed in the study of donor-acceptor dyads with C_{60} bearing nitrogen based ligands based on metal-ligand interaction.^{39, 45-46} The coordination of zinc porphyrin and pyridine was utilized in *chapter 2* to construct a dynamic miktoarm star polymer.



Scheme 1.1 The structure of zinc porphyrin and the complex, and the most used ligands in literature.

1.1.3.2 Host-guest interactions based on cyclodextrin, cucurbit[n]urils and anthracene

In the world of supramolecular chemistry, one of the frequently employed host compounds are cyclodextrins. Cyclodextrins are cyclic oligomers built up from six, seven or eight glucopyranose units, linked by α -(1-4)-glycosidic linkages, named α -, β - and γ -cyclodextrins, respectively.⁴⁷ The three-dimensional structure of CDs is like a truncated cone with all hydroxyl groups located at the surface of the molecule, making it soluble in water. On the other hand, the interior cavity of CDs is relatively hydrophobic, allowing lipophilic molecules with proper size to be included by host/guest interaction. The physical properties of the three cyclodextrins are shown in Figure 1.7.

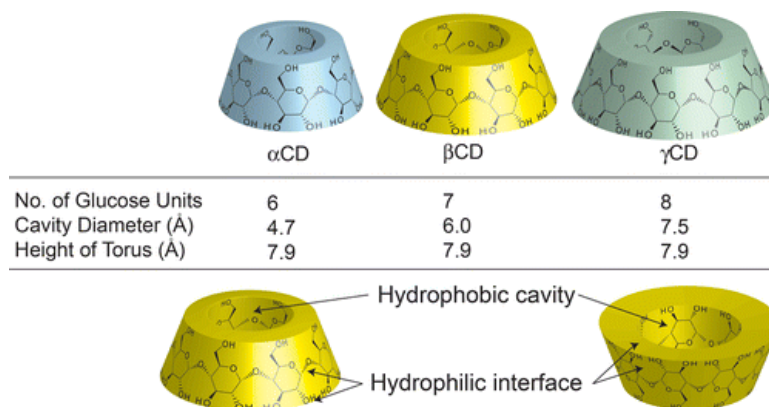
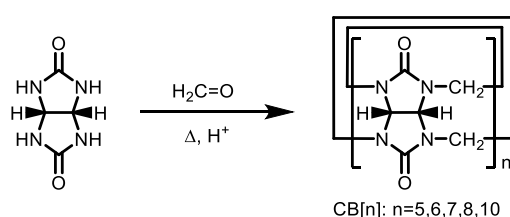


Figure 1.7 Chemical structures, approximate geometric, dimensions, and physical properties of α -, β - and γ -cyclodextrins. Reprinted with permission from ref. ⁴⁸ Copyright © 2014, American Chemical Society.

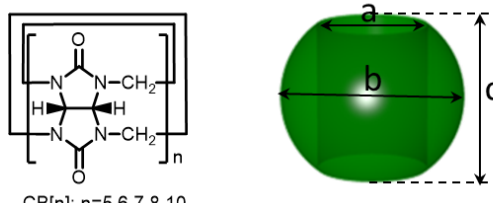
Among the three common CDs, α -CD is able to form a stable supramolecular complex with small hydrophobic guests, such as monocyclic aromatics, including azobenzene (Azo) and its derivatives; β -CD tends to interact with medium sized hydrophobic compounds, such as anthraquinone, cholesterol,⁴⁹ ferrocene (Fc),⁵⁰ adamantane (Ada),⁵¹⁻⁵³ cyclic diene, azo compound and some derivatives. α -CD and β -CD are the most utilized CDs to form inclusion complexes for a wide range of applications, *e.g.* supramolecular hydrogels,^{46, 49-52} supramolecular polymer,^{48, 53} supramolecular nanoparticles,⁵⁴ and so on. γ -CD has a relatively large cavity allowing complex two guest molecules in its cavity yielding ternary inclusion complexes. For example, pyrene,⁵⁵⁻⁵⁷ anthracene⁵⁸ or their derivatives have been reported to form ternary inclusion complexes with γ -CD where two guest molecules are included in the hydrophobic cavity. Inspired by this feature, the γ -CD was employed in Chapter 3 to prepare supramolecular networks using the ternary complex formation as dynamic crosslinks.

Cucurbit[n]urils (CB[n]), each of which consists of *n* glycoluril units, have a hydrophobic cavity and two identical carbonyl-laced portals and are an important family of macrocyclic compounds. CB[n]s can be prepared from the acid-catalyzed condensation reaction of glycoluril and formaldehyde (Scheme 1.2).⁵⁹ The structures and physical properties of CB[n]s are shown in Figure 1.8. Similar to CDs, the hydrophobic interior of CBs provides a potential site for inclusion of hydrophobic molecules with very high binding constants. Comparing to CDs, the utilization of CB[n] as host to form non-covalent interactions is, however, limited by: (i) poor solubility in aqueous and organic media, especially CB [6] and CB[8]; (ii) more difficult access to (functional) CB[n] derivatives, compared to CDs.



Scheme 1.2 Synthesis of CB[n] homologues by condensation of glycoluril and formaldehyde under acidic conditions.

However, the electrostatic potential of the carbonyl groups at the portals of the CB[n] cavity, which play a crucial role in molecular recognition in aqueous solution, is obviously more electronegative than the hydroxyl portals in CDs. Figure 1.9 shows the electrostatic potentials of CB[7] and β -CD as an example. Another advantage of CB[n] family is that the average binding affinity to hydrophobic guests is generally an order of magnitude higher than with CDs, which was reviewed by Houk et al.⁶⁰ In the wide field of host-guest chemistry, CB[n] is an important young family member of macrocyclic hosts, able to form inclusion complexes with various guest molecules, such as cations, drug molecules, amino acids and peptides, and even high molecular weight guests. The excellent recognition properties of the CB[n] family have led to their extensive use in various applications, including catalysis, self-assembled monolayers, waste-stream remediation of textile industry, DNA binding and gene transfection, which was summarized by Isaacs et al.⁶¹ Among the CB[n] family, the cavity of CB[8] is similar in terms of size to γ -CD. In contrast to CB[5] to CB[7], the larger cavity provides the capability to simultaneously bind two aromatic guests to form ternary host-guest complexes.⁶²⁻⁶⁸ Even more strikingly, the ternary complex can be formed when mixing the host and guest at a ratio of 1:1 indicating strong cooperativity for the binding of the two guests. We took this advantage of CB[8] in Chapter 3 to prepare supramolecular hydrogels using the ternary complexes as dynamic supramolecular crosslinks. Furthermore, CB[8] can form hetero-ternary complexes resulting in enhanced interaction of the two different guests, which has not been reported for γ -CD until now.



The figure shows the chemical structure of CB[n] on the left, which is a macrocyclic cage with n repeating units of a 1,3-dimethyl-2-imidazolidinone ring. To the right is a green cartoon representation of the cage, with dimensions a (width), b (depth), and c (height) indicated by dashed lines and arrows.

	M_r	a [Å]	b [Å]	c [Å]	S_{H_2O} [mM]
CB[5]	830	2.4	4.4	9.1	20-30
CB[6]	996	3.9	5.8	9.1	0.018
CB[7]	1163	5.4	7.3	9.1	20-30
CB[8]	1329	6.9	8.8	9.1	<0.01
CB[10]	1661	9.0-11.0	10.7-12.6	9.1	---

Figure 1.8 The chemical structures, cartoon representation, dimensions and physical properties of CB[n]. (note that: the values quoted for a, b, and c take into account the van der Waals radii of relevant atoms). Adapted from ref.⁶¹

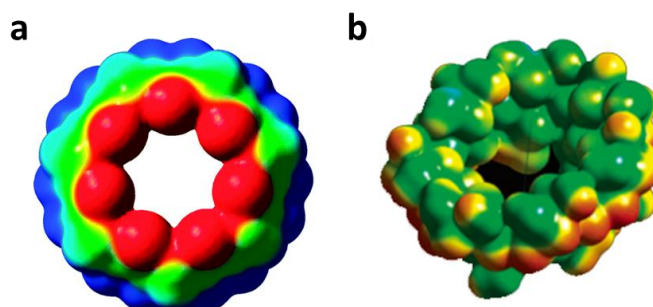
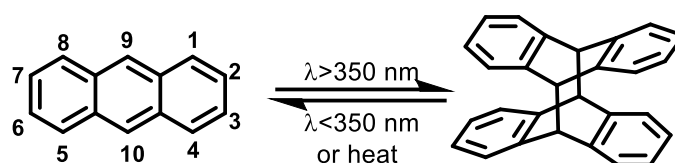


Figure 1.9 Electrostatic potential map of (a) CB[7] and (b) β -CD, indicating the negatively charged carbonyl portals of CB[7] (in red) and neutral portal and cavity of β -CD (in green). Adapted from ref.⁶⁹ and ref.⁷⁰

Anthracene is a polycyclic aromatic hydrocarbon consisting of three fused benzene rings. The ring is willing to act as a light induced electron donor or acceptor, which is easily tuned by the substitution pattern. The reversible photodimerization ability of anthracene (Scheme 1.3) has attracted a great interest in recent years, which was employed to prepare dynamic and/or reversible polymeric networks.⁷¹⁻⁷³ Moreover, the hydrophobicity of anthracene makes it an excellent guest for γ -CD and CB[8] resulting in the formation of ternary complexes.^{66, 74-76} In the most recent reports, the two properties were combined and it was demonstrated that the constructed system can undergo a reversible conversion of the formed supramolecular ternary inclusion complex to a binary complex of the macrocyclic host with the anthracene dimer facilitated by the photodimerization of anthracene.^{66, 74, 76}



Scheme 1.3 Photoinduced conversion between anthracene and its dimer.

1.1.3.3 π - π Interactions and electrostatic effects (charge transfer interaction)

Cyclobis(paraquat-*p*-phenylene) (CBPQT⁴⁺, Blue Box (BB)) was one of the flagships in the history of host-guest chemistry and was first report in 1988 by J. Fraser Stoddart's group.⁷⁷ The structure of CBPQT⁴⁺ is composed of two π -electron-deficient 4,4'-bipyridinium (BIPY²⁺) recognition units linked by two para-xylylene spacers in a cyclic manner (Figure 1.10). The π -electron-deficient host can form strong host-guest complexes by taking advantage of the formation of strong charge-transfer donor-acceptor interactions with electron-rich aromatic guest molecules. Furthermore, the α -hydrogen atoms of the BIPY²⁺ are electron deficient due to the positively charged nitrogen atoms, potentially allowing hydrogen bonding interaction with functional groups in the guest molecules, such as oligo-ethylene glycol spacers. A number of host-guest complexes with various size- and electronic constitution-matched guests were studied and employed to build topological structures as well as molecular machines based on CBPQT⁴⁺.⁷⁸⁻⁸⁶ Some of the most used electron-rich guests, 1,5-dialkoxynaphthalene (DNP), tetrathiafulvalene (TTF), dialkoxybenzene (DB), for blue box are depicted in Figure 1.10.

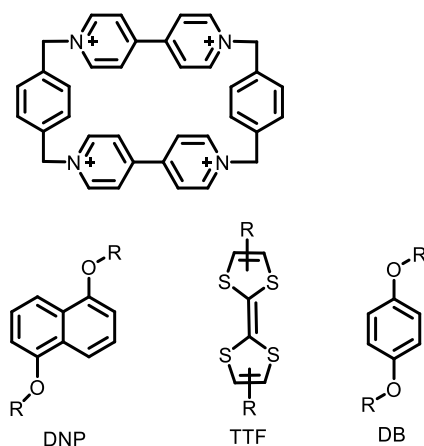


Figure 1.10 The structure of cyclobis(paraquat-*p*-phenylene) (counterions are omitted, but are crucial in determining the solubility in different solvents) and the typical guests.

1.2 The development of supramolecular star polymers

Since it was first proposed and demonstrated by Staudinger⁸⁷ that polymers consist of a covalently bonded macromolecular structure consisting of many repeating units, polymers have become an inextricable and irreplaceable part of our everyday life owing to its extraordinary versatility of property profile and application range. The properties of polymers are dominated by the chemical composition and the topology of polymer. It has been demonstrated that branching of polymers gives rise to a more compact structure compared to the linear polymer with similar molecular weight resulting in higher segment density, which further affects the crystalline, mechanical, viscoelastic and solution properties of the polymers.^{88,89}

Star polymers were first prepared by Schaeffgen and Flory in 1948,⁹⁰ representing the simplest branched polymer structure. Such star polymers have attracted significant attention in recent years.⁹¹⁻⁹³ Star polymers can be divided into homoarm star polymers and miktoarm star polymers according to the chemical composition of the arms. Star polymers are typically synthesized by divergent, convergent and coupling-onto strategies.⁹⁴ A major effort in polymer chemistry is focusing on the synthesis of polymers with desired properties by the precise control of molecular weight, polydispersity, composition and topology of the polymer chains.⁹³

However, conventional polymers also pose challenges as they can be difficult to process and recycle. Supramolecular polymers are polymeric arrays of monomeric units that are held together by highly directional and reversible non-covalent interactions, including hydrogen bonding, host-guest interaction, metal-ligand coordination and so on. These reversible and dynamic non-covalent interactions play a leading role in the assembly and conformation of the supramolecular system, and have been widely employed to construct different types of supramolecular polymers. Parameters that control the polymer properties, e. g. molecular weight, conformation, degree of polymerization and life-time of the chain, are highly depending on the strength of the non-covalent interactions, which can be tuned by adopting different arrays or different types of non-covalent interactions. The combination of the versatility of custom-made synthetic polymers and the

flexibility of the non-covalent dynamic interactions provide supramolecular polymers with unique properties catering applications in sensing, stimuli-responsive, self-healing and shape-memory materials.⁹⁵⁻⁹⁹ Moreover, significant efforts have been dedicated to elucidate the mechanism of the supramolecular polymerization, which has been well documented by Meijer *et al.*⁹⁶

Even though most efforts have been dedicated to linear supramolecular polymers, supramolecular star polymers are also interesting materials as the supramolecular association controls the topology of the polymer chains, thereby enriching material science with new potentials.¹⁰⁰⁻¹⁰² The non-covalent interactions provide new opportunities in dynamic and potentially stimuli-responsive materials. It is especially appealing to control the association of polymer chains to a core *via* supramolecular interactions as this provides supramolecular control over the number of arms and/or over the formation of homo-arm or mikto-arm star polymers. In this section, we will provide a brief overview of the use of different supramolecular interactions for linking of polymer chains to a core structure yielding dynamic supramolecular star-polymers.

1.2.1 Hydrogen bonding interaction based supramolecular star-polymers

The self-complementary ditopic hydrogen-bonding module, Bis-DeAP (Figure. 1.11), was developed by Zimmerman *et al.* in 1996 and used to assemble dendrimers at first.¹⁰³ Inspired by the formation of stable discrete cyclic assemblies, the authors further used this module to prepare supramolecular star polymers by modifying it with initiators for ring opening polymerization or atom transfer radical polymerization (ATRP).^{104,105} The Bis-DeAP functionalized initiators were used to polymerize styrene or methylmethacrylate. The resulting polymers self-assembled into higher molecular weight structures with narrow molecular weight distribution that could be observed by SEC, showing a single peak at high molecular weight range with a small polymer dispersity.

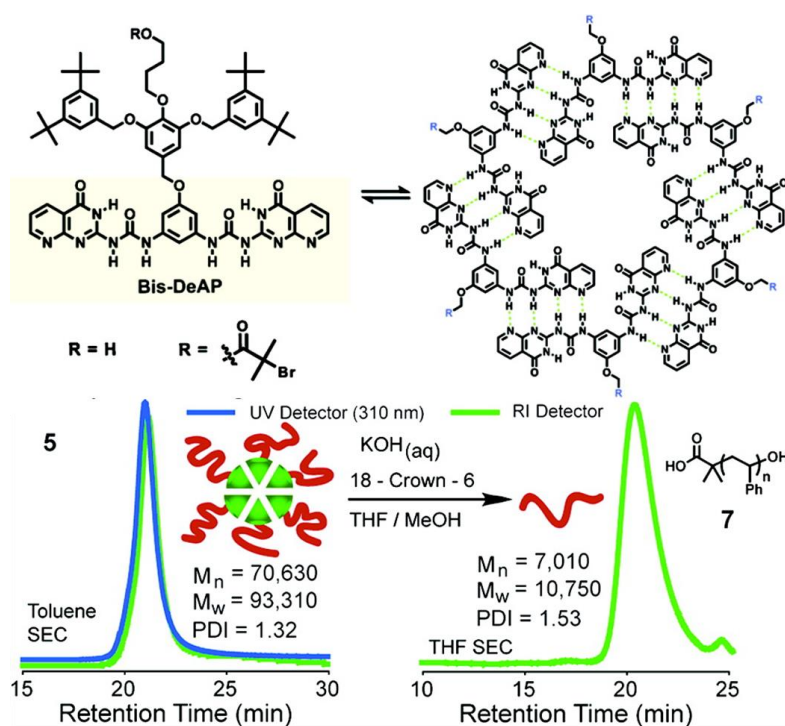


Figure 1.11 The structure of ditopic hydrogen bonding module Bis-DeAP and its hexameric assembly (top); the SEC traces of the assembled supramolecular polymer and one free arm polymer. (bottom). Reproduced with permission from ref.¹⁰⁴ Copyright © 2007, American Chemical Society

Barner-Kowollik *et al.* recently reported the formation of miktoarm (AB_2 ¹⁰⁶ and ABC ¹⁰⁷) and homoarm (A_3)¹⁰⁶ supramolecular star polymers based on the hydrogen bonding interaction of the Hamilton wedge (HW) and cyanuric acid (CA) (Figure 1.12.). The supramolecular (mikto)arm polymers were formed by mixing the HW mid-chain functionalized poly(styrene) and CA end-functionalized poly(styrene) or poly(methyl methacrylate). The more complicated ABC-type supramolecular star polymer was prepared by a similar strategy, for which the HW mid-chain functionalized polymer was poly(ethylene glycol)-*b*-polystyrene (PEG-HW-PS) block copolymer and cyanuric acid chain-end functional linear polymer was poly(*n*-butylacrylate) (PnBA).

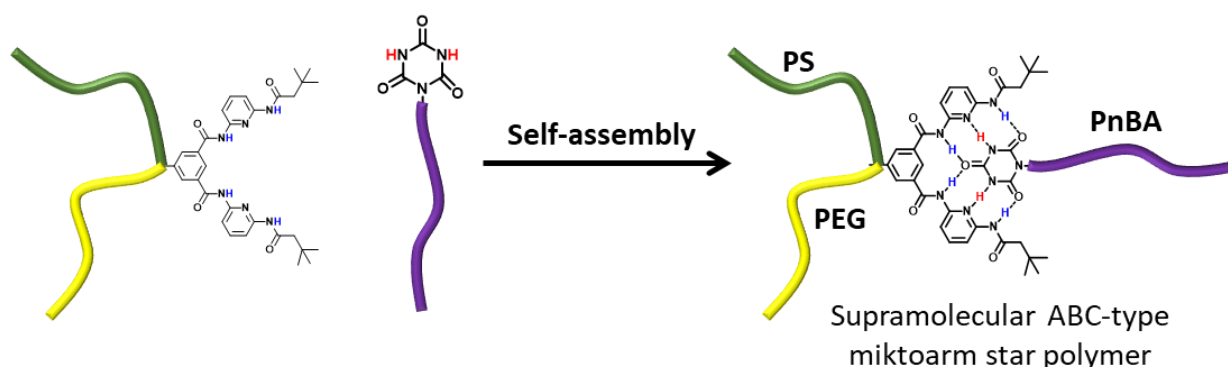


Figure 1.12. General strategy for the preparation of ABC type miktoarm terpolymers. The HW building blocks are generated by a combined ATRP/CuAAC strategy. The linear α -CA functional PnBA is synthesized by raft polymerization. ABC-type miktoarm terpolymers are subsequently generated *via* the supramolecular self-assembly of HW/CA complementary recognitions motifs. Adapted from ref.¹⁰⁷

Bernard and co-workers also prepared supramolecular poly(vinyl acetate) (PVAc) 3-arm star polymers by the formation of hydrogen bonded heterocomplexes between polymer chains functionalized with heterocomplementary associating units (thymine and diaminophridine), prepared by RAFT polymerization.¹⁰⁸⁻¹⁰⁹

1.2.2 Host-guest interaction based supramolecular star-polymers

Although a large number of host/guest complexes have been reported, the most common host molecules involved in fabricating supramolecular star polymers include cyclodextrins (CDs), crown ethers, and cucurbit[8]urils (CB[8]). Guest molecules are generally the small hydrophobic organic compounds that can be incorporated inside the hydrophobic cavity of host. Until now, cyclodextrins have been mostly applied for the construction of supramolecular star polymers.

CD-based supramolecular star polymers can be constructed based on a covalent star polymer with CD as the core moiety and a guest molecule that is functionalized with a polymer through host/guest complexation. An interesting architecture in that regard is the connection of CD-centered star polymers with linear polymers bearing one or two guest end-groups as reported by Li and

coworkers.¹¹⁰⁻¹¹¹ The first report presented a system comprising a β -CD-core Poly(*N*-isopropylacrylamide) (PNIPAm) star polymer which forms a supramolecular mikto-arm star polymer with poly(ethylene glycol) (PEG) bearing an adamantyl end-group through host-guest complexation (Figure 1.13a). The complex formation was proven *via* NOESY. The thermoresponsive properties of the supramolecular polymer could be tuned over a temperature scale around the body temperature by varying the number of guest moieties and the molecular weight of the employed PEG.¹¹⁰ Later, two β -CD centered PNIPAm star polymers were connected by complexation with poly(propylene glycol) (PPG) having two adamantane end-groups. As this system contains two kinds of thermoresponsive segments, PPG and PNIPAAm, it exhibited dual thermoresponsive behavior in aqueous solution. The supramolecular polymer underwent a reversible temperature-induced transition from solution to micelle and further to larger aggregates upon heating.¹¹¹

More recently, the same group reported a supramolecular star polymer as multifunctional gene carrier system.¹¹² The supramolecular star polymer is self-assembled from two molecular building blocks: a star polymer host polymer, β -CD-SS-P, consisting of multiple arms of poly(2-dimethylaminoethyl methacrylate) (PDMAEMA) linked to a β -CD core *via* bioreducible disulfide bonds, and a polymeric guest, adamantyl end capped poly(2-methacryloyloxyethyl phosphorylcholine) (Ada-PMPC), being an adamantane end capped poly(2-methacryloyloxyethyl phosphorylcholine) (PMPC) (Figure 1.13b). The host and guest polymers self-assemble to integrate both the gene complexing function of the PDMAEMA and the non-fouling function of pMPC into one system, based on the host/guest interaction between β -CD and adamantane moieties.

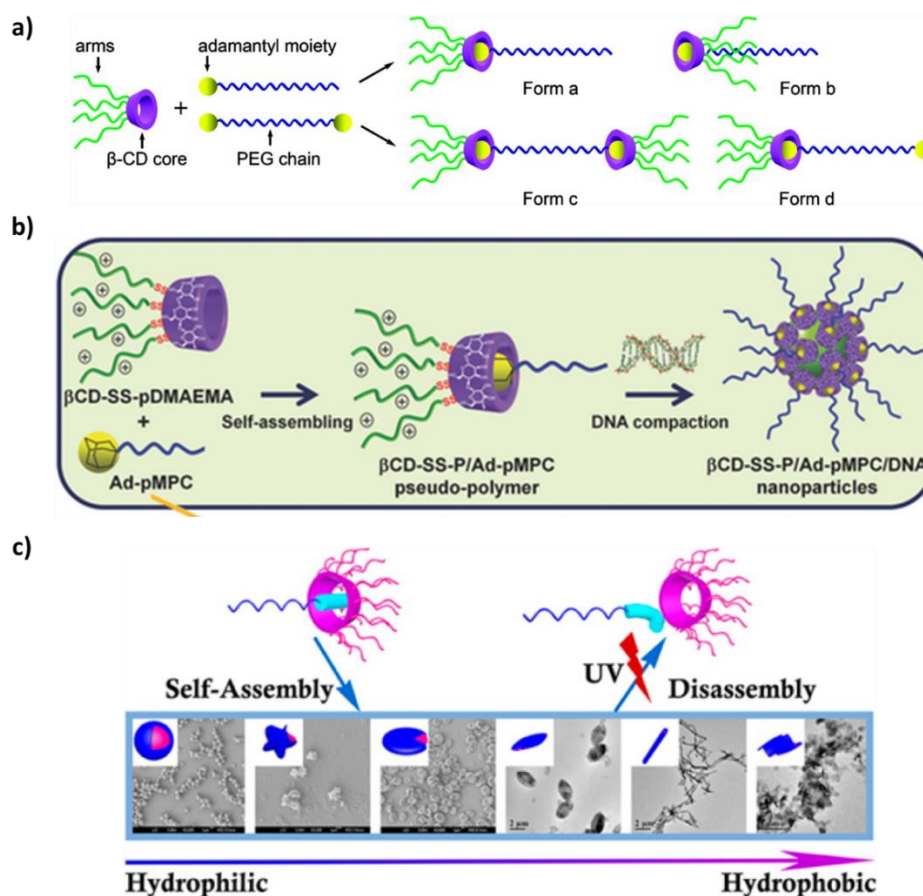


Figure 1.13 (a) Supramolecular complexation formed *via* host/guest interaction between β -CD centered star polymer and adamantly functionalized PEGs. Reprinted with permission from ref.¹¹⁰ Copyright © 2008, American Chemical Society; (b) Formation of β -CD-SS-P/Ad-pMPC pseudo-diblock copolymer *via* host-guest interaction, followed by DNA compaction to form β -CD-SS-P/Ad-pMPC/DNA polyplex. Reprinted with permission from ref.¹¹² Copyright © 2014, John Wiley and Sons; (c) Supramolecular star polymers *via* azobenzene functionalized PEG and star polymer β -CD-PLLA. Reprinted with permission from ref.¹¹³ Copyright © 2014, American Chemical Society.

Wu and coworkers constructed a series of supramolecular star polymers by assembling a linear guest polymer, azobenzene-functionalized poly(ethylene glycol) (Azo-PEG), and multi-arm star host polymers consisting of β -CD functionalized with 14 poly(L-lactide) chains (β -CD-PLLA) (Figure 1.13c).¹¹³ Different morphologies were obtained through aqueous self-assembly of these supramolecular polymers.

An alternative approach of constructing supramolecular star polymers based on CD is based on a mono-polymer functionalized cyclodextrin and a guest modified polymer having the guest at the middle of the polymer. Barner-Kowollik and coworkers described the synthesis of such a miktoarm star polymer *via* supramolecular complexation between β -CD functionalized poly(*N,N*-diethylacrylamide) (PDEAAM) and poly(*N,N*-dimethylacrylamide) (PDMAAM) mid-chain functionalized with adamantane (Figure 1.14a).¹¹⁴ The formation of the supramolecular miktoarm star polymer was proven *via* DLS, ROESY and turbidimetry. Additionally, the temperature induced aggregation behavior was studied by temperature sequenced DLS measurements. Furthermore, a wide variety of complex macromolecular X- and H- shaped star copolymers were reported based on similar self-assembly strategies by the same group (Figure 1.14b).¹¹⁵ Several building blocks including adamantyl mid-chain poly (*N, N*-dimethylacrylamide) (pDMA), poly (*N, N*-diethylacrylamide) (pDEA) and p(DEA-b-DMA) as well as double adamantyl end-functional pDMA and pDEA, along with mid-chain β -CD functionalized PDMA, PDEA and P(DEA-b-DMA), were synthesized *via* the combination of RAFT polymerization and copper catalyzed azide alkyne cycloaddition. Subsequently, the formation of the target architectures *via* supramolecular association of CD- and adamantyl-functionalized building blocks was evidenced by NOESY and DLS. Furthermore, the temperature responsive behavior of the obtained star block copolymers was investigated.

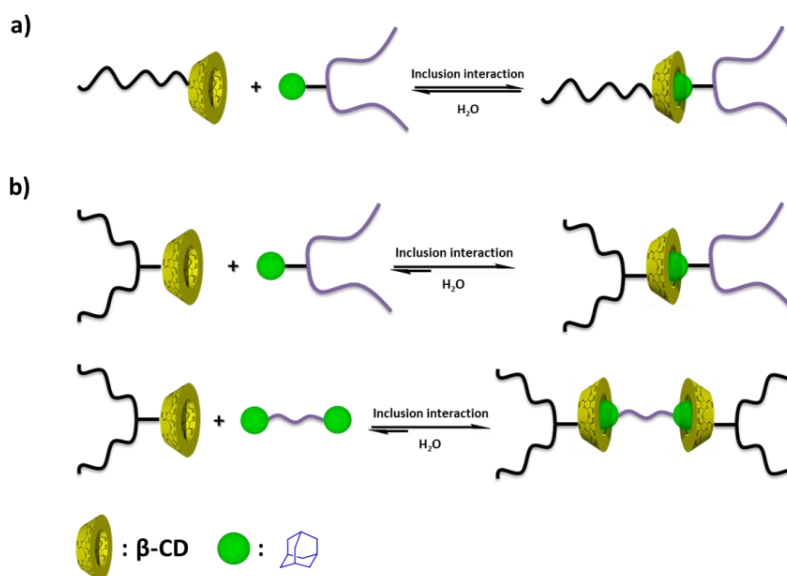


Figure 1.14 (a) Supramolecular miktoarm star formation *via* mid-chain adamantyl functionalized PDMMAm and β -CD end functionalized PDEAAm. (b) Examples of supramolecular X-shaped and H-shaped star block copolymers. adapted from ref. ¹¹⁴⁻¹¹⁵

Another strategy for preparing supramolecular star polymers based on CD host-guest complexation is based on a multifunctional core molecule bearing multiple CD or guest molecules in combination with the complementary polymers having the guest or CD as chain end. Barner-Kowollik and coworkers utilized a core with three β -CDs and adamantyl-functionalized polyacrylamides to form three armed star polymers *via* the formation of inclusion complexes (Figure 1.15a).¹¹⁶ In brief, the Ada-PDMAAm and Ada-PDEAAm were synthesized *via* RAFT polymerization with adamantyl-functionalized chain transfer agent. The core, β -CD₃, was synthesized *via* CuAAC techniques. The formation of supramolecular star polymers was carried out in D₂O and proven *via* DLS and ROSY NMR. In the case of star polymers with pDEAAm arms, the temperature-dependent solution behavior was studied by turbidity measurements. More recently, Ritter and coworkers utilized a core with six CDs to connect six phenolphthalein-functionalized methoxypoly(ethylene glycol) (PP-mPEG) chains.¹¹⁷ The synthesis of the arms (PP-mPEG) and the core (β -CD₆) was carried out *via* cycloaddition reaction. The formation of stable complexes based on supramolecular interactions between both building blocks was proven by UV-Vis measurement. The great advantage of the system is the possibility to follow the star polymer formation with the naked eye due to the introduction of phenolphthalein as guest leading to a color change upon complexation. Chen and coworkers described the construction of supramolecular star polymers based on the native protein concanavalin A (ConA) and adamantyl-functionalized PEGs (Ada-PEG).¹¹⁸ A dual linker (β -CD-Man) consisting of β -cyclodextrin (β -CD) and α -mannopyranoside (Man) was utilized to bind both adamantane end-functionalized PEG and the lectin ConA in an orthogonal manner (Figure 1.15b). The supramolecular association was probed *via* isothermal titration calorimetry (ITC). The complex formation was additionally investigated *via* DLS and SEC evidencing a strong dependence of the number of attached PEG chains on the concentration of the solution. Addition of free α -CD molecules was demonstrated to lead to hydrogel formation *via* threading of α -CD over the PEG

chains and further association of the form pseudorotaxane structures through hydrogen bonding of the α -CDs.

An interesting macromolecular architecture star-star polymer was described by Li and coworkers.⁵³ A dendritic supramolecular star polymer was formed by complexation of a star shaped 8-armed poly(ethylene glycol) having adamantane end-groups and a β -CD centered star poly(*N*-isopropylacrylamide) through inclusion complexation (Figure 1.15c). The formed structure further aggregated into a 3D network in response to temperature change, forming a thermoresponsive reversible “smart” hydrogel.

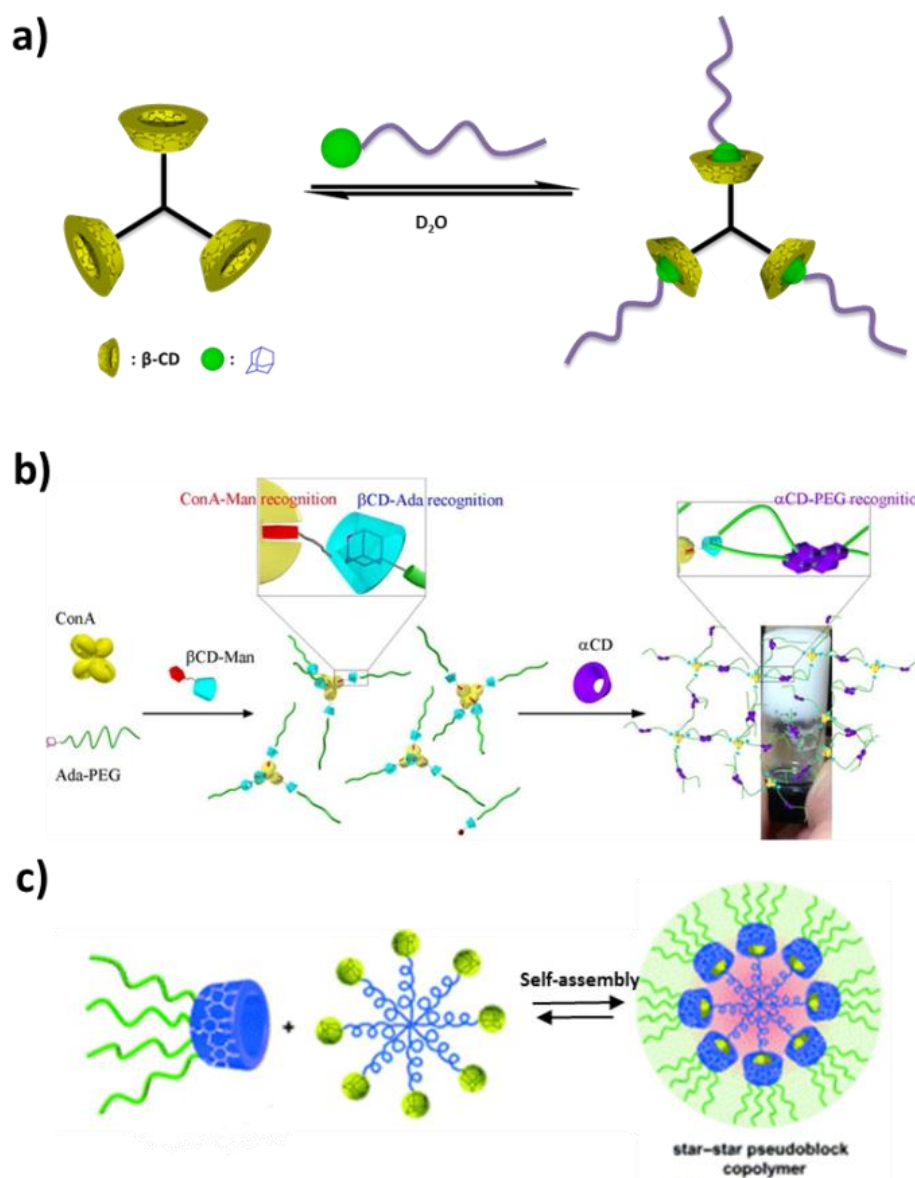


Figure 1.15 (a) The formation supramolecular star polymers via host/guest inclusion complexes between adamantyl-functionalized polyacrylamides and a three-pronged β -CD linker; (b) Schematic representation of supramolecular star polymer and further hydrogel formation. Reprinted from ref.¹¹⁸ Copyright © 2013, American Chemical Society; (c)

Formation of a dendritic supramolecular star polymer and the formation of a supramolecular hydrogel at a temperature above the LCST. Reprinted with permission from ref.⁵³ Copyright © 2013, John Wiley and Sons.

In addition to cyclodextrins, crown ethers and cucurbit[8]urils can also be employed in the fabrication of supramolecular star polymers. Crown ethers are cyclic chemical compounds consisting of a ring which contains several ether groups. The most popular guest molecules, which were utilized in the construction of supramolecular star polymers, are paraquat (*N, N'*-dimethyl-4, 4'-bipyridinium) dications and secondary ammonium salts. To date, all these systems were reported by Gibson's group. The first supramolecular star polymer based on crown ethers as supramolecular host was reported in 2005¹¹⁹ based on the self-assembly of a core molecule having three crown ether hosts and a complementary paraquat-terminated polystyrene guest. The formation of the 3-armed star polymer was confirmed by viscometry. Additionally, the relationship among the three crown ether binding sites during the complexation with the polymeric guests was studied by NMR spectroscopy.

The reverse system was reported five years later based on the complexation of a core molecule with three secondary ammonium salts or four paraquats as guests with crown ether (dibenzo-24-crown-8) terminated polystyrene.¹²⁰ The self-assembly processes were examined by NMR spectroscopy and viscometry revealing the formation of the supramolecular star polymers. It should be mentioned that the tetrafunctional paraquat core formed only 3-armed supramolecular star polymers instead of 4 armed, perhaps due to the steric effects. Similarly, the same group also designed and synthesized a C₆₀ derivative having multiple ammonium groups as multitopic guest that complexed with crown ether end functionalized polystyrene to form supramolecular star polymers with up to 12 arms *via* supramolecular complexation.¹²¹ In the same year, polymers that incorporate paraquat or crown ether moieties as chain ends or central units were synthesized by stable free radical polymerization and atom transfer radical polymerization. Supramolecular star polymers were formed by mixing the appropriate end- or center-functionalized polymers.¹²² Complexation studies to determine the stoichiometry and association constants were performed by NMR spectroscopy and isothermal microcalorimetric titration (ITC). A supramolecular 3-armed star polymer based on CB[8] was reported by Scherman and coworkers.¹²³ In this study, viologen functional macromolecules were achieved by CuAAC type click reaction and the reaction conditions were optimized. The authors also prepared a viologen trifunctional trimer by this method. Through formation of a ternary complex, self-assembly between the viologen trimer, CB[8] and a naphthol-terminated PEG polymer, a 7-component supramolecular 3-armed star polymer was formed in aqueous solution and characterized by ¹H NMR and DOSY.

1.2.3 Metal-ligand interaction based supramolecular star-polymers

In this section, the use of metal-ligand interactions to construct supramolecular star polymers will be summarized. One of the earliest supramolecular star polymers was reported by Chujo and co-workers based on complexation of 2,2'-bipyridine end-functionalized polymers that were prepared *via* post-polymerization chain end modification. The supramolecular star polymers were constructed by the coordination of 2,2'-bipyridyl terminated PEG¹²⁴⁻¹²⁵ and PPG¹²⁶ with various transition metal ions such as Ni(II), Ru(II), Co(II) and Pd(II). Fraser and co-workers pioneered in new

methodology of employing metalloinitiators for the living cationic polymerization of 2-oxazolines by using iron(II) tris(bipyridine)¹²⁷ and di-, tetra-, hexa-functional ruthenium tris(bipyridine) initiators.¹²⁸ The same research group performed the polymerization of different monomers, namely 2-methyl-, 2-phenyl-, 2-undecyl-2-oxazolines, with the same halomethyl substituted bipyridine.¹²⁹ Schubert *et al.* contributed to this methodology by using the complex of 6,6'-bis(bromomethyl)-2,2'-bipyridine with tetrahedral Cu(I) as initiator producing 4-arm poly(2-ethyl-oxazoline).¹³⁰

Fraser and co-workers reported polylactide and polycaprolactone supramolecular star polymers based on the assembly of 2,2'-bipyridines with one or two polymer chains with Fe(II) or Ru(II).¹³¹ Zhou and Haruna synthesized a 2,2'-bipyridine functionalized dithioester and successfully used it as RAFT agent for the polymerization of styrene and NIPAM.¹³² Supramolecular star polymers were formed by the addition of ruthenium(II) ions. Schubert *et al.* reported 4-arm homoleptic supramolecular star- polymers based on tridentate ligands.¹³³ Terpyridine was employed as bifunctional initiator for the ring opening polymerization of 2-ethyl-2-oxazoline followed by metal complexation to form the metallo-supramolecular star-polymers.

Dipyridinepyridazine (dpp) based metallo-supramolecular star polymers were reported based on the self-assembly of polymer functionalized dpp ligands into grid-like metal complexes with Cu(I) and Ag(I).¹³⁴ The polymer functionalized dpp ligands were prepared by either polymerization using a dpp initiator or by post-polymerization end group functionalization (Figure 1.16)¹³⁵.

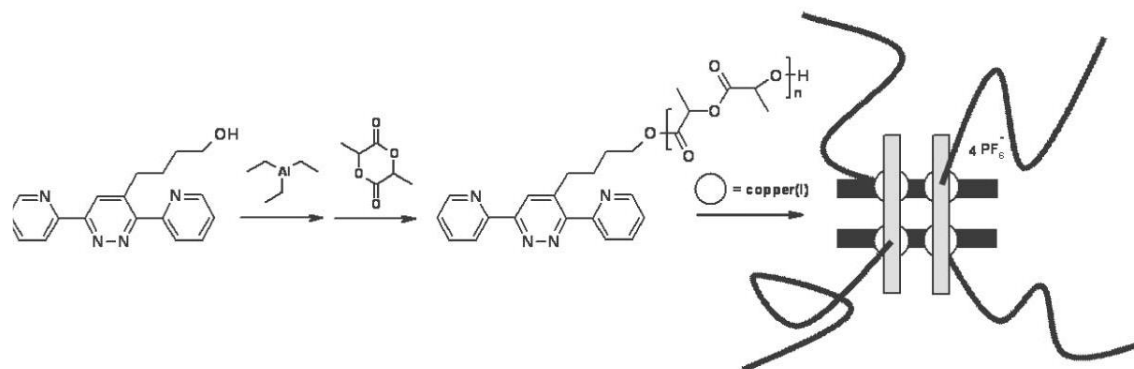


Figure 1.16 Schematic representation of the synthesis of a poly(L-lactide) 3,6-di(2-pyridyl)pyridazine macroligand and the subsequent self-assembly into grid-like complexes with copper(I) ions. Adapted from ref.¹³⁵

1.3 Supramolecular hydrogels

Hydrogels are 3-dimensional (polymeric) networks that trap large amounts of waters within their structure. Hydrogels found widely employed applications in industrial, environmental and biological areas.¹³⁶⁻¹³⁷ Natural hydrogels form an essential part of life, including chitosan, agarose, alginate, gellan gum and collagen based hydrogels, and even though they are still widely used in all kinds of applications, they were gradually replaced by synthetic hydrogels owing to the higher water absorption ability and robustness of synthetic hydrogels. Generally, the synthetic hydrogels can be classified in two categories based on the mechanism of cross-linking, chemical hydrogels and

physical hydrogels. Chemical hydrogels are formed by covalent bonds, whereas physical hydrogels, also called supramolecular hydrogels, are formed by non-covalent interactions, such as hydrogen bonds, metal-ligand interactions, host-guest interactions and hydrophobic interactions. Both of the two types of hydrogels have already been summarized in many reviews regarding the preparation, application and processing.^{11, 138-143} In the following section, we will give a brief overview of the development of covalent and physical hydrogels focusing on reports from the past few years.

Chemical hydrogels, in which polymer chains are connected by chemical bonds, can be prepared by the following methods: (i) cross-linking by radical polymerization in presence of bifunctional monomers; (ii) cross-linking of preformed polymers having complementary reactive groups; (iii) cross-linking by high energy radiation. When performing free radical polymerization, hydrogels can be prepared by adding multifunctional crosslinkers, which are the most commonly used methods to prepare chemical hydrogel.

Crosslinking of preformed polymers through coupling of reactive side chains is another popular method for the preparation of hydrogels. Various reactive groups, such as NH_2 , COOH , OH , present in hydrophilic polymers can be used to crosslink the material resulting in chemical hydrogels. For example, Zu Y. and coworkers synthesized hydrogels by adding the crosslinker glutaraldehyde to a solution of poly(vinyl alcohol), in which the chemical cross-links were formed by the reaction between the alcohol and the aldehyde.¹⁴⁴ Polymers bearing amine groups can also be crosslinked by the same cross-linker resulting in Schiff bases. Polysaccharides have been crosslinked to form hydrogels by the addition of a bifunctional crosslinker, such as 1,6-hexamethylenediisocyanate,¹⁴⁵ divinylsulfone,¹⁴⁶ or 1,6-hexanedibromide¹⁴⁷.

Hydrogels based on Tarragum/acrylic acid and bacterial cellulose were reported based on irradiation of the polymer solution with gamma rays¹⁴⁸ and electron beam¹⁴⁹, respectively. This method is more broadly applicable as the formation of poly(2-ethyl-2-oxazoline) and PEG hydrogels have also recently been reported based on gamma or beta irradiation of aqueous polymer solutions.¹⁵⁰

The chemical hydrogels possess excellent mechanical properties, but they are often brittle, lack transparency, and do not provide the possibility for reshaping or self-healing. In contrast, physical hydrogels overcame these issues relying on the reversible dynamic interaction, which has gained increasing interest. Physical crosslinking is made available through the use of supramolecular interactions. However, the dynamics of the crosslinks come at the cost of lower mechanical strength compared to covalent hydrogels.

Host-guest inclusion complexation has been applied as non-covalent interaction for the formation of supramolecular hydrogels. The most common host motifs are cyclodextrins (CD) and cucurbit[n]urils (CB[n]). Many reports have shown that hydrogels could be prepared by grafting host and guest molecules onto polymer backbones. Hydrogels can be formed in a system where both the host and the guest are grafted onto the same polymer chain (Figure 1.17a),¹⁵¹⁻¹⁵³ polymers grafted with either the host or the guest are mixed (Figure 1.17b),^{50, 154-157} or polymers grafted with guest

are mixed with dimers of the host (Figure 1.17c)^{52, 158}. When it comes to larger macrocyclic hosts, e. g. γ -CD or CB[8], that form ternary complexes with two guest molecules, hydrogels can be formed by mixing the polymers grafted with the guest and the free host molecule as employed in Chapter 3 of this thesis (Figure 1.17d).¹⁵⁹⁻¹⁶⁴

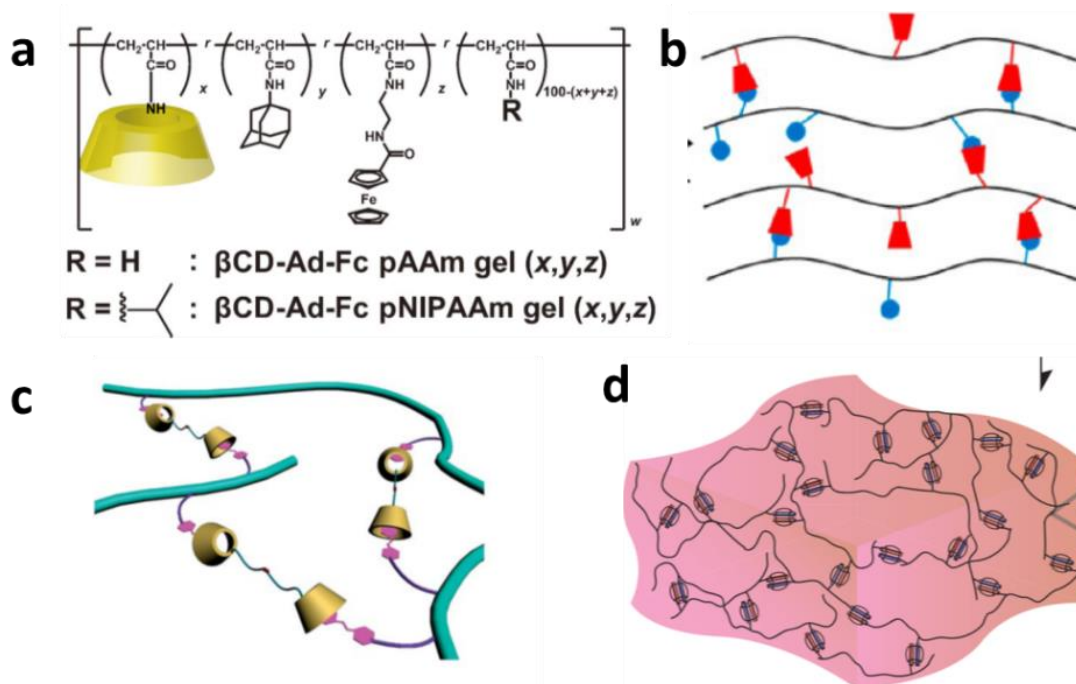


Figure 1.17 Schematic illustration of the different ways that hydrogels can be formed through host/guest interactions: a) both host and guest were grafted onto one polymer, reprinted with permission from ref.¹⁵¹ Copyright © 2015, John Wiley and Sons; b) polymer grafted with either host or guest, reprinted with permission from ref.¹⁵⁴ Copyright © 2013, American Chemical Society; c) polymer grafted with guest mixing with dimer of host, reprinted with permission from ref.¹⁵⁸ Copyright © 2013, Royal Society of Chemistry; d) polymer grafted with guest mixing with larger macrocyclic host, reprinted with permission from ref.^{158, 164} Copyright © 2012, American Chemical Society.

Hydrogen bonds are directional supramolecular interactions in which a hydrogen atom bound to an electronegative atom forms a weak interaction with an electronegative atom. Single hydrogen bonds are not strong enough to form hydrogels, but several motifs which can form multiple hydrogen bonds can be used for preparation of hydrogels. 2-Ureido-4-pyrimidone (UPy) is an example of a multiple hydrogen bonding motif. Campo and coworkers reported a self-healing hydrogel based on UPy units. A UPy side-chain functionalized copolymer was prepared by copolymerization and the resulting polymer formed self-healing hydrogels above pH = 8 (Figure 1.18).¹⁶⁵ The multiple hydrogen motif UPy was also employed to form hydrogels in other reports.¹⁶⁶⁻¹⁶⁷

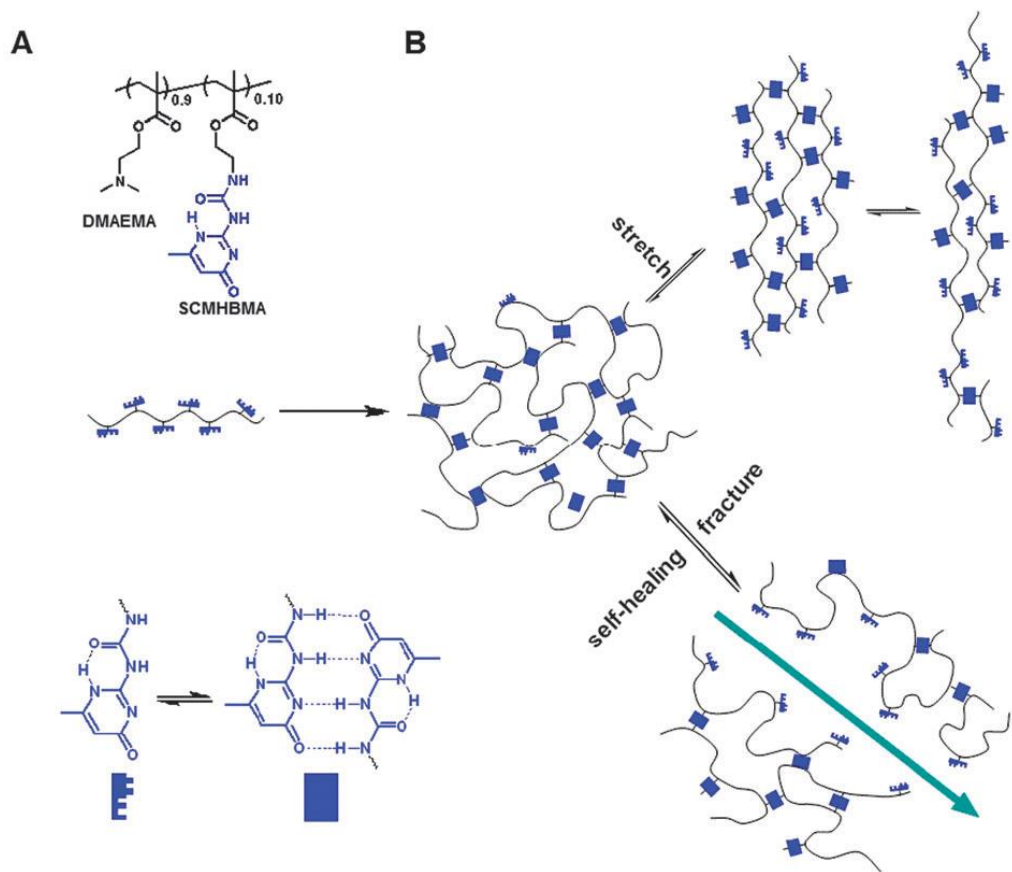


Figure 1.18 Chemical structure of the copolymer decorated by UPy (A) and the schematic model of self-healing and stretching of the hydrogel formed by the copolymers (B). Reprinted with permission from ref.¹⁶⁵ Copyright © 2012, Royal Society of Chemistry.

Another important type of non-covalent interactions for the formation of physical hydrogels are electrostatic interactions. A recently reported approach, to form supramolecular hydrogels is based on mixing of a charged ABA triblock copolymers with oppositely charged homopolymer (C)¹⁶⁸ or oppositely charged triblock copolymer (CBC)¹⁶⁹⁻¹⁷⁰ (Figure 1.19).

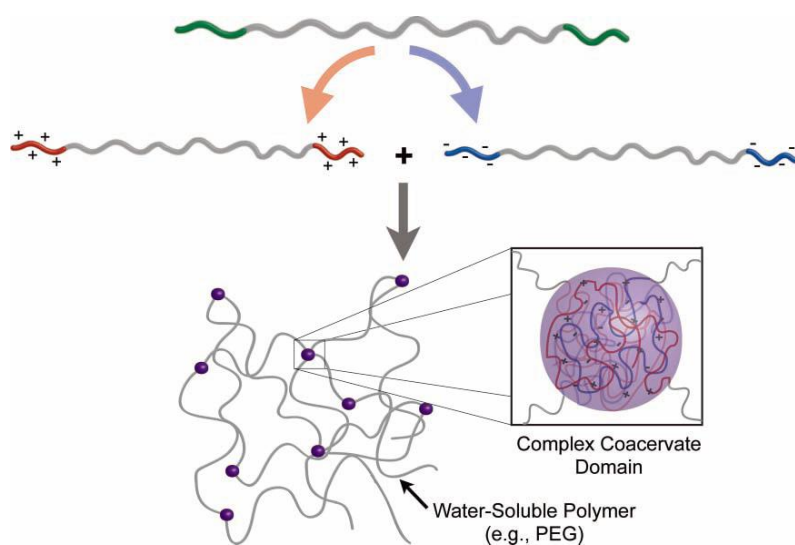


Figure 1.19 Schematic representation of hydrogel formation from two triblock copolymers. Reprinted with permission from ref.¹⁶⁹ Copyright © 2012, Royal Society of Chemistry.

1.4 Rotaxanes via click chemistry

Rotaxanes are mechanically interlocked molecules (MIMs) comprising a linear species (guest; axle) on which a cyclic species (host) is bound together by a mechanical bond, i.e. the presence of sterically demanding end-groups on the axle ensure that the cycle cannot slide off. Such rotaxanes have been used in molecular devices, e. g. molecular nanovalves,¹⁷¹ molecular motors and muscles.¹⁷² A cartoon representation of a rotaxane is shown in Figure 1.20. The rotaxane structure is considered to provide a versatile platform for the construction of functional artificial nanomachines. Therefore, a more efficient synthetic strategy to prepare rotaxanes should significantly facilitate the development in this research area. Cyclobis(paraquat-*p*-phenylene) (CBPQT⁴⁺) as an electron-deficient macrocyclic host for electron-rich guests, such as 1,5-dialkoxynaphthalene (DNP) and tetrathiafulvalene (TTF), has frequently been employed for the construction of [2]rotaxanes. In this section, we will give an overview of [2]rotaxanes, consisting of CBPQT⁴⁺/DNP or (and) TTF, focusing on the synthetic approach.

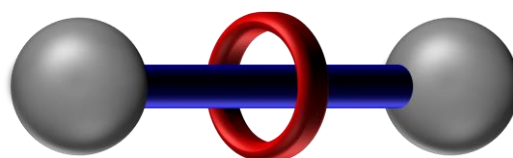
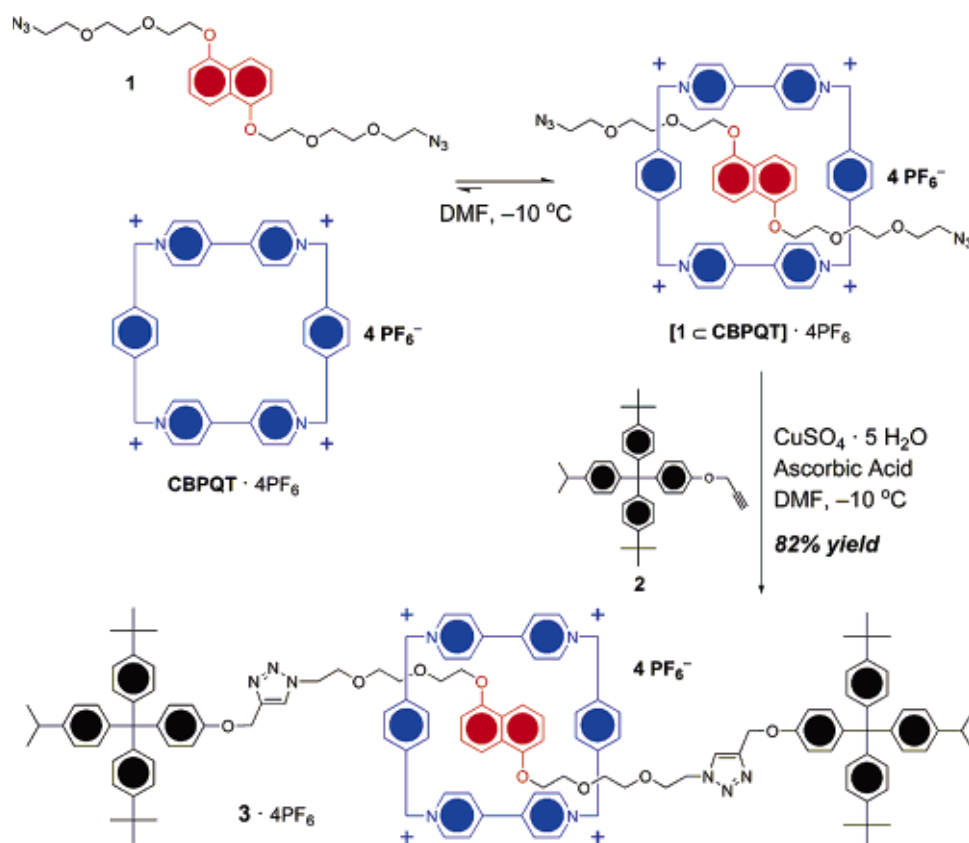


Figure 1.20 Cartoon representation of rotaxane.

The first rotaxane based on CBPQT⁴⁺ was reported by Anelli and coworkers through the clipping method.¹⁷³ A half blue box (1,4-bis(bromomethyl)benzene) and a dumbbell component were mixed, and the resulting supramolecular complex was further reacted with *p*-xylene dibromide to afford the [2] rotaxane. After that first report, the clipping method was also utilized to synthesize rotaxanes in Stoddart's group.¹⁷⁴ An alternative synthetic approach towards the [2]rotaxanes is the "stopping" strategy. Stoddart and coworker employed CuAAC click chemistry to prepare such a [2]rotaxane in 2006,¹⁷⁵ which greatly facilitated the development of rotaxane applications. (Scheme 1.4) Afterwards, the click reaction has widely been utilized for the preparation of CBPQT⁴⁺ based [2]rotaxanes,¹⁷⁶⁻¹⁷⁷ as well in other macrocyclic host based rotaxanes.¹⁷⁸⁻¹⁷⁹ The click reaction for the synthesis of rotaxane has a number of advantages: (i) high regioselectivity; (ii) tolerance of sensitive functional groups; (iii) quite mild reaction conditions; and (iv) excellent yields. It should be pointed that the reaction can be performed at room temperature or lower, which is ideal for strong binding of CBPQT⁴⁺ to guest. Inspired by the advantages of CuAAC for the preparation of rotaxanes as well as the drawback of using copper(I), we introduced a new reactive stopper for the preparation of CBPQT⁴⁺-based [2]rotaxanes using strain promoted azide-alkyne cycloaddition in Chapter 4.



Scheme 1.4 Synthesis of [2]rotaxane *via* click reaction. Reprinted with permission from ref.¹⁷⁵ Copyright © 2012, Royal Society of Chemistry.

1.5 Reversible addition-Fragmentation Chain Transfer Polymerization

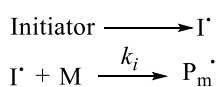
Within this thesis, the polymers that form the basis for the supramolecular materials were designed to have rather narrow molar mass distribution facilitating the analysis of the formed materials as well as to potentially derive structure-property relationships.

In polymer chemistry, living polymerization is regarded as a chain propagation reaction, which still has the ability of propagation after full monomer conversion via the addition of further monomer.¹⁸⁰ Chain termination and chain transfer reactions are absent and the rate of initiation is faster than the rate of chain propagation and, as a result, the polymer chains grow at a more constant rate yielding polymer chains with low dispersity (\bar{D}).¹⁸¹⁻¹⁸³ Anionic and some cationic polymerization were considered as truly living polymerizations, which are, however, not always easy to perform, especially in presence of functional (supramolecular) units. The most recently developed controlled radical polymerization (CRP) techniques, such as atom transfer radical polymerization (ATRP),¹⁸⁴⁻¹⁸⁶ nitroxide-mediated polymerization (NMP)^{182, 187-189} and the reversible addition fragmentation chain transfer polymerization (RAFT)¹⁹⁰⁻¹⁹⁴ also yield polymers with low \bar{D} , but are more functional group tolerant making them more attractive for developing supramolecular materials.¹⁹⁵

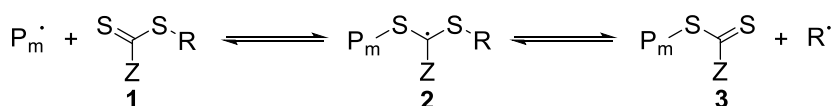
The polymers in this thesis were synthesized by RAFT polymerization, which is the most functional group tolerant from the different CRP methods while allowing polymerization of most monomer classes. RAFT polymerization is a reversible deactivation radical polymerization, in which the

equilibrium between active chains and dormant chains is regulated by a chain transfer agent (CTA), also known as RAFT agent. The CTA is the central element in the RAFT process that makes the polymerization controllable. The CTA is typically a thiocarbonyl thio compound bearing two substituents that are usually abbreviated as R- and Z- group (refer to the structure of **1** in Figure 1.21). The R-group is the radical leaving group and the Z-group is the stabilizing group. The generally accepted mechanism for RAFT polymerization is illustrated in Figure 10. The first step is the initiation step, where the radical is formed when the initiator, such as AIBN, is activated by heat or light. The radicals will react with monomers and oligomeric radicals are formed. Then the oligomeric radicals reversibly react with the RAFT agent **1** in step (ii). The R-group of the RAFT agent is ideally a better leaving group than the monomer adduct, so that all the RAFT agents are consumed in this step.¹⁹⁶ The intermediate radical **2** can further fragment to oligomeric RAFT agent **3** and the R radical. It should be pointed out that the R group should also be a good reinitiating group. Polymer chains with a free radical end-group will grow by adding monomer at the reinitiation step, which quickly exchanges with the oligomeric RAFT agent **3**. The formation of intermediate **4** in the chain transfer step limits the concentration of polymer chains with free radical end-groups and, thus, limits termination reactions. However, some termination reactions will still occur as depicted in step v. During the reaction, the concentration of active radicals in the system is very low as only a small fraction of the polymer chains carry free radicals, which together with the stable radical intermediate minimize termination reactions.

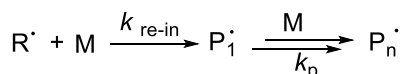
i Initiation



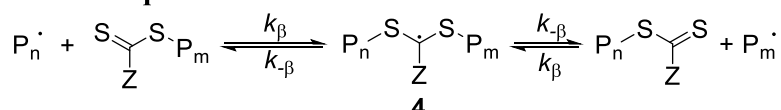
ii Initial equilibrium



iii Reinitiation



iv Main equilibrium



v Termination

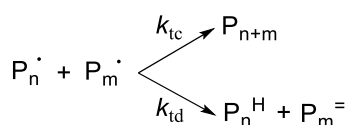


Figure 1.21 **Generally accepted mechanism for RAFT polymerization.** Following initiation, as in conventional free-radical polymerization (i), the radical reversibly adds onto the chain transfer agent **1** to form an intermediate radical **2**,

which can fragment to liberate a reinitiating group and form a new dormant chain **3** (ii). The new radical reinitiates polymerization by reaction on monomers (iii). The rapid establishment of this reversible addition-fragmentation equilibrium (iv) allows for control over molecular weight and molecular-weight distribution, although irreversible termination reactions still occur, mainly due to the free radical introduced initially to initiate polymerization (v).

Reprinted with permission from ref.¹⁹⁷ Copyright © 2010, Springer Nature.

RAFT polymerization is a kind of CRP, which should follow the first order kinetic behavior with regard to the concentration of monomer $[M]$. This can be derived from the equation of the polymerization rate (R_p):

$$R_p = -\frac{d[M]}{dt} = k_p[P^*][M]$$

Where t is reaction time, k_p is the propagation rate constant, $[P^*]$ is the concentration of propagating radical and $[M]$ is the real-time concentration of monomer. This equation was integrated to give the following equation:

$$\ln \frac{[M]_0}{[M]} = k_p[P^*]t$$

Where $[M]_0$ is the initial concentration of monomer. The plot of $\ln \frac{[M]_0}{[M]}$ against reaction time can be used to evaluate the kinetics of polymerization, in which $\ln \frac{[M]_0}{[M]}$ can be determined by gas chromatography (GC) or proton nuclear magnetic resonance spectroscopy.

As with the controlled living polymerization techniques, the degree of polymerization (DP) should be linear to the monomer conversion during polymerization, and the number average molecular weight M_n can be calculated from the conversion of monomer:

$$M_n = DP \times M + M_{CTA} = \frac{[M]_0 \times C}{[CTA]} \times M + M_{CTA}$$

Where M is the molecular weight of monomer, M_{CTA} is the molecular weight of RAFT agent, $[CTA]$ is the concentration of the RAFT agent, and C is the conversion of monomer. The linear relationship can be confirmed by plotting the M_n against the monomer conversion, in which M_n is usually measured by size exclusion chromatography (SEC), and the conversion can be calculated from the data of GC. Here it should be pointed out that the M_n from SEC is a relative molecular weight compared to polymer standards. The different properties between the measured polymer and the polymer standards lead to an inaccurate values due to the different hydrodynamic radius in the used solvent.

As aforementioned, the controlled living polymerization should lead to polymers with low dispersity, which is defined by

$$D = \frac{M_w}{M_n}$$

where M_w is the weight-average molecular weight. The polymer dispersity can be determined directly by SEC.

1.6 Summary

The rationale and recent developments for supramolecular star polymers, supramolecular hydrogels and rotaxanes were highlighted in this section. The dynamic reversible properties make these systems very promising for application in the life and materials science, e.g. drug delivery, biocompatible materials or artificial nanomachines. The advances in supramolecular bonding, *e. g.* reversibility, stimulus-responsivity and dynamics, are a welcome addition to the properties of the traditional materials. In addition, a broad variety of supramolecular motifs as toolbox is available which offers large number of possibilities to form the intended structure with desired properties.

Branched macromolecules are more compact than linear homologous ones due to their higher segment densities. The increased segment density results in a decreased tendency for these macromolecules to interpenetrate in solution as well as in bulk. A broad range of applications have been proposed for different branched polymers, therefore, the design of branched polymer with complex architectures would provide the opportunity to generate a broad range of material. Star polymers are characterized as the simplest case of branched polymers that have attracted significant attention in the last few years. To extend the applications, the non-covalent bonds were introduced in the construction of polymers, featuring a degree of flexibility, tunability and dynamics that was impossible using covalent chemistry. To date, various supramolecular star polymers have been prepared based on non-covalent interactions. However, to the best of our knowledge, there has been no report on the use of metalloporphyrin for the construction of supramolecular branched polymer, even though this kind of interactions were widely employed in other fields and it provides a highly tunable supramolecular interaction, both with regard to binding stoichiometry as well as interaction strength. The metal-ligand interaction based on metalloporphyrin and pyridine is firstly utilized to explore the construction of branched polymers, and a supramolecular miktoarm star polymer was selected to begin this research in **Chapter 2**.

As previously stated, the hydrogels have attracted considerable interest of chemists during the past few decades, due to their wide application as an ideal class of materials. Chemical hydrogels are stable and exhibit robust mechanical properties due to the stability of the covalent bonds, and have been commonly employed when tough and stable hydrogels are required. However, the poor shapability and processability and their brittleness limited their applications. In contrast, physical hydrogels are formed by dynamic non-covalent bonds between polymer chains, which avoid the deleterious implications of chemical hydrogels (brittleness, limited reshaping etc.) at the price of mechanically weaker systems. In recent years, hydrogels combining physical and chemical crosslinking have been developed. The resulting materials exhibited combined properties. However, the fact that the covalent crosslinks are presented in the hydrogels lead to irreversible damage when large ruptures occur. A system that can be switched between physical and chemical hydrogels could

be hypothesized to address this issue. To the best of our knowledge, no study regarding the reversible conversion between physical and chemical hydrogels was reported. In **Chapter 3**, a new kind of hydrogel that undergoes the conversion based on supramolecular assembly and dimerization of anthracene group was designed and explored.

Mechanically interlocked molecules (MIMs) have attracted increasing attention for over 50 years owing to their wide range of potential application in molecular devices. The rotaxane structure has been considered as a versatile platform for the construction of functional MIMs. Therefore, the development of highly efficient synthetic strategies for the preparation of rotaxanes should facilitate the further development of this research. Even though copper(I) catalyzed azide-alkyne cycloadditions have been used for this purpose, this leads to the incorporation of additional triazole linkers and may complicate purification by the presence of copper ions in the product. Therefore, in **Chapter 4**, a strained dibenzoazacyclooctyne (DIBAC) derivative was introduced for the preparation of a rotaxane by strain-promoted azide-alkyne cycloaddition (SPAAC). The carboxyl group present on the stopper would be further used to construct more complex mechanically interlocked molecules.

1.7 References

1. Lehn, J.-M., Molecular Recognition. In *supramolecular chemistry Concepts and Perspectives*, Lehn, J.-M., Ed. 1995.
2. Liu, Z.; Sun, X.; Nakayama-Ratchford, N., *et al.*, *ACS Nano* **2007**, *1* (1), 50-56.
3. Fernando, I. R.; Ferris, D. P.; Frasconi, M., *et al.*, *Nanoscale* **2015**, *7* (16), 7178-7183.
4. Lehn, J.-M., *Proc. Natl. Acad. Sci.* **2002**, *99* (8), 4763-4768.
5. Beck, J. B.; Rowan, S. J., *J. Am. Chem. Soc.* **2003**, *125* (46), 13922-13923.
6. Ulijn, R. V., *J. Mater. Chem.* **2006**, *16* (23), 2217-2225.
7. Yarimaga, O.; Jaworski, J.; Yoon, B., *et al.*, *Chem. Commun.* **2012**, *48* (19), 2469-2485.
8. Descalzo, A. B.; Martínez - Máñez, R.; Sancenón, F., *et al.*, *Angew. Chem. Int. Ed.* **2006**, *45* (36), 5924-5948.
9. Liu, Y.; Huang, Z.; Tan, X., *et al.*, *Chem. Commun.* **2013**, *49* (51), 5766-5768.
10. Houton, K. A.; Wilson, A. J., *Polym. Int.* **2015**, *64* (2), 165-173.
11. Folmer, B. J. B.; Sijbesma, R. P.; Versteegen, R. M., *et al.*, *Adv. Mater.* **2000**, *12* (12), 874-878.
12. Zhang, M.; Xu, D.; Yan, X., *et al.*, *Angew. Chem.* **2012**, *124* (28), 7117-7121.
13. Lehn, J.-M., *Science* **1985**, *227* (4689), 849-856.
14. Feringa, B. L.; Koumura, N.; van Delden, R. A., *et al.*, *Appl. Phys. A* **2002**, *75* (2), 301-308.
15. Feringa, B. L.; Jager, W. F.; de Lange, B., *Tetrahedron* **1993**, *49* (37), 8267-8310.
16. Tian, H.; Yang, S., *Chem. Soc. Rev.* **2004**, *33* (2), 85-97.
17. Taylor, A. I.; Beuron, F.; Peak - Chew, S. Y., *et al.*, *ChemBioChem* **2016**, *17* (12), 1107-1110.
18. Rajagopal, K.; Schneider, J. P., *Curr. Opin. Struct. Biol.* **2004**, *14* (4), 480-486.
19. <https://bodytomy.com/structure-of-hemoglobin/>; <http://www.ks.uiuc.edu/Research/folding/>;
<https://www3.nd.edu/~aseriann/entrop.html>.
20. Lehn, J.-M., Definition and Development of Supramolecular Chemistry. In *Supramolecular chemistry*, Steed, J. W.; Atwood, J. L., Eds. John Wiley & Sons: 2009; pp 1-4.
21. Kyba, E. P.; Helgeson, R. C.; Madan, K., *et al.*, *J. Am. Chem. Soc.* **1977**, *99* (8), 2564-2571.
22. Xu, Y.; Zhang, H.; Li, F., *et al.*, *J. Mater. Chem.* **2012**, *22* (4), 1592-1597.
23. Goshe, A. J.; Steele, I. M.; Ceccarelli, C., *et al.*, *Proc. Natl. Acad. Sci.* **2002**, *99* (8), 4823-4829.
24. Hartlieb, K. J.; Witus, L. S.; Ferris, D. P., *et al.*, *ACS Nano* **2015**, *9* (2), 1461-1470.
25. Witus, L. S.; Hartlieb, K. J.; Wang, Y., *et al.*, *Org. Biomol. Chem.* **2014**, *12* (32), 6089-6093.
26. Thordarson, P., *Chem. Soc. Rev.* **2011**, *40* (3), 1305-1323.
27. El-Khouly, M. E.; Ito, O.; Smith, P. M., *et al.*, *J. Photochem. Photobiol., C: Photochem. Rev.* **2004**, *5* (1), 79-104.
28. Ros, T. D.; Prato, M.; Guldi, D. M., *et al.*, *Chem. Eur. J.* **2001**, *7* (4), 816-827.
29. Diederich, F.; Gomez-Lopez, M., *Chem. Soc. Rev.* **1999**, *28* (5), 263-277.
30. D'Souza, F.; Deviprasad, G. R.; El-Khouly, M. E., *et al.*, *J. Am. Chem. Soc.* **2001**, *123* (22), 5277-5284.
31. D'Souza, F.; Chitta, R.; Gadde, S., *et al.*, *Chem. Commun.* **2005**, (10), 1279-1281.
32. Sandanayaka, A. S. D.; Ikeshita, K.-i.; Araki, Y., *et al.*, *J. Mater. Chem.* **2005**, *15* (23), 2276-2287.

33. D'Souza, F.; Chitta, R.; Gadde, S., *et al.*, *Chem. Eur. J.* **2005**, *11* (15), 4416-4428.
34. Del Sole, R.; De Luca, A.; Mele, G., *et al.*, *J. Porphyrins Phthalocyanines* **2005**, *09* (07), 519-527.
35. Maiya, B. G., *J. Porphyrins Phthalocyanines* **2004**, *08* (09), 1118-1128.
36. Sandanayaka, A. S. D.; Araki, Y.; Ito, O., *et al.*, *Chem. Commun.* **2006**, (41), 4327-4329.
37. Kamm, J. M.; Iverson, C. P.; Lau, W.-Y., *et al.*, *Langmuir* **2016**, *32* (2), 487-495.
38. Follana-Berna, J.; Seetharaman, S.; Martin-Gomis, L., *et al.*, *Phys. Chem. Chem. Phys.* **2018**, *20* (11), 7798-7807.
39. D'Souza, F.; Rath, N. P.; Deviprasad, G. R., *et al.*, *Chem. Commun.* **2001**, (3), 267-268.
40. Alvaro, M.; Atienzar, P.; de la Cruz, P., *et al.*, *J. Am. Chem. Soc.* **2006**, *128* (20), 6626-6635.
41. Lin, C.-I.; Fang, M.-Y.; Cheng, S.-H., *J. Electroanal. Chem.* **2002**, *531* (2), 155-162.
42. Khade, R. L.; Zhang, Y., *J. Am. Chem. Soc.* **2015**, *137* (24), 7560-7563.
43. Patra, R.; Chaudhary, A.; Ghosh, S. K., *et al.*, *Inorg. Chem.* **2010**, *49* (5), 2057-2067.
44. Wondimagegn, T.; Rauk, A., *J. Phys. Chem. B* **2012**, *116* (34), 10301-10310.
45. D'Souza, F.; Smith, P. M.; Zandler, M. E., *et al.*, *J. Am. Chem. Soc.* **2004**, *126* (25), 7898-7907.
46. Abdul Karim, A.; Loh, X. J., *Soft matter* **2015**, *11* (27), 5425-5434.
47. Szejtli, J., *Chemical Reviews* **1998**, *98* (5), 1743-1754.
48. Harada, A.; Takashima, Y.; Nakahata, M., *Acc. Chem. Res.* **2014**, *47* (7), 2128-2140.
49. van de Manakker, F.; Vermonden, T.; el Morabit, N., *et al.*, *Langmuir* **2008**, *24* (21), 12559-12567.
50. Nakahata, M.; Takashima, Y.; Yamaguchi, H., *et al.*, *Nat. Commun.* **2011**, *2*, 511.
51. Charlot, A.; Auzély-Velty, R., *Macromolecules* **2007**, *40* (26), 9555-9563.
52. Kretschmann, O.; Choi, S. W.; Miyauchi, M., *et al.*, *Angew. Chem. Int. Ed.* **2006**, *45* (26), 4361-4365.
53. Zhang, Z. X.; Liu, K. L.; Li, J., *Angew. Chem. Int. Ed.* **2013**, *52* (24), 6180-6184.
54. Hu, Q.-D.; Tang, G.-P.; Chu, P. K., *Acc. Chem. Res.* **2014**, *47* (7), 2017-2025.
55. Yorozu, T.; Hoshino, M.; Imamura, M., *J. Phys. Chem.* **1982**, *86* (22), 4426-4429.
56. Herkstroeter, W. G.; Martic, P. A.; Evans, T. R., *et al.*, *J. Am. Chem. Soc.* **1986**, *108* (12), 3275-3280.
57. Chen, B.; Liu, K. L.; Zhang, Z., *et al.*, *Chem. Commun.* **2012**, *48* (45), 5638-5640.
58. Wang, Q.; Yang, C.; Ke, C., *et al.*, *Chem. Commun.* **2011**, *47* (24), 6849-6851.
59. Freeman, W. A.; Mock, W. L.; Shih, N. Y., *J. Am. Chem. Soc.* **1981**, *103* (24), 7367-7368.
60. Houk, K. N.; Leach Andrew, G.; Kim Susanna, P., *et al.*, *Angew. Chem. Int. Ed.* **2003**, *42* (40), 4872-4897.
61. Lagona, J.; Mukhopadhyay, P.; Chakrabarti, S., *et al.*, *Angew. Chem. Int. Ed.* **2005**, *44* (31), 4844-4870.
62. Kim, J.; Jung, I.-S.; Kim, S.-Y., *et al.*, *J. Am. Chem. Soc.* **2000**, *122* (3), 540-541.
63. Mu, T. W.; Liu, L.; Zhang, K. C., *et al.*, *Chin. Chem. Lett.* **2001**, *12* (9), 783-786.
64. Carvalho, C. P.; Domínguez, Z.; Da Silva, J. P., *et al.*, *Chem. Commun.* **2015**, *51* (13), 2698-2701.
65. Zhang, Q.; Qu, D.-H.; Ma, X., *et al.*, *Chem. Commun.* **2013**, *49* (84), 9800-9802.
66. Biedermann, F.; Ross, I.; Scherman, O. A., *Polym. Chem.* **2014**, *5* (18), 5375-5382.
67. Yang, C.; Mori, T.; Origane, Y., *et al.*, *J. Am. Chem. Soc.* **2008**, *130* (27), 8574-8575.
68. Appel, E. A.; Biedermann, F.; Rauwald, U., *et al.*, *J. Am. Chem. Soc.* **2010**, *132* (40), 14251-14260.

69. Assaf, K. I.; Nau, W. M., *Chem. Soc. Rev.* **2015**, 44 (2), 394-418.
70. Lee, J. W.; Samal, S.; Selvapalam, N., *et al.*, *Acc. Chem. Res.* **2003**, 36 (8), 621-630.
71. Yokoe, M.; Yamauchi, K.; Long, T. E., *J. Polym. Sci., Part A: Polym. Chem.* **2016**, 54 (15), 2302-2311.
72. Zheng, Y.; Micic, M.; Mello, S. V., *et al.*, *Macromolecules* **2002**, 35 (13), 5228-5234.
73. Chujo, Y.; Sada, K.; Nomura, R., *et al.*, *Macromolecules* **1993**, 26 (21), 5611-5614.
74. Tamaki, T.; Kokubu, T., *J. Inclusion Phenom.* **1984**, 2 (3-4), 815-822.
75. Zhang, X.; Gao, Y.; Lin, Y., *et al.*, *Polym. Chem.* **2015**, 6 (22), 4162-4166.
76. Ji, Z.; Li, Y.; Ding, Y., *et al.*, *Polym. Chem.* **2015**, 6 (38), 6880-6884.
77. Odell, B.; Reddington, M. V.; Slawin, A. M. Z., *et al.*, *Angew. Chem. Int. Ed. Engl.* **1988**, 27 (11), 1547-1550.
78. Nielsen, M. B.; Li, Z.-T.; Becher, J., *J. Mater. Chem.* **1997**, 7 (7), 1175-1187.
79. Belal, K.; Stoffelbach, F.; Lyskawa, J., *et al.*, *Angew. Chem.* **2016**, 128 (45), 14180-14184.
80. Bigot, J.; Bria, M.; Caldwell, S. T., *et al.*, *Chem. Commun.* **2009**, (35), 5266-5268.
81. Bigot, J.; Charleux, B.; Cooke, G., *et al.*, *Macromolecules* **2010**, 43 (1), 82-90.
82. Sambe, L.; Stoffelbach, F.; Poltorak, K., *et al.*, *Macromol. Rapid Commun.* **2014**, 35 (4), 498-504.
83. Sambe, L.; Belal, K.; Stoffelbach, F., *et al.*, *Polym. Chem.* **2014**, 5 (3), 1031-1036.
84. Wang, Y.; Sun, J.; Liu, Z., *et al.*, *Chem. Sci.* **2017**, 8 (4), 2562-2568.
85. Gibbs-Hall, I. C.; Vermeulen, N. A.; Dale, E. J., *et al.*, *J. Am. Chem. Soc.* **2015**, 137 (50), 15640-15643.
86. Fahrenbach, A. C.; Zhu, Z.; Cao, D., *et al.*, *J. Am. Chem. Soc.* **2012**, 134 (39), 16275-16288.
87. Rolf, M., *Angew. Chem. Int. Ed.* **2004**, 43 (9), 1054-1063.
88. Roovers, J., *Star and Hyperbranched Polymers*, Marcel Dekker Inc.: 1998; p P285.
89. Pitsikalis, M.; Pispas, S.; Mays, J., *et al.*, Nonlinear Block Copolymer Architectures. In *Blockcopolymers - Polyelectrolytes - Biodegradation*, Bellon-Maurel, V.; Calmon-Decriaud, A.; Chandrasekhar, V.; Hadjichristidis, N.; Mays, J. W.; Pispas, S.; Pitsikalis, M.; Silvestre, F., Eds. Springer Berlin Heidelberg: 1998; Vol. 135, pp 1-137.
90. Schaeffgen, J. R.; Flory, P. J., *J. Am. Chem. Soc.* **1948**, 70 (8), 2709-2718.
91. Hadjichristidis, N.; Pitsikalis, M.; Iatrou, H., *et al.*, 6.03 - Polymers with Star-Related Structures: Synthesis, Properties, and Applications A2 - Matyjaszewski, Krzysztof. In *Polymer Science: A Comprehensive Reference*, Möller, M., Ed. Elsevier: Amsterdam, 2012; pp 29-111.
92. Higashihara, T.; Hayashi, M.; Hirao, A., *Prog. Polym. Sci.* **2011**, 36 (3), 323-375.
93. Altintas, O.; Vogt, A. P.; Barner-Kowollik, C., *et al.*, *Polym. Chem.* **2012**, 3 (1), 34-45.
94. Gao, H.; Matyjaszewski, K., *Prog. Polym. Sci.* **2009**, 34 (4), 317-350.
95. Brunsveld, L.; Folmer, B. J. B.; Meijer, E. W., *et al.*, *Chem. Rev.* **2001**, 101 (12), 4071-4098.
96. De Greef, T. F. A.; Smulders, M. M. J.; Wolfs, M., *et al.*, *Chem. Rev.* **2009**, 109 (11), 5687-5754.
97. Yang, L.; Tan, X.; Wang, Z., *et al.*, *Chem. Rev.* **2015**, 115 (15), 7196-7239.
98. Hager, M. D.; Bode, S.; Weber, C., *et al.*, *Prog. Polym. Sci.* **2015**, 49-50, 3-33.
99. Jean - Marie, L., *Polym. Int.* **2002**, 51 (10), 825-839.
100. Aida, T.; Meijer, E. W.; Stupp, S. I., *Science* **2012**, 335 (6070), 813-817.
101. Yan, X.; Wang, F.; Zheng, B., *et al.*, *Chem. Soc. Rev.* **2012**, 41 (18), 6042-6065.

102. Whittell, G. R.; Hager, M. D.; Schubert, U. S., *et al.*, *Nat. Mater.* **2011**, *10*, 176.
103. Zimmerman, S. C.; Zeng, F.; Reichert, D. E. C., *et al.*, *Science* **1996**, *271* (5252), 1095-1098.
104. Todd, E. M.; Zimmerman, S. C., *J. Am. Chem. Soc.* **2007**, *129* (47), 14534-14535.
105. Todd, E. M.; Zimmerman, S. C., *Tetrahedron* **2008**, *64* (36), 8558-8570.
106. Altintas, O.; Tunca, U.; Barner-Kowollik, C., *Polym. Chem.* **2011**, *2* (5), 1146-1155.
107. Altintas, O.; Schulze-Suenninghausen, D.; Luy, B., *et al.*, *Eur. Polym. J* **2015**, *62* (0), 409-417.
108. Bernard, J.; Lortie, F.; Fenet, B., *Macromol. Rapid Commun.* **2009**, *30* (2), 83-88.
109. Chen, S.; Bertrand, A.; Chang, X., *et al.*, *Macromolecules* **2010**, *43* (14), 5981-5988.
110. Zhang, Z.-X.; Liu, X.; Xu, F. J., *et al.*, *Macromolecules* **2008**, *41* (16), 5967-5970.
111. Zhang, Z.-X.; Liu, K. L.; Li, J., *Macromolecules* **2011**, *44* (5), 1182-1193.
112. Yuting, W.; Zhongxing, Z.; Jun, L., *Adv. Funct. Mater.* **2014**, *24* (25), 3874-3884.
113. Wang, J.; Wang, X.; Yang, F., *et al.*, *Langmuir* **2014**, *30* (43), 13014-13020.
114. Schmidt, B. V. K. J.; Hetzer, M.; Ritter, H., *et al.*, *Polym. Chem.* **2012**, *3* (11), 3064-3067.
115. Schmidt, B. V. K. J.; Barner-Kowollik, C., *Polym. Chem.* **2014**, *5* (7), 2461-2472.
116. Schmidt, B. V. K. J.; Rudolph, T.; Hetzer, M., *et al.*, *Polym. Chem.* **2012**, *3* (11), 3139-3145.
117. Fleischmann, C.; Wöhlk, H.; Ritter, H., *Beilstein J. Org. Chem.* **2014**, *10*, 2263-2269.
118. Wei, K.; Li, J.; Chen, G., *et al.*, *ACS Macro Lett.* **2013**, *2* (3), 278-283.
119. Huang, F.; Nagvekar, D. S.; Slebodnick, C., *et al.*, *J. Am. Chem. Soc.* **2005**, *127* (2), 484-485.
120. W., G. H.; Aurica, F.; W., J. J., *et al.*, *J. Polym. Sci., Part A: Polym. Chem.* **2009**, *47* (14), 3518-3543.
121. W., G. H.; Zhongxin, G.; W., J. J., *et al.*, *J. Polym. Sci., Part A: Polym. Chem.* **2009**, *47* (23), 6472-6495.
122. Lee, M.; Schoonover, D. V.; Gies, A. P., *et al.*, *Macromolecules* **2009**, *42* (17), 6483-6494.
123. Emma - Rose, J.; Urs, R.; Jesús, d. B., *et al.*, *Macromol. Rapid Commun.* **2013**, *34* (19), 1547-1553.
124. Naka, K.; Yaguchi, M.; Chujo, Y., *Chem. Mater.* **1999**, *11* (4), 849-851.
125. Chujo, Y.; Naka, A.; Krämer, M., *et al.*, *J. Macromol. Sci., Part A* **1995**, *32* (6), 1213-1223.
126. Konishi, G.-i.; Chujo, Y., *Polym. Bull.* **1999**, *43* (1), 9-12.
127. Lamba, J. J. S.; Fraser, C. L., *J. Am. Chem. Soc.* **1997**, *119* (7), 1801-1802.
128. McAlvin, J. E.; Fraser, C. L., *Macromolecules* **1999**, *32* (21), 6925-6932.
129. McAlvin, J. E.; Scott, S. B.; Fraser, C. L., *Macromolecules* **2000**, *33* (19), 6953-6964.
130. Georg, H.; Oskar, N.; S., S. U., *Macromol. Rapid Commun.* **1998**, *19* (6), 309-313.
131. Corbin, P. S.; Webb, M. P.; McAlvin, J. E., *et al.*, *Biomacromolecules* **2001**, *2* (1), 223-232.
132. Guangchang, Z.; Jibao, H.; I., H. I., *J. Polym. Sci., Part A: Polym. Chem.* **2007**, *45* (18), 4225-4239.
133. Schubert, U. S.; Eschbaumer, C.; Nuyken, O., *et al.*, *J. Inclusion Phenom. Macrocycl. Chem.* **1999**, *35* (1), 23-34.
134. Hoogenboom, R.; Kickelbick, G.; Schubert, U. S., *Eur. J. Org. Chem.* **2003**, *2003* (24), 4887-4896.
135. Hoogenboom, R.; Wouters, D.; Schubert, U. S., *Macromolecules* **2003**, *36* (13), 4743-4749.
136. Rosiak, J. M.; Yoshii, F., *Nucl. Instrum. Methods Phys. Res. Sect. B* **1999**, *151* (1), 56-64.
137. Khan, A.; Othman, M. B. H.; Razak, K. A., *et al.*, *J. Polym. Res.* **2013**, *20* (10), 273.

138. Ullah, F.; Othman, M. B. H.; Javed, F., *et al.*, *Mater. Sci. Eng., C* **2015**, *57*, 414-433.
139. Ahmed, E. M., *J. Adv. Res.* **2015**, *6* (2), 105-121.
140. Mann, J. L.; Anthony, C. Y.; Agmon, G., *et al.*, *Biomater. Sci.* **2018**, *6* (1), 10-37.
141. Webber, M. J.; Appel, E. A.; Meijer, E. W., *et al.*, *Nat. Mater.* **2015**, *15*, 13.
142. Appel, E. A.; del Barrio, J.; Loh, X. J., *et al.*, *Chem. Soc. Rev.* **2012**, *41* (18), 6195-6214.
143. Voorhaar, L.; Hoogenboom, R., *Chem. Soc. Rev.* **2016**, *45* (14), 4013-4031.
144. Zu, Y.; Zhang, Y.; Zhao, X., *et al.*, *Int. J. Biol. Macromol.* **2012**, *50* (1), 82-87.
145. Hovgaard, L.; Brøndsted, H., *J. Controlled Release* **1995**, *36* (1), 159-166.
146. Gehrke, S. H.; Uhden, L. H.; McBride, J. F., *J. Controlled Release* **1998**, *55* (1), 21-33.
147. Coviello, T.; Grassi, M.; Rambone, G., *et al.*, *J. Controlled Release* **1999**, *60* (2), 367-378.
148. Abd Alla, S. G.; Sen, M.; El-Naggar, A. W. M., *Carbohydr. Polym.* **2012**, *89* (2), 478-485.
149. Mohd Amin, M. C. I.; Ahmad, N.; Halib, N., *et al.*, *Carbohydr. Polym.* **2012**, *88* (2), 465-473.
150. Sedlacek, O.; Kucka, J.; Monnery, B. D., *et al.*, *Polym. Degrad. Stab.* **2017**, *137*, 1-10.
151. Miyamae, K.; Nakahata, M.; Takashima, Y., *et al.*, *Angew. Chem. Int. Ed.* **2015**, *54* (31), 8984-8987.
152. Kakuta, T.; Takashima, Y.; Harada, A., *Macromolecules* **2013**, *46* (11), 4575-4579.
153. Takashima, Y.; Sawa, Y.; Iwaso, K., *et al.*, *Macromolecules* **2017**, *50* (8), 3254-3261.
154. Rodell, C. B.; Kaminski, A. L.; Burdick, J. A., *Biomacromolecules* **2013**, *14* (11), 4125-4134.
155. Rodell, C. B.; Wade, R. J.; Purcell, B. P., *et al.*, *ACS Biomater. Sci. Eng.* **2015**, *1* (4), 277-286.
156. Tamesue, S.; Takashima, Y.; Yamaguchi, H., *et al.*, *Angew. Chem. Int. Ed.* **2010**, *49* (41), 7461-7464.
157. Rodell, C. B.; Highley, C. B.; Chen, M. H., *et al.*, *Soft matter* **2016**, *12* (37), 7839-7847.
158. Guan, Y.; Zhao, H.-B.; Yu, L.-X., *et al.*, *RSC Adv.* **2014**, *4* (10), 4955-4959.
159. Rowland, M. J.; Appel, E. A.; Coulston, R. J., *et al.*, *J. Mater. Chem. B* **2013**, *1* (23), 2904-2910.
160. Li, C.; Rowland, M. J.; Shao, Y., *et al.*, *Adv. Mater.* **2015**, *27* (21), 3298-3304.
161. Appel, E. A.; Forster, R. A.; Rowland, M. J., *et al.*, *Biomaterials* **2014**, *35* (37), 9897-9903.
162. Appel, E. A.; Forster, R. A.; Koutsoubas, A., *et al.*, *Angew. Chem. Int. Ed.* **2014**, *53* (38), 10038-10043.
163. Appel, E. A.; Biedermann, F.; Rauwald, U., *et al.*, *J. Am. Chem. Soc.* **2010**, *132* (40), 14251-14260.
164. Appel, E. A.; Loh, X. J.; Jones, S. T., *et al.*, *J. Am. Chem. Soc.* **2012**, *134* (28), 11767-11773.
165. Cui, J.; Campo, A. d., *Chem. Commun.* **2012**, *48* (74), 9302-9304.
166. Dankers, P. Y. W.; Hermans, T. M.; Baughman, T. W., *et al.*, *Adv. Mater.* **2012**, *24* (20), 2703-2709.
167. Chirila, T. V.; Lee, H. H.; Odon, M., *et al.*, *J. Appl. Polym. Sci.* **2014**, *131* (4).
168. Lemmers, M.; Sprakel, J.; Voets, I. K., *et al.*, *Angew. Chem. Int. Ed.* **2010**, *49* (4), 708-711.
169. Hunt, J. N.; Feldman, K. E.; Lynd, N. A., *et al.*, *Adv. Mater.* **2011**, *23* (20), 2327-2331.
170. Krogstad, D. V.; Lynd, N. A.; Choi, S.-H., *et al.*, *Macromolecules* **2013**, *46* (4), 1512-1518.
171. Nguyen, T. D.; Liu, Y.; Saha, S., *et al.*, *J. Am. Chem. Soc.* **2007**, *129* (3), 626-634.
172. Saha, S.; Stoddart, J. F., Molecular Motors and Muscles. In *Functional Organic Materials: Syntheses, Strategies and Applications*, 2007; pp 293-327.
173. Anelli, P. L.; Spencer, N.; Stoddart, J. F., *J. Am. Chem. Soc.* **1991**, *113* (13), 5131-5133.

174. Hartlieb, K. J.; Liu, W. G.; Fahrenbach, A. C., *et al.*, *Chem. Eur. J.* **2016**, *22* (8), 2736-2745.
175. Dichtel, W. R.; Miljanić, O. Š.; Spruell, J. M., *et al.*, *J. Am. Chem. Soc.* **2006**, *128* (32), 10388-10390.
176. Bruns, C. J.; Liu, H.; Francis, M. B., *J. Am. Chem. Soc.* **2016**, *138* (47), 15307-15310.
177. Li, H.; Zhu, Z.; Fahrenbach, A. C., *et al.*, *J. Am. Chem. Soc.* **2012**, *135* (1), 456-467.
178. Li, H.-G.; Wang, G.-W., *J. Org. Chem.* **2017**, *82* (12), 6341-6348.
179. Jacquot de Rouville, H.-P.; lehl, J.; Bruns, C. J., *et al.*, *Org. Lett.* **2012**, *14* (20), 5188-5191.
180. WEBSTER, O. W., *Science* **1991**, *251* (4996), 887-893.
181. Hsieh, H.; Quirk, R. P., *Anionic polymerization: principles and practical applications*, CRC Press: 1996.
182. Moad, G.; Rizzardo, E.; Thang, S. H., *Acc. Chem. Res.* **2008**, *41* (9), 1133-1142.
183. Szwarc, M.; Van Beylen, M., *Ionic polymerization and living polymers*, Springer Science & Business Media: 2012.
184. Matyjaszewski, K.; Xia, J., *Chem. Rev.* **2001**, *101* (9), 2921-2990.
185. Braunecker, W. A.; Matyjaszewski, K., *Prog. Polym. Sci.* **2007**, *32* (1), 93-146.
186. Ouchi, M.; Terashima, T.; Sawamoto, M., *Chem. Rev.* **2009**, *109* (11), 4963-5050.
187. Solomon, D.; Rizzardo, E.; Cacioli, P. In *US Patent 4,581,429, 1985*, Chem. Abstr, 1985; p 221335q.
188. Hawker, C. J.; Bosman, A. W.; Harth, E., *Chem. Rev.* **2001**, *101* (12), 3661-3688.
189. Grubbs, R. B., *Polym. Rev.* **2011**, *51* (2), 104-137.
190. Chiefari, J.; Chong, Y.; Ercole, F., *et al.*, *Macromolecules* **1998**, *31* (16), 5559-5562.
191. D'Agosto, F., *Handbook of RAFT polymerization*. Wiley Online Library: 2008.
192. Barner - Kowollik, C.; Perrier, S., *J. Polym. Sci., Part A: Polym. Chem.* **2008**, *46* (17), 5715-5723.
193. Moad, G.; Rizzardo, E.; Thang, S. H., *Polymer* **2008**, *49* (5), 1079-1131.
194. Moad, G.; Rizzardo, E.; Thang, S. H., *Aust. J. Chem.* **2009**, *62* (11), 1402-1472.
195. Odian, G., *Principles of polymerization*, John Wiley & Sons: 2004.
196. McLeary, J.; Calitz, F.; McKenzie, J., *et al.*, *Macromolecules* **2005**, *38* (8), 3151-3161.
197. Semsarilar, M.; Perrier, S., *Nat. Chem.* **2010**, *2*, 811.

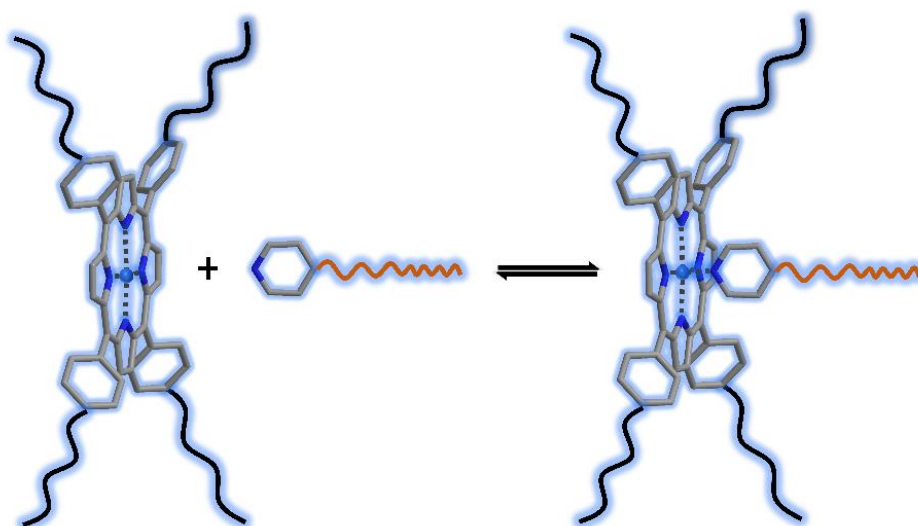
Chapter 2 A Supramolecular Miktoarm Star Polymer Based on Porphyrin Metal Complexation in water

This chapter was published as:

Z. Hou, W. Dehaen, J. Lyskawa, P. Woisel, R. Hoogenboom, A supramolecular miktoarm star polymer based on porphyrin metal complexation in water, *Chem. Commun.*, 2017,53, 8423-8426.

The 5, 10, 15, 20-tetra(4-acetylphenyl)porphyrin was provided by Prof. Wim Dehaen and the ITC measurements were performed by Joel Lyskawa.

Abstract: A novel supramolecular miktoarm star polymer was successfully constructed in water from a pyridine end-functionalized poly(methoxy diethylene glycol acrylate) (Py-PmDEGA) and a metalloporphyrin based four-arm star poly(ethylene glycol) methyl ether (ZnTPP-(PEGME)₄) *via* metal-ligand coordination. The Py-PmDEGA moiety was prepared *via* a combination of reversible addition-fragmentation chain transfer polymerization (RAFT) and subsequent aminolysis and Michael addition reaction to introduce the pyridine end-group. The ZnTPP(PEGME)₄ star-polymer was synthesized by reaction between tetrakis (*p*-hydroxyphenyl)porphyrin and toluenesulfonyl poly(ethylene glycol) methyl ethers (PEGME-TOS), and followed by insertion of a zinc ion into the porphyrin core. The formation of a well-defined supramolecular AB₄-type miktoarm star polymer was unambiguously demonstrated *via* UV-Vis spectroscopic titration, isothermal titration calorimetry (ITC) and diffusion ordered NMR spectroscopy (DOSY).



2.1 Introduction

Polymer properties are mainly influenced by the chemical composition and topology of the constituting macromolecules. A broad range of applications have been proposed for different polymer architectures, *e.g.* stabilization of polymer blends with block copolymers,¹ drug delivery *via* amphiphilic block copolymers² or drug-delivery with star polymers.³ Therefore, the design of complex macromolecular architectures represents an important field in modern polymer chemistry and provides the opportunity to generate a broad range of materials with tunable properties.⁴⁻⁶ Star polymers are an important class of polymers that have attracted significant attention in the last few years.⁷⁻⁹ They are typically synthesized *via* one of three common methodologies, *i.e.* core-first, arm-first and coupling-onto.¹⁰ Various combinations of these three approaches can be employed to make even more complex miktoarm star block copolymers, unavoidably involving a significant number of synthetic steps. Miktoarm star polymers, also called asymmetric or mixed-arm star polymer, have polymer arms that vary in chemical structure and/or molecular weight. They exhibit unique and unusual phase separation behavior in bulk and selected solvents, which tremendously increased the variety of morphological structures. Thus, miktoarm star polymers are promising materials with many potential applications in fields of nanoscience and nanotechnology such as electronic and optical nanodevices, nanomaterials for lithography, nanoreactors carrying metal catalysts and enzymes, nanoscale microfilters and complex self-assembly.¹¹⁻¹⁷

The advent of supramolecular chemistry, which utilizes noncovalent, reversible bonds for the assembly of materials, has had a tremendous influence on the synthesis and applications of macromolecular architectures.¹⁸ It has introduced the possibility of using noncovalent interactions for the creation of polymers, featuring a degree of flexibility, tunability and dynamics that was impossible using covalent chemistry.¹⁹⁻²⁰ Hence, supramolecular polymers have received growing interest in recent years due to their unique dynamic properties making them applicable to a broad range of fields in chemistry, biology and physics.^{18, 21} To date, various supramolecular polymers with different architectures, such as linear,²²⁻²⁴ branched, star-shaped,²⁵⁻²⁹ and dendronized,³⁰ have been prepared based on hydrogen bonding,^{24, 27-28, 30} π - π interactions,³¹⁻³² metal-ligand binding,^{29, 33-38} and host-guest interactions.²⁵⁻²⁶ Among the non-covalent interactions, metal-ligand coordination is particularly interesting for the synthesis of supramolecular polymers. Indeed, in addition of being highly directional, metal-ligand coordination can be prepared from a wide range of easily functionalized ligands and metal ions, thereby allowing a large panoply of tunable metal-ligand complexes to be prepared both in organic and aqueous media.²² Moreover, the presence of a metal complex in the polymer structure can impart further properties of interest including electrochemical, photophysical, catalytic and magnetic properties.

Porphyrins and their metal derivatives have attracted interest of chemists and biologists due to their importance and applications in biological fields. In particular, they represent a key-component of haemoglobin as well as for the inhibition of protease-resistant prion protein formation or for thermotherapy due to their strong affinity towards cancer cells.³⁹⁻⁴⁰ Also, owing to their ability of

forming π - π interactions or metal-ligand coordination, they constitute an important class of supramolecular building blocks,⁴¹⁻⁴² which has been widely employed in supramolecular chemistry.⁴³ However, to the best of our knowledge, there has been no report on the use of metalloporphyrin for the construction of supramolecular block copolymers, star polymers or other even more complex polymer structures based on this interaction.

In this chapter, we present a straightforward strategy allowing the formation of an AB₄-type miktoarm star polymer in water, governed by the complexation of a pyridine unit and a metalloporphyrin moiety, based on a zinc-porphyrin based star poly(ethylene glycol) methyl ether ((ZnTPP(PEGME)₄) and a pyridine end-functionalized poly(methoxy diethylene glycol acrylate) (Py-PmDEGA) (Figure 2.1). These two building blocks were synthesized and characterized by proton nuclear magnetic resonance (¹H NMR) spectroscopy, size exclusion chromatography (SEC) and MALDI-TOF mass spectrometry. Finally, in aqueous solution, the effective formation of the supramolecular star polymer was proven *via* diffusion ordered NMR spectroscopy (DOSY), isothermal titration calorimetry (ITC) and UV-Visible spectroscopy (UV-Vis).

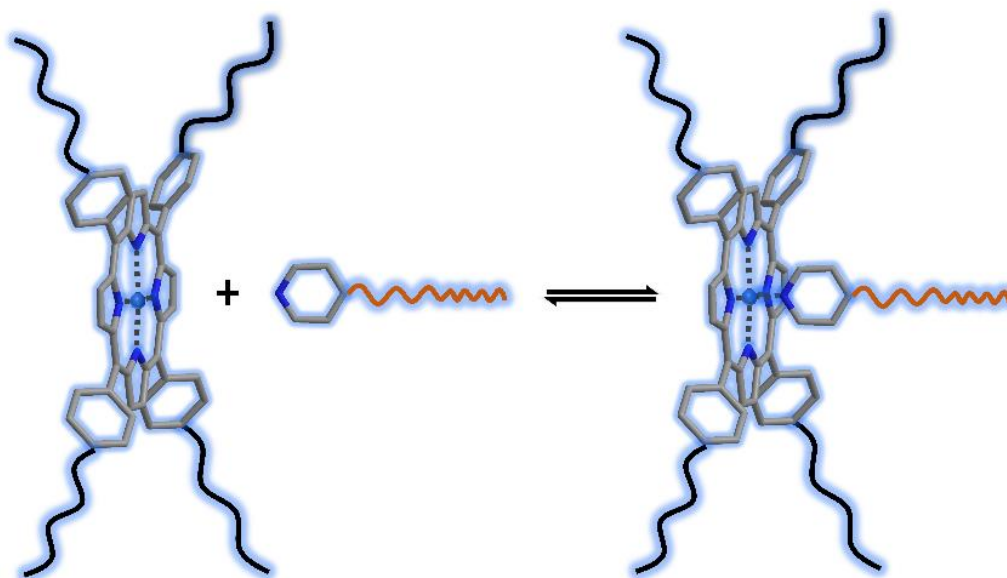
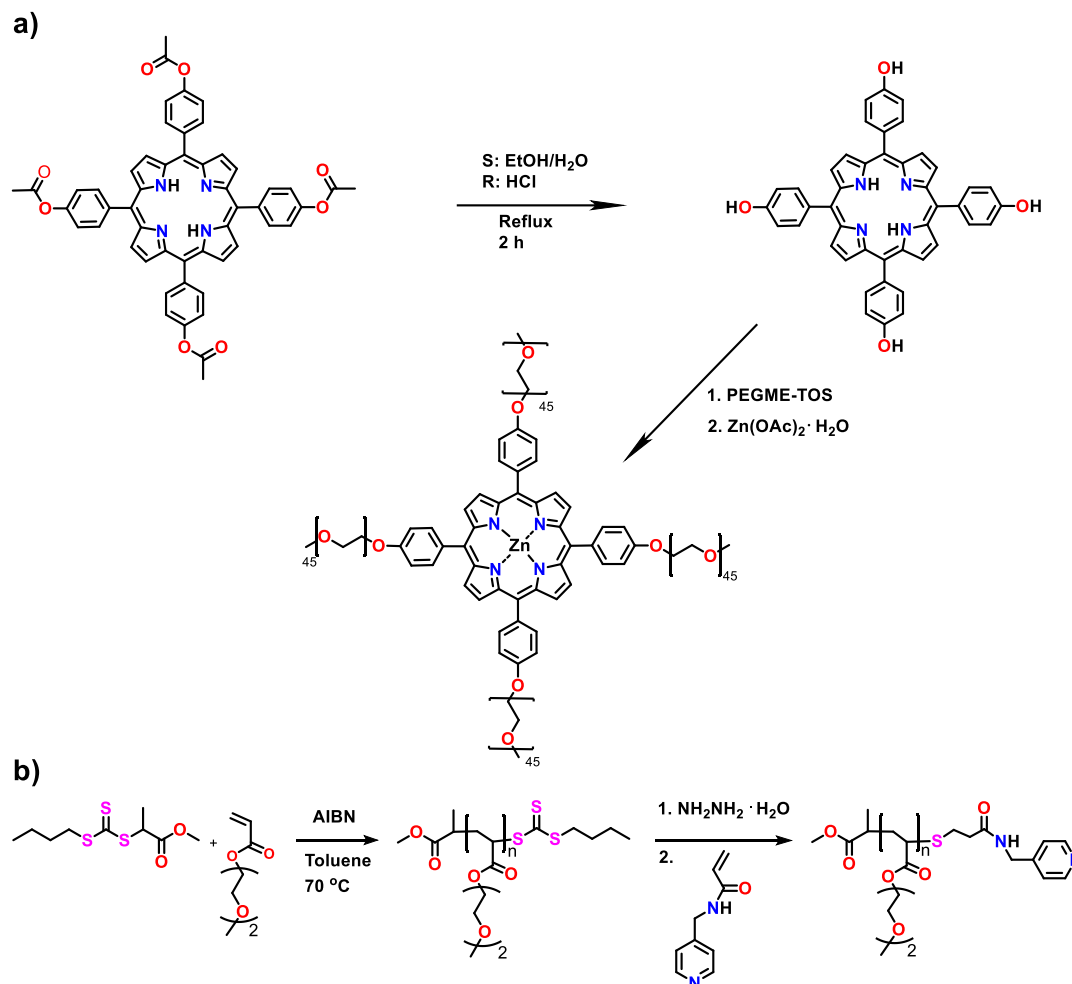


Figure 2.1 Graphical representation of the formation of a supramolecular miktoarm star polymer in water by complexation of a zinc-porphyrin with four PEGME chains and a pyridine end-functionalized poly(methoxydiethylene glycol acrylate). (Gray framework with blue bend line: porphyrin and pyridine; Light blue sphere: zinc ion; black curve: PEGME chain; Orange curve: PmDEGA chain)

2.2 Results and discussion

The molecular design of the supramolecular miktoarm star-block copolymer is based on the metal-ligand interaction between a zinc-porphyrin and pyridine, as they can form noncovalent interactions with high association constants up to 10^5 M^{-1} in water.⁴⁴ The synthetic strategy towards these two building blocks is illustrated in Scheme 2.1.



Scheme 2.1 Synthetic routes of building blocks: (a) star polymer with zinc-porphyrin (ZnTPP(PEGME)₄); (b) pyridine end-functionalized PmDEGA (Py-PmDEGA).

The coupling of four poly(ethylene glycol) methyl ether (PEGME) ($M_n = 2000$ Da) chains to the porphyrin core was performed by the reaction between tetrakis(*p*-hydroxyphenyl) porphyrin and *p*-toluenesulfonyl-poly(ethylene glycol) methyl ethers followed by the subsequent insertion of the zinc(II) ion into the porphyrin core (Scheme 2.1a). The metal-free porphyrin star polymer was purified *via* precipitation into a mixture of diethyl ether and dichloromethane followed by column chromatography and then analyzed *via* ^1H NMR spectroscopy, SEC and MALDI-TOF MS. The ^1H NMR spectrum of the metal-free porphyrin star polymer indicated that all four PEGME chains were successfully attached based on the integration ratio of the peaks from the porphyrin (8.78, 8.05 and -2.83 ppm) and the PEGME (4.37 and 3.99 ppm) (Figure 2.2). In addition, the star polymer was analyzed by SEC and MALDI-TOF MS (Figure 2.3 and 2.4), confirming the formation of a four-arm star polymer architecture. The molecular weight (31 kDa) measured by SEC was calculated against poly(methyl methacrylate) (PMMA) standards leading to a significant overestimation while the molecular weight from MALDI-TOF MS measurement is more accurate. Furthermore, the MALDI-TOF MS spectrum revealed two distributions, both corresponding to the four-arm star polymer ionized with a sodium or a potassium ion, respectively.

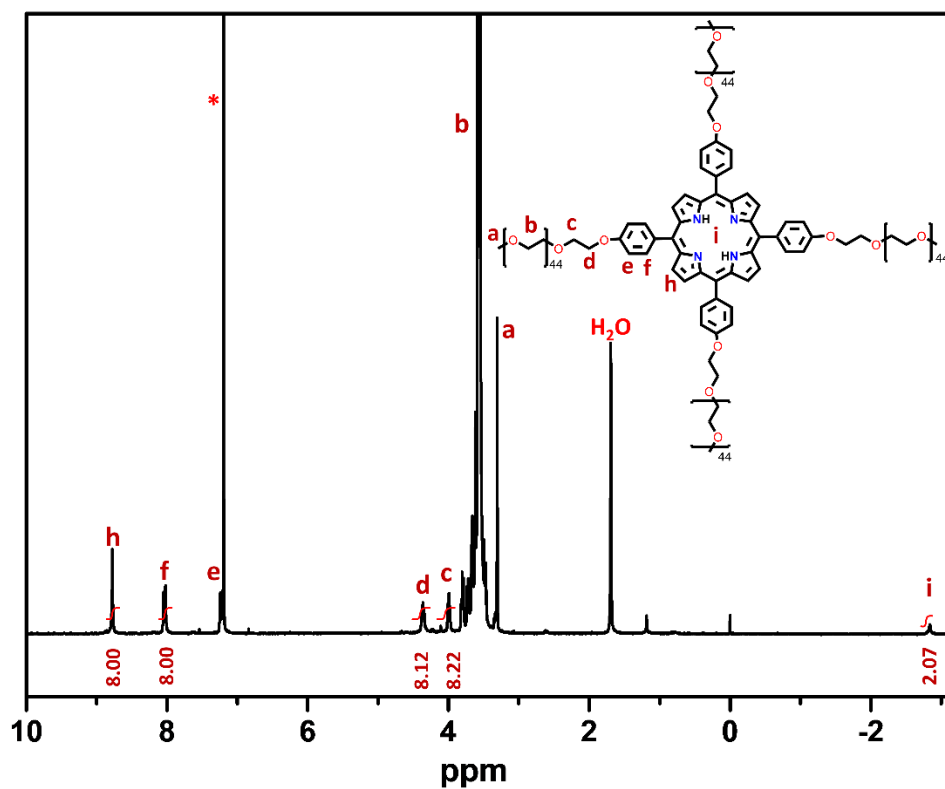


Figure 2.2 The ¹H NMR spectrum of H₂TPP(PEGME)₄ recorded in CDCl₃ at 25 °C.

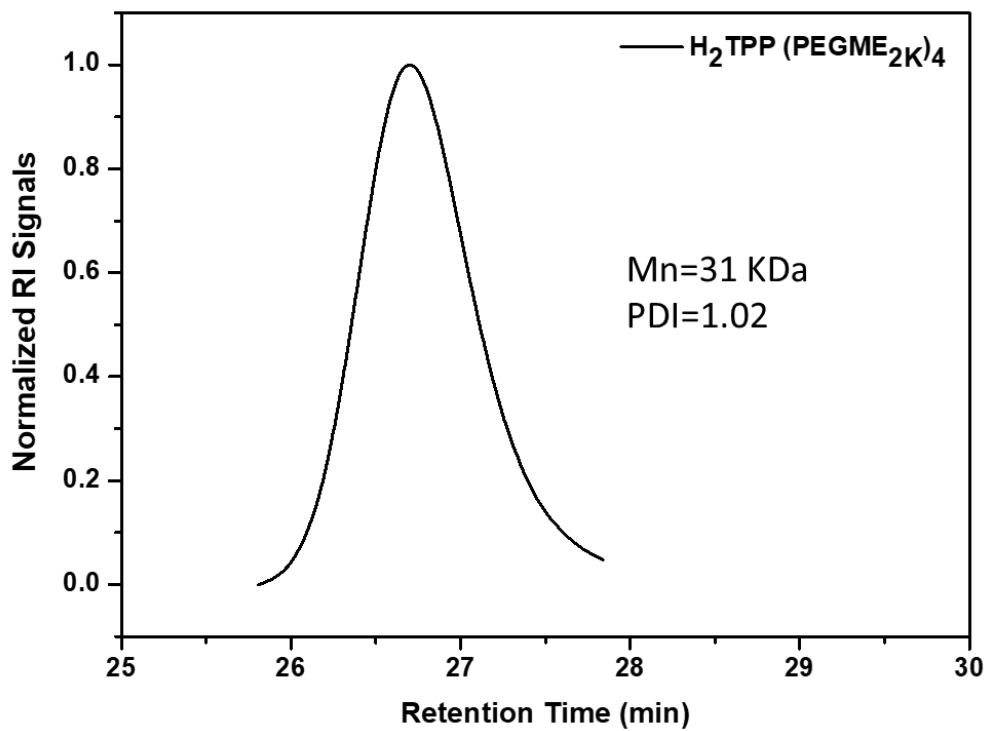


Figure 2.3 SEC trace of metal-free star polymer H₂TPP(PEGME)₄.

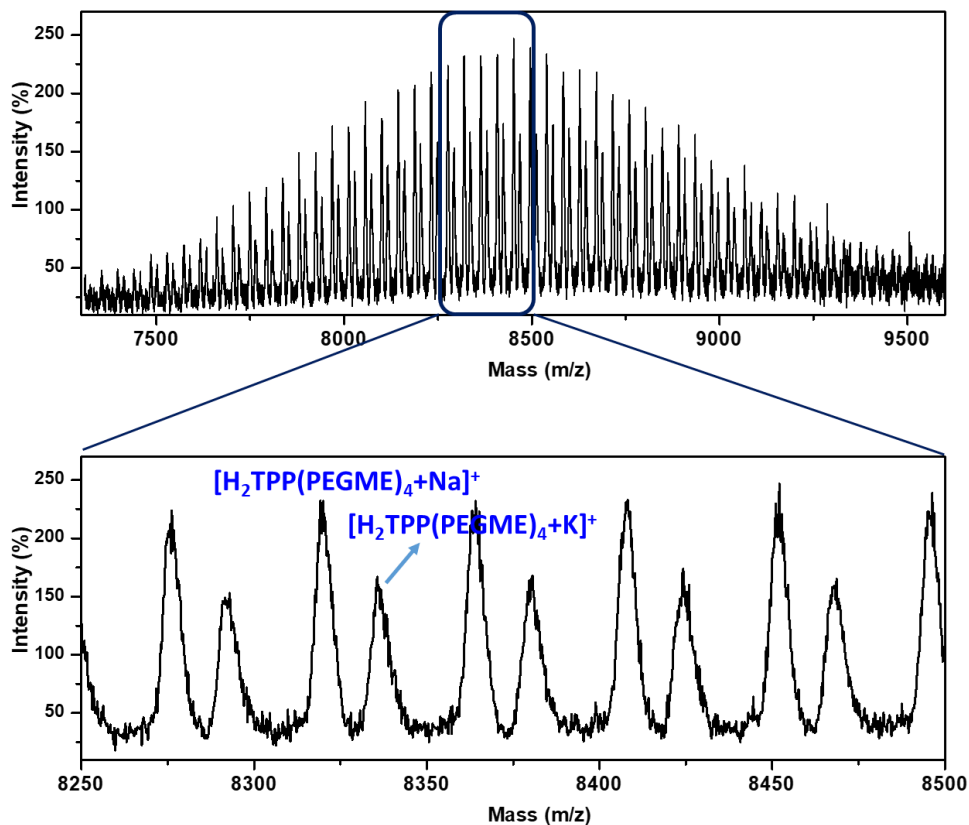


Figure 2.4 Full MALDI-TOF MS spectrum of metal-free star polymer $H_2TPP(PEGME)_4$ (top) and the zoomed in spectrum (bottom)

After insertion of the zinc(II) ion by Zn metalation, the peak of the N-H pyrrole protons in the 1H NMR spectrum disappeared, revealing that the pyrrole protons were successfully replaced by the zinc(II) ion (Figure 2.5). Furthermore, UV-Vis spectroscopy was performed evidencing the successful metalation based on the red-shift of the Soret band of the porphyrin unit to 428 nm and the disappearance of the main Q-band at 520 nm (Figure 2.6).

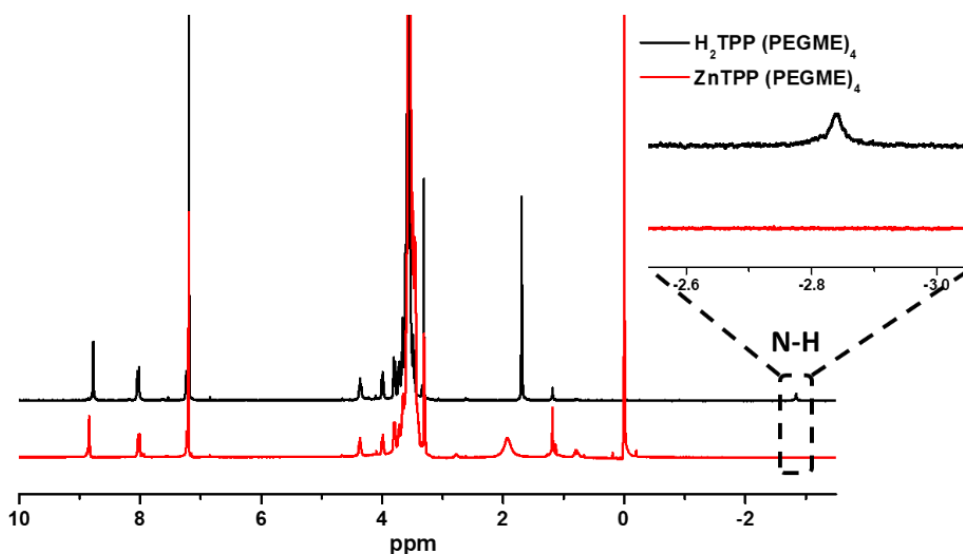


Figure 2.5 1H NMR spectra of $H_2TPP(PEGME)_4$ and $ZnTPP(PEGME)_4$, recorded in $CDCl_3$ at $25^\circ C$.

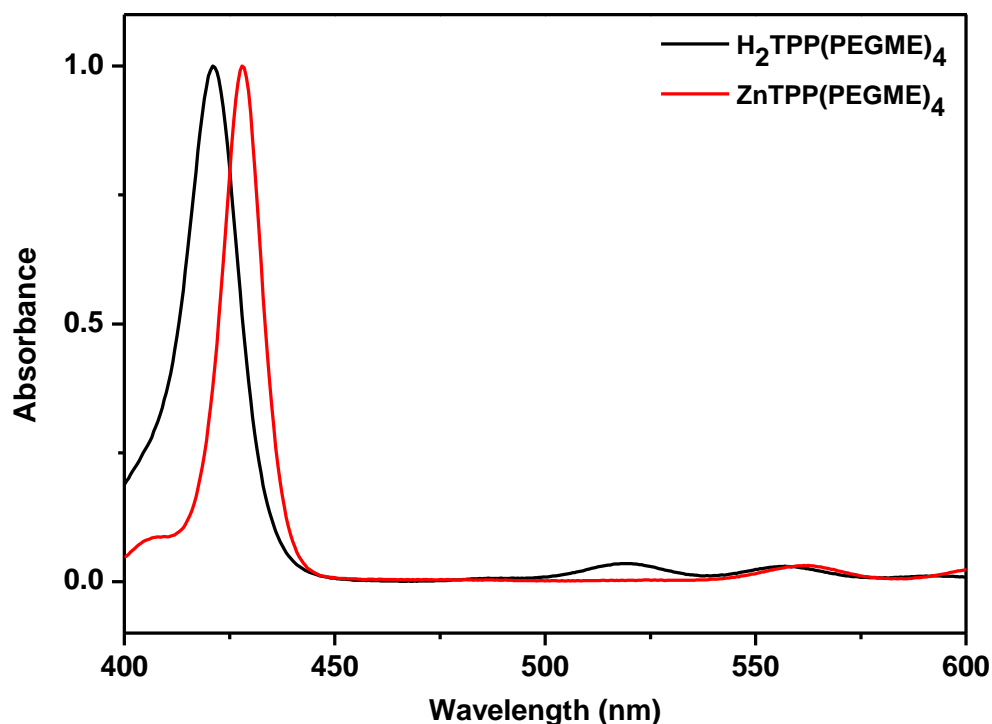


Figure 2.6. UV-Vis spectra of $\text{H}_2\text{TPP}(\text{PEGME})_4$ and $\text{ZnTPP}(\text{PEGME})_4$ in aqueous solution.

The second part required for the supramolecular miktoarm star complex is a pyridine end-decorated poly(methoxy-diethyleneglycol acrylate) (PmDEGA). The PmDEGA polymer was synthesized by RAFT polymerization using methyl-2-(*n*-butyltrithiocarbonyl)propanoate as chain transfer agent (CTA) and azobutyronitrile as radical initiator, at 70 °C in toluene.⁴⁵ After determination of the polymerization kinetics (Figure 2.7), a well-defined polymer was prepared with a degree of polymerization of 56. The polymer was purified by precipitation in diethyl ether (4x) and analyzed by ^1H NMR spectroscopy and SEC. The acquired polymer was subjected to an aminolysis reaction to convert the CTA end-group into a thiol group followed by introducing *N*-(pyridine-4-ylmethyl) acrylamide by thiol-ene Michael addition.⁴⁶⁻⁴⁷ Hydrazine was employed for the aminolysis because of its strong nucleophilicity and antioxidant effect which significantly improved the aminolysis rate compared to primary alkyl amine and effectively suppressed the formation of disulfides. The polymers obtained before and after end group modification were characterized by SEC with refractive index (RI) detection, which revealed a minor change in the M_n and dispersity (\mathcal{D}) giving a first indication of successful end group modification (Figure 2.8). Furthermore, no additional shoulder was present in the SEC trace of the polymer after end group transformation indicating the absence of disulfide formation after aminolysis, which could only be achieved when working in oxygen free conditions. The transformation was also assessed by UV-Vis spectroscopy using the characteristic absorbance of the trithiocarbonate group around 310 nm (Figure 2.9). The original polymer exhibits a strong absorption at this wavelength while no absorption can be detected for the resulting pyridine end-decorated polymer.

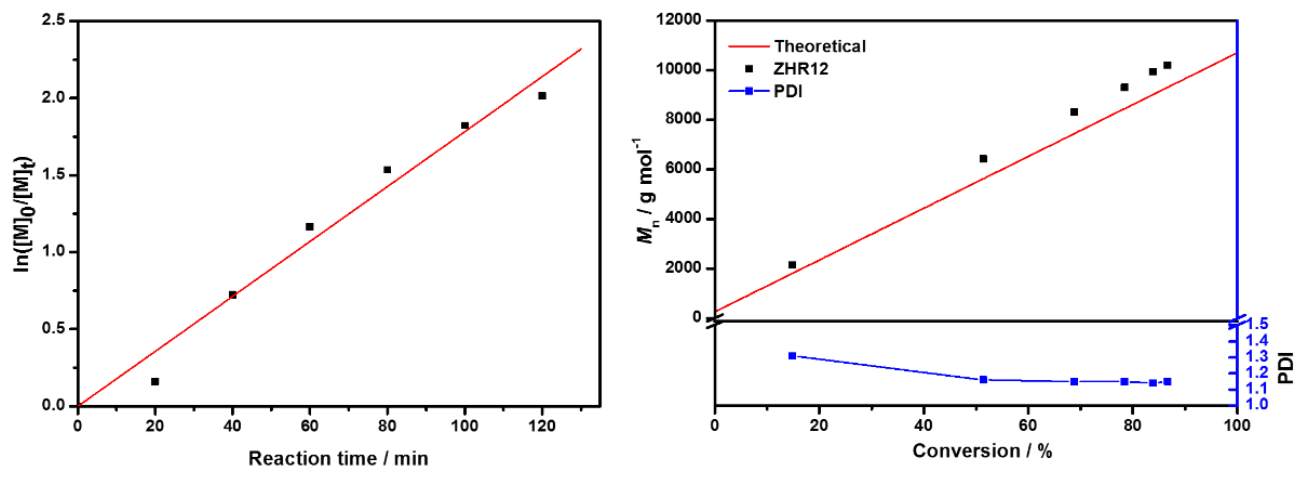


Figure 2.7. The kinetic data for the polymerization of mDEGA.

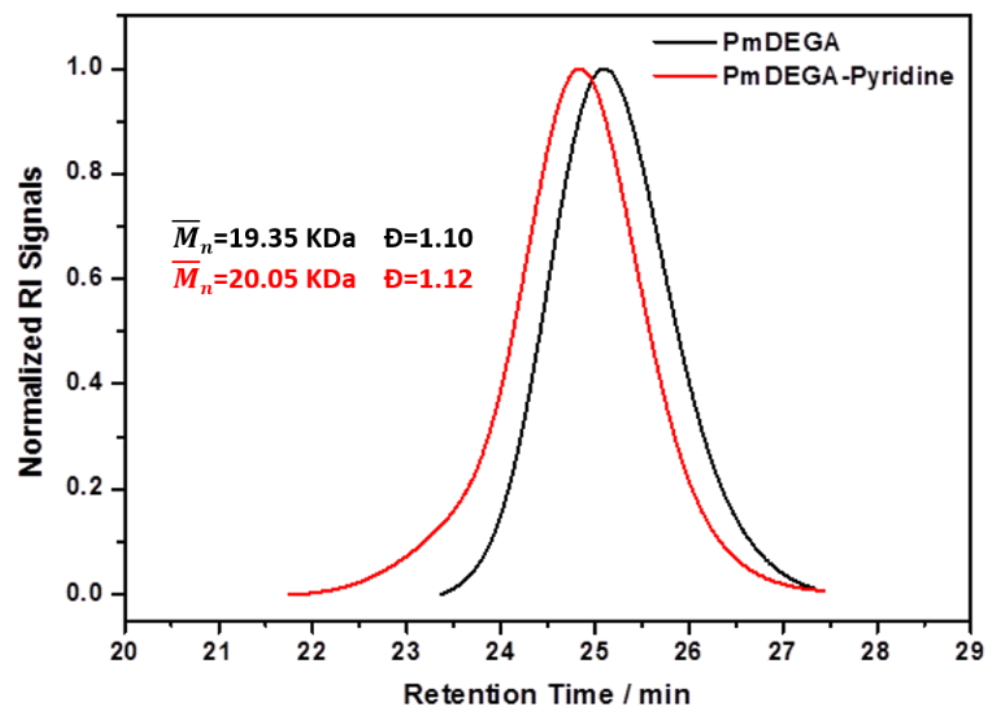


Figure 2.8. SEC traces of PmDEGA and pyridine end-functionalized PmDEGA.

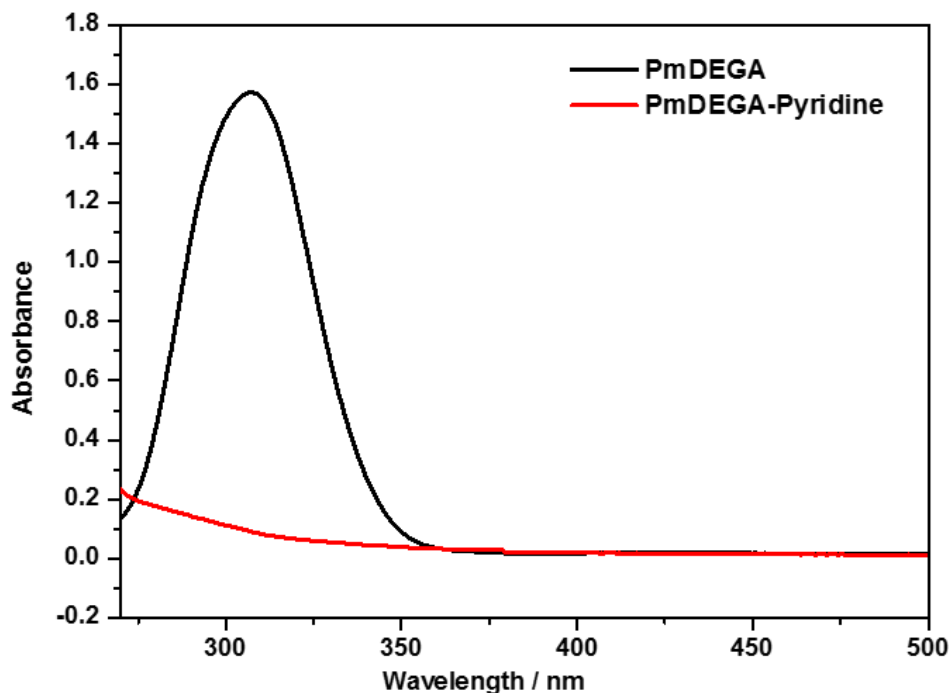


Figure 2.9. Comparison of the UV-vis absorption spectra of PmDEGA before and after aminolysis of the CTA end-group with hydrazine and modification with pyridine by thiol-ene modification.

In the next step, the formation of the supramolecular miktoarm star block copolymer *via* metal-ligand coordination—between the ZnTPP(PEGME)₄ and Py-PmDEGA was assessed. The assembly process of the two building blocks can be efficiently followed by the characteristic changes in the absorption intensity of the porphyrin *via* UV-Visible spectroscopy.

Detailed information regarding the stoichiometry of the self-assembly is very important for the study of the supramolecular system, as it directly affects the arm number of the miktoarm star polymer. Herein, we determined the stoichiometry by the continuous variation approach (Job plot) based on the change of the absorption intensity of the zinc-porphyrin upon complexation with Py-PmDEGA in water. The total concentration of the two building blocks was kept constant at 5.05 μM , while the ratio was changed between 0:1 and 1:0. The anticipated 1:1 stoichiometry between the two blocks was indeed confirmed by the Job plot diagram (Figure 2.10a) by the minimum absorption intensity at the ratio 1:1 of the two blocks at 25 °C. The stoichiometry was also determined by fluorescence spectroscopy supporting the UV-Vis results (Figure 2.10b).

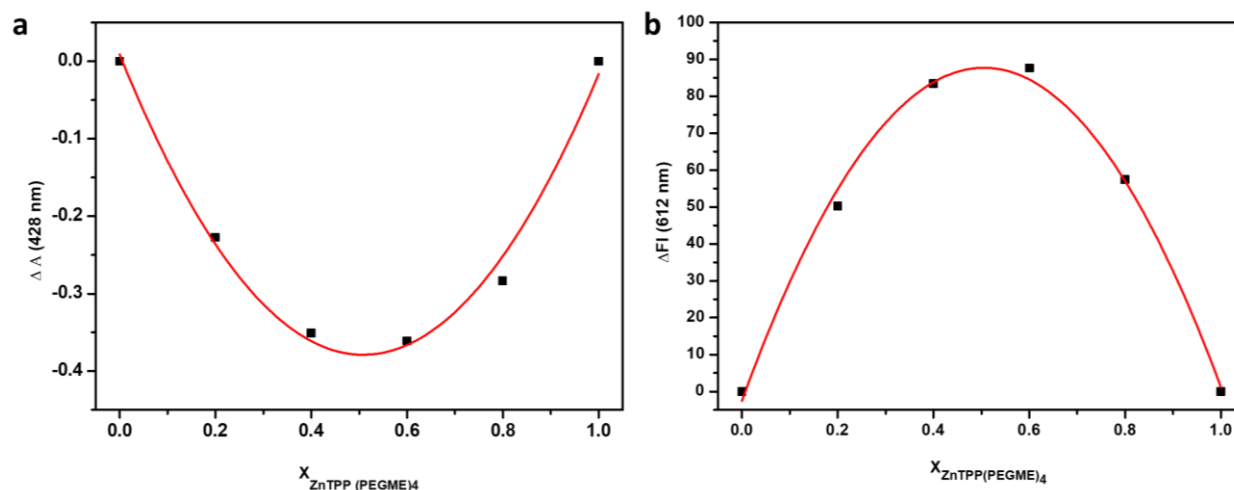


Figure 2.10 Continuous variation plot (Job plot) of ZnTPP(PEGME)₄ with Py-PmDEGA in Milli-Q water at 25 °C, a). by UV-Vis spectroscopy; b). by fluorescence spectroscopy, showing a minimum/maximum at 0.5 mole fraction of ZnTPP(PEGME)₄.

After confirming the stoichiometry of the two building blocks, we focused our attention on the strength of the supramolecular assembly characterized by the thermodynamic association constant, K_a , of the Py-PmDEGA@ZnTPP(PEGME)₄ complex. A UV-Vis spectrophotometric titration was employed to determine the binding constant in which a concentrated aqueous solution of Py-PmDEGA was added to a dilute aqueous solution of ZnTPP(PEGME)₄. As shown in Figure 2.11a, the addition of Py-PmDEGA resulted in a small red shift and a hyperchromicity of the Soret maximum in accordance with literature reports.⁴⁸⁻⁴⁹ The binding isotherm shown in Figure 2.11b was used for fitting with a 1:1 binding model, as confirmed by the Job plot, revealing a K_a of $(2.9 \pm 0.2) \times 10^4 \text{ M}^{-1}$ for this supramolecular system. This value is similar to the K_a reported for small molecule analogues indicating that the polymer chains do not significantly affect the supramolecular interaction strength.⁴⁸ Furthermore, the ITC binding isotherm resulting from addition of a concentrated aqueous solution of Py-PmDEGA (14.28 mM) to a dilute aqueous solution of Zn-TPP(PEGME)₄ (1.49 mM) showed exothermic responses (Figure 2.12), indicating the binding events. Fitting of the ITC curve was, however, not straightforward due to the strong exothermic dilution of Py-PmDEGA in water. Nonetheless, the ITC confirms exothermic binding of Py-PmDEGA to ZnTPP(PEGME)₄ with a K_a in the range of $10^3 - 10^4 \text{ M}^{-1}$. For comparison, the binding affinity of ZnTPP(PEGME)₄ with pyridine was also determined revealing a K_a of $(1.9 \pm 0.1) \times 10^4 \text{ M}^{-1}$, which is close to the K_a of ZnTPP(PEGME)₄ with Py-PmDEGA confirming that the polymer does not strongly influence the supramolecular association. Furthermore, the association constant was investigated at different temperatures indicating that there was no significant effect of temperature at 10 °C, 25 °C and 40 °C, which are all below the cloud point transition temperature of PmDEGA, on the association constant (Figure 2.13a). The association constant at the temperature above the cloud point transition temperature of PmDEGA was not studied as this is not possible due to the turbid phase separated solution. At last, the effect of pH of the solution (pH=1.68, 7.00 and 10.01) on the binding affinity was studied at 25 °C, also demonstrating roughly similar association constants (Figure 2.13b).

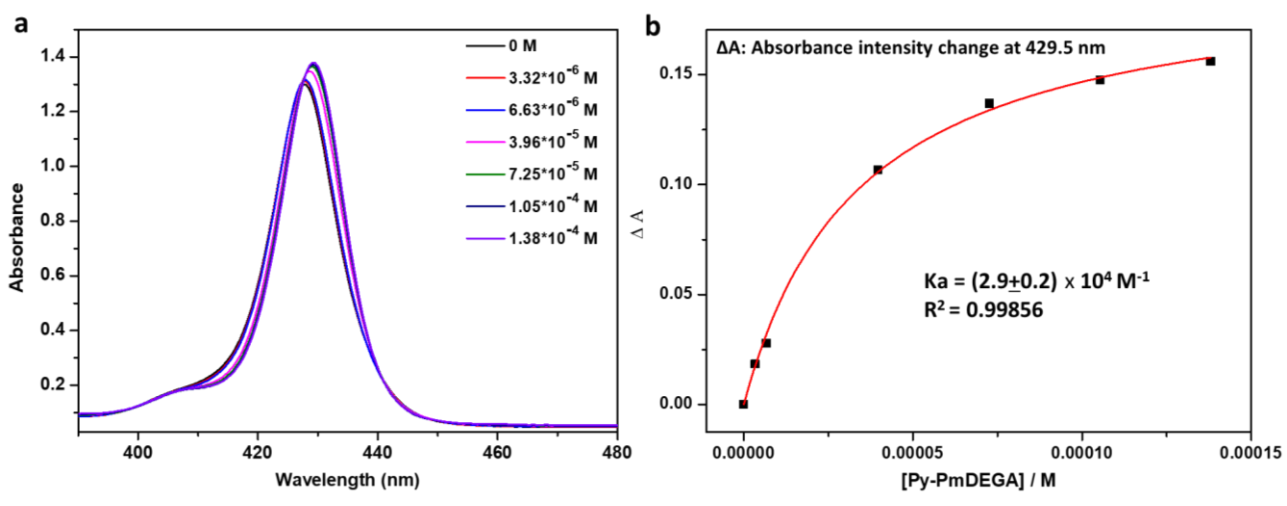


Figure 2.11 a: UV-Vis titration of Py-PmDEGA to a 5 μM ZnTPP(PEGME)₄ solution in Milli-Q water at 25 °C; b: absorbance changes of ZnTPP(PEGME)₄ at 429.5 nm upon the addition of Py-PmDEGA; the red solid line is the binding isotherm obtained by the least-squares fit to the experimental data ($R^2 = 0.99856$).

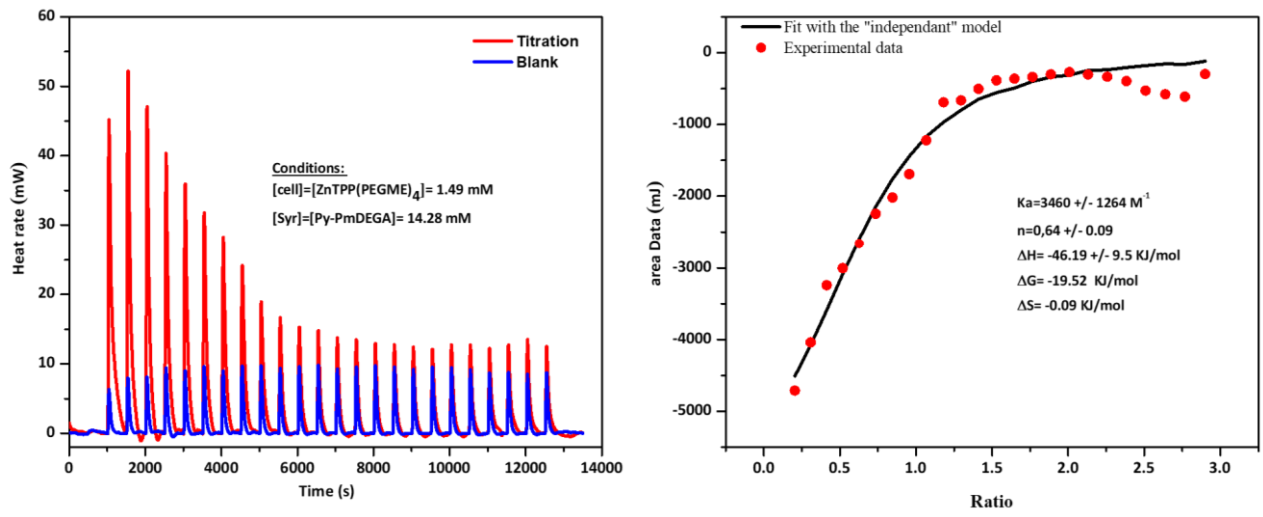


Figure 2.12 Isothermal titration calorimetry data for the addition of Py-PmDEGA to Zn-Tpp(PEGME)₄. Recorded in Milli-Q water at 20 °C.

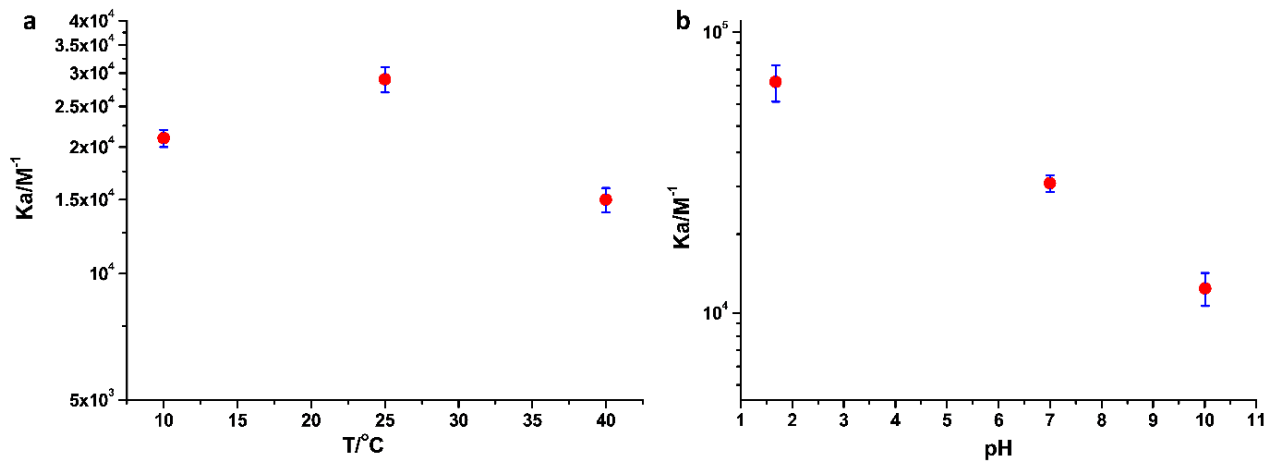


Figure 2.13 The association constants of Py-PmDEGA and ZnTPP(PEGME)₄ as function of (a) temperature and (b) pH value. All the UV-Vis titration experiments were performed in aqueous solution.

Next, to further prove that such metal-ligand interactions could effectively lead to the formation of supramolecular miktoarm star polymers from zinc porphyrin and pyridine functionalized polymer building blocks, two-dimensional diffusion-ordered ^1H NMR spectroscopy (DOSY) experiments were carried out (Figure 2.14). 2D-DOSY is a simple and fast technique to determine diffusion coefficients of species in solution. It was expected that the metal-ligand interactions driven self-assembled structures would exhibit lower diffusion coefficients compared to the lower molar mass precursors and that all components have the same diffusion coefficient. The results revealed for the individual components $\text{ZnTPP}(\text{PEGME})_4$ and Py-PmDEGA diffusion coefficient values of $(1.89 \pm 0.02) \times 10^{-10}$ and $(2.25 \pm 0.03) \times 10^{-10} \text{ m}^2/\text{s}$, respectively. When a DOSY experiment was undertaken on the 1:1 complex between $\text{ZnTPP}(\text{PEGME})_4$ and Py-PmDEGA , the diffusion coefficients associated with the single polymers moved to an identical diffusion coefficient value $((2.09 \pm 0.04) \times 10^{-10} \text{ m}^2/\text{s})$ indicating that they are associated. The lowest diffusion coefficient of the $\text{ZnTPP}(\text{PEGME})_4$ is rather surprising and indicates association of this component in water, presumably through π - π stacking interactions of the porphyrins. The intermediate diffusion coefficient of the mixture of the two components demonstrates the existence of the uniform miktoarm star block copolymer and, apparently, the suppression of the $\text{ZnTPP}(\text{PEGME})_4$ agglomerates. Moreover, no signals for the free polymer building blocks were detected, which suggest the efficient association between the two building blocks, $\text{ZnTPP}(\text{PEGME})_4$ and Py-PmDEGA , at least at this concentration. The reversibility of the metal-ligand complexation can also be assessed by DOSY spectroscopy. The addition of a large excess of the competitive low molecular weight pyridine ligand induced the disassembly process of the complexation, observed from the diffusion coefficient value transition of Py-PmDEGA . Hence, based on the DOSY measurements, it is evident that the supramolecular copolymer is capable of undergoing a reversible transition triggered by the addition of a competitive ligand.

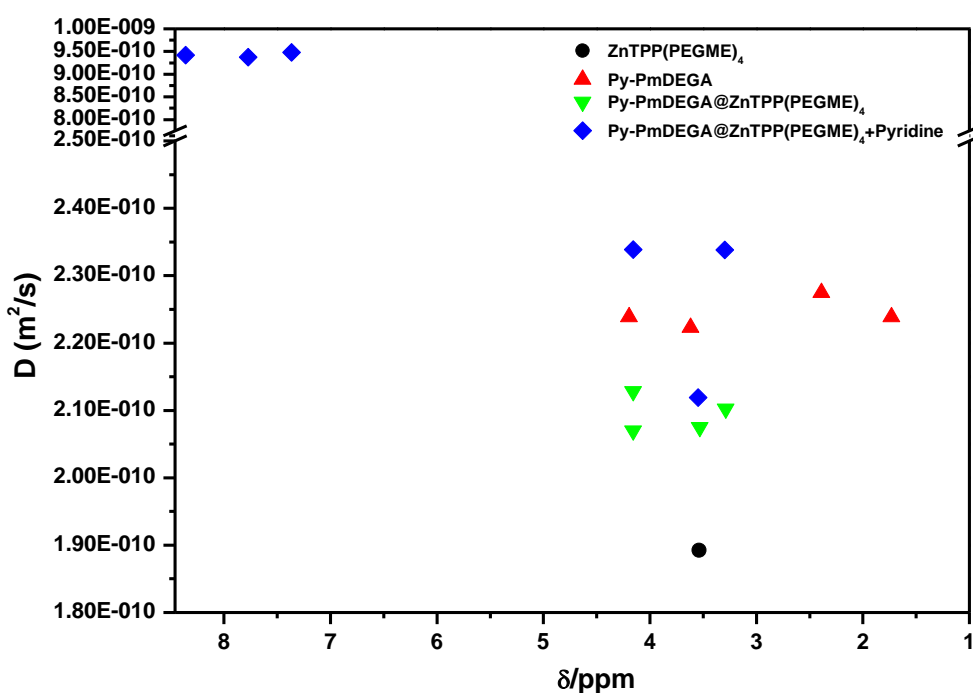


Figure 2.14 Diffusion coefficients, D , as function of the chemical shifts of the resonances associated with the initial polymer blocks (ZnTPP(PEGME)₄ and Py-PmDEGA), the supramolecular AB₄ complex and the complex in the presence of large excess amount of pyridine. The DOSY experiments were carried out at 2.02 mM in D₂O solution.

Apart from the investigation of the supramolecular interaction between the two building blocks, we also studied the effect of the complexation on the thermoresponsive behaviors of Py-PmDEGA. The phase transitions were determined by turbidimetry for Py-PmDEGA and the complex Py-PmDEGA@ZnTPP(PEGME)₄ (Figure 2.15). The results indicated that the cloud point temperature of Py-PmDEGA (*ca.* 54 °C) did not significantly change after complexation. However, the hysteresis diminished after complexation, which may indicate that the hysteresis of PmDEGA could result from (de)protonation of the pyridine group upon phase transition and that this is no longer the case upon complexation.

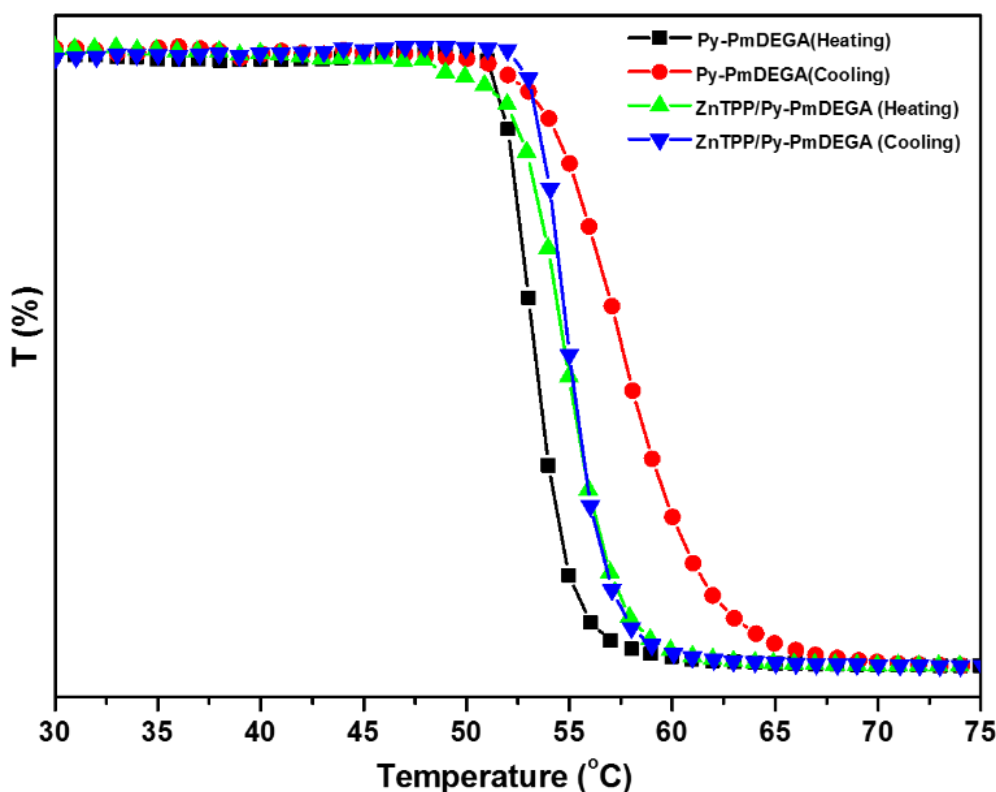


Figure 2.15 Plots of transmittance as a function of temperature measured for aqueous solutions (5 mg/mL) of Py-PmDEGA and complex Py-PmDEGA@ZnTPP(PEGME)₄.

2.3 Conclusions

In summary, a novel strategy is demonstrated for the preparation of supramolecular AB₄ miktoarm star block copolymers by association of a four-armed star-polymer with a Zn-porphyrin core and a pyridine end-functionalized polymer. The metalloporphyrin based star polymer was prepared by reaction between tetrakis (*p*-hydroxyphenyl)porphyrin and *p*-toluenesulfonyl poly(ethylene glycol) methyl ethers followed by insertion of the metal ion into the porphyrin core. The synthesis of the pyridine end-functionalized linear polymer was carried out *via* RAFT polymerization and subsequent aminolysis and Michael addition reaction. The building blocks were characterized by SEC, MALDI-TOF MS and ¹H NMR spectroscopy. The formation of the supramolecular miktoarm star polymer

was investigated in H₂O or D₂O at 25 °C and successful formation was confirmed *via* a combination of UV-Vis spectrophotometric titration, ITC and DOSY NMR spectroscopy, while the stoichiometry was determined by Job plot analysis.

We propose that other even more complex dynamic macromolecular architectures can be constructed *via* metalloporphyrin-pyridine interaction in future work. Taking into account that the supramolecular interaction and thermoresponsive polymer based architecture may be reversibly disassembled by applying various stimuli (temperature and the addition of competitive metal ion), this approach may open the way for the creation of a new family of responsive materials which expand the application areas of the conventional miktoarm star polymers.

2.4 Experimental section

2.4.1 Materials

All solvents and basic materials were commercially available (Sigma-Aldrich) and used as received, unless otherwise stated. Dichloromethane (DCM) and dimethylformamide (DMF) were dried in a solvent purification system (JC Meyer) before use as reaction solvents. Milli-Q Water (18.2 MΩ/cm) was generated using a Millipore Milli-Q academic water purification system. The buffer solutions for UV-Vis titration were potassium tetraoxalate dihydrate (50 mM, pH= 1.68), sodium carbonate and sodium bicarbonate (25 mM, pH=10.01) in Milli-Q water. Azobisisobutyronitrile (AIBN, 98%, Aldrich) was recrystallized twice from methanol prior to use. Methyl-2-(*n*-butyltrithiocarbonyl)propanoate (MBTTCP) was prepared according to the established procedures.⁵⁰ Poly(ethylene glycol) monomethyl ether (average M_n= 2000, Sigma Aldrich) was characterized by size exclusion chromatography with dimethylacetamide as eluent (M_n = 2400, PDI = 1.06) and ¹H NMR spectroscopy using CDCl₃ as solvent (DP=48). 5, 10, 15, 20-tetra(4-acetylphenyl)porphyrin (H₂TPP(OAc)₄) was synthesis according to a literature procedure.⁵¹

2.4.2 Analytical Techniques

¹H NMR and ¹³C NMR spectra were acquired on a Bruker Avance 400 MHz spectrometer. Samples were dissolved in CDCl₃ or D₂O. Chemical shifts are expressed in ppm by comparison with the signal of TMS used as an internal standard.

Size Exclusion Chromatography (SEC) was performed on an Agilent 1260-series HPLC system equipped with a 1260 online degasser, a 1260 ISO-Pump, a 1260 automatic liquid sampler, a thermostatted column compartment, a 1260 diode array detector (DAD) and a 1260 refractive index detector (RID). Analyses were performed on a PPS Gram30 column in series with a PPS Gram 1000 column at 50 °C. DMA containing 50 mM of LiCl was used as an eluent at a flow rate of 0.6 mL/min. The SEC traces were analyzed using the Agilent Chemstation software with the GPC add on. Molar mass and PDI values were calculated against PMMA standards.

Gas Chromatography (GC) was performed on 7890A from Agilent Technologies with an Agilent J&W Advanced Capillary GC column (30 m, 0.320 mm and 0.25 μm). Injections were performed with an Agilent Technologies 7693 auto sampler. Detection was done with a FID detector. Injector and detector temperatures were kept constant at 250 $^{\circ}\text{C}$ and 280 $^{\circ}\text{C}$, respectively. The column was initially set at 50 $^{\circ}\text{C}$, followed by two heating stages: from 50 $^{\circ}\text{C}$ to 100 $^{\circ}\text{C}$ with a rate of 20 $^{\circ}\text{C}/\text{min}$ and from 100 $^{\circ}\text{C}$ to 300 $^{\circ}\text{C}$ with a rate of 40 $^{\circ}\text{C}/\text{min}$. and then held at this temperature for 0.5 minutes. Conversion was determined based on the integration of monomer peaks using DMA as internal standard.

MALDI-TOF mass spectra were acquired with a Voyager DE-STR (PerSeptive Biosystem) using a simultaneous delay extraction procedure (20 kV applied after 233 ns with a potential gradient of 2545 V/mm and a wire voltage of 200 V) and detection in reflection mode. The instrument was equipped with a nitrogen laser (emission at 337 nm for 3 ns) and a flash AD converter (time base 2 ns). Trans-2-[3-(4-t-butylphenyl)-2-methyl-2-propenylidene]malononitrile (DCTB) was used as matrix.

UV/Vis spectra were recorded on a Varian Cary 300 Bio UV/VIS spectrophotometer equipped with a Cary temperature and stir control.

Fluorescence measurement for Job plot were carried out on a Cary Eclipse fluorescence spectrophotometer (Agilent Technologies) equipped with a Varian Cary Temperature Controller. The emission spectra resulting from excitation by a 428.5 nm laser were monitored from 500 -700 nm, and the slit width was kept at 5 nm during the measurements.

2.4.3 Job plots (continuous variation method)

The stoichiometry of the self-assembly was determined *via* Job's method of continuous variation.⁵² A stock solution was prepared for each complementary recognitions motif dissolved in Milli-Q water in a 5 mL round bottom flask. The appropriate amount from the stock solution was transferred to the UV-Visible cuvette or fluorescence cuvette in which the total concentration of the recognition motifs was kept constant at 5.05 μM . The molar fraction of the motifs was varied between 0 and 1. The changes in absorption intensity were multiplied by the molar fraction and plotted vs. molar fraction to construct the Job plot.

2.4.4 UV-Vis spectrophotometric titration experiment

UV-Visible titration was performed by adding solutions containing the Py-PmDEGA polymer to a solution of the ZnTPP(PEGME)₄ in a 1 cm path quartz cuvette by using microliter syringes. In all cases the ZnTPP(PEGME)₄ was present in the Py-PmDEGA solution at the same concentration as that in the cuvette to avoid dilution effects. Milli-Q water (18.2 m Ω /cm) was used as solvent for UV-Visible titration. UV-Visible scanning conditions were as follows: Scanning rate =300 nm/min, bandwidth = 0.5 nm, response time = 0.1 s, accumulations = 1 scan.

2.4.5 Isothermal titration calorimetry (ITC) experiment

ITC experiments were performed at 20 °C using a nano-ITC titration calorimeter from TA Instruments with a standard sample cell volume of 1 mL, following standard procedures. A 250 μ L injection syringe was used with stirring at 400 rpm. Host molecules were dissolved in Milli-Q water and the solutions were degassed gently under vacuum before use. Each titration comprised an initial 2 μ L preinjection followed by 24 \times 10 μ L injections of Py-PmDEGA (14.28 mM) into Zn-TPP(PEGME)₄ solution (1.49 mM). Control experiments with identical injections of Py-PmDEGA into water alone were used to correct titration data.

2.4.6 Diffusion ordered spectroscopy (DOSY) NMR experiment

DOSY NMR experiments were performed on a 400 MHz Bruker Avance II spectrometer equipped with a broadband ¹H decoupling probe (PABBO) using double stimulated echo, 2 spoil gradients and alternative phase cycle provided by Garreth Morris at a temperature of 298.2 K. Proton pulse lengths were determined to be 10.12 μ s and bipolar gradient of $\delta=2.5$ ms length were incremented from G=2.588 G/cm to 49.163 G/cm in 64 steps. 16 scans with 12 k complex data points were recorded for each increment with 16 dummy scans per experiment. The diffusion delay Δ was set to 1000 μ s. Processing was achieved using TopSpin 3.2 with the Dynamic Center 2.0.4. After zero filling to 24 k points and apodization using an exponential window function with an additional linewidth of 0.1 Hz, 1D increment spectra were Fourier transformed and the Signal decay due to Gradients was fitted using

$$f(G) = I_0 \cdot e^{\left(-\gamma_H^2 \cdot G^2 \cdot \delta^2 \cdot \left(\Delta - \frac{\delta}{3}\right)\right) \cdot D}$$

with the proton gyromagnetic ratio γ_H and the full signal intensity I_0 . Corresponding diffusion coefficients D of the polymer signals and the solvent are the result of the fitting procedure and are plotted against chemical shifts.

2.4.7 Turbidity measurements

The turbidity measurements were performed on UV-Vis spectrophotometer at a wavelength of 700 nm. The concentration of all the sample were 5 mg/mL. The transmittance was measured during at least two controlled cooling/heating cycles with a cooling/heating rate of 0.5 °C under stirring.

2.4.8 Synthesis and characterizations

2.4.8.1 Synthesis of α -methoxy- ω -toluenesulfonyl-PEG (PEGME-TOS)

A solution of poly(ethylene glycol) methyl ether (4.0 g, 2.0 mmol) in 30 mL THF was added to a 7.5 mL aqueous solution of NaOH (1.4 g, 36 mmol). The resulting mixture was cooled in an ice bath. A

solution of *p*-toluenesulfonyl chloride (4.4 g, 23 mmol) in 6 mL THF was added. The reaction solution was stirred at room temperature overnight. The solution was extracted with CH₂Cl₂ two times and the organic phase was combined and washed three times with water. The organic phase was dried over MgSO₄, filtered and concentrated under reduced pressure. Then, precipitation in cold diethyl ether yielded a white solid (3.6 g, 83.5 %). ¹H NMR (400 MHz, CDCl₃, δ/ppm): 2.38 (s, CH₃-C₆H₅), 3.37 (s, CH₃-O), 3.51-3.72 (m, -CH₂CH₂-O), 3.81 (t, -CH₂CH₂-TOS), 4.09 (t, -CH₂-CH₂-TOS), 7.28 (d, arom), 7.73 (d, arom).

2.4.8.2 Synthesis of 5, 10, 15, 20-tetra(4-hydroxyphenyl)porphyrin (H₂TPP(OH)₄)

In a 10 mL flask, 0.8 g H₂TPP(OAc)₄ (ca. 0.95 mmol) was dissolved in 6 mL of a EtOH/H₂O (1:3) solution. Then 1 mL concentrated HCl was added and the mixture solution was refluxed for 2 hours. After cooling to room temperature, the reaction solution was diluted with H₂O (40 mL), neutralized with 5% NaOH until the color of the green solution turned dark red and pH was 7.5. The mixture was stirred vigorously for 1 hour, then ethyl acetate was added, and the mixture was stirred for another 1.5 hours. The organic layer was separated, washed twice with water, dried over anhydrous MgSO₄, filtered, and the solvent was removed at reduced pressure. Chromatography (silica, toluene/ethyl acetate = 2:1) was employed to isolate the pure product (506 mg, 79% yield). ¹H NMR (400 MHz, acetone-*d*₆, δ/ppm): -2.69 (s, N-H pyrrole protons), 7.30(d, C-H phenyl protons in β-position with respect to the phenolic oxygen), 8.07(d, C-H phenyl protons γ to the phenolic oxygen), 8.87 (s, O-H phenolic protons), 8.93(s, C-H pyrrole protons).

2.4.8.3 Synthesis of H₂TPP(PEGME)₄

Firstly, PEGME-TOS was melted at 80 °C in vacuum for 2 hours before use to removed traces of moisture. Then, a mixture of [H₂TPP(OH)₄] (100 mg, 0.147 mmol) and PEGME-TOS (2528 mg, 1.179 mmol) was dissolved in 12 mL of dimethylformamide. To this solution, potassium carbonate (164 mg, 1.179 mmol) was added and the solution was stirred at 80 °C for 48 hours. After cooling to room temperature, the solution was poured into water and extracted three times with CH₂Cl₂. The combined organic phase was washed with water three times and then with brine, dried over MgSO₄, filtered and the solvent was evaporated under reduced pressure. The crude product was purified by precipitation into CH₂Cl₂/diethyl ether (4/45 v/v) from CH₂Cl₂ and column chromatography on silica gel using CH₂Cl₂/C₂H₅OH/N(C₂H₅)₃ (50:1:0.5) as eluent to yield the desired product (H₂TPP(PEGME)₄) (1.1 g, 80.6%). UV-Vis (H₂O) λ_{max} = 421 nm. ¹H NMR (400 MHz, CDCl₃, δ/ppm): -2.83 (s, N-H pyrrole protons), 3.31 (s, O-CH₃), 3.46-3.82 (m, OCH₂CH₂O), 3.99 (t, O-CH₂CH₂OPh), 4.37 (t, O-CH₂-CH₂OPh), 7.24(d, C-H phenyl protons in β-position with respect to the phenolic oxygen), 8.05(d, C-H phenyl protons γ to the phenolic oxygen), 8.78 (s, C-H pyrrole protons).

2.4.8.4 Synthesis of ZnTPP(PEGME)₄

To a well stirred solution of H₂TPP(PEGME)₄ (14.5 mg, 0.002 mmol) in 24 mL CH₂Cl₂/CH₃OH (3/1 v/v) was added 4.0 mg Zn(OAc)₂·2H₂O (0.018 mmol). The mixture was refluxed for 3 h. After the solution

cooled, it was diluted by CH_2Cl_2 , washed three times with water, dried over MgSO_4 and concentrated to give 13 mg product (90%). UV-Vis (H_2O) $\lambda_{\text{max}} = 428 \text{ nm}$. ^1H NMR (300 MHz, CDCl_3 , δ/ppm): 3.31 (s, O- CH_3), 3.46-3.82 (m, O $\text{CH}_2\text{CH}_2\text{O}$), 3.99 (t, O- $\text{CH}_2\text{CH}_2\text{OPh}$), 4.37 (t, O- $\text{CH}_2\text{CH}_2\text{OPh}$), 7.24(d, C-H phenyl protons in β -position with respect to the phenolic oxygen), 8.05(d, C-H phenyl protons γ to the phenolic oxygen), 8.78 (s, C-H pyrrole protons).

2.4.8.5 Synthesis of di(ethylene glycol) methyl ether acrylate (mDEGA)

Diethylene glycol monomethyl ether (87.72 g, 0.73 mol) and trimethylamine (74.36 g, 0.73 mol) were dissolved in 400 mL dichloromethane. To this stirred solution, acryloyl chloride (73.85 g, 0.82 mol) was added dropwise at 0°C . After stirring for 10 hours at room temperature, the precipitated salt was removed by filtration. The filtrate was washed with aqueous NaHCO_3 solution, and distilled water. Then the solution was dried over MgSO_4 , followed by filtration. The solvent (DCM) was evaporated under reduced pressure at room temperature. Then 113.7 g (89.5%) product was collected by reduced-pressure distillation in presence of hydroquinone as inhibitor. ^1H NMR (300 MHz, CDCl_3 , δ/ppm): 3.36 (s, 3H, O CH_3), 3.49-3.78 (m, 6H, $-\text{CH}_2\text{OCH}_2\text{CH}_2-\text{OCH}_3$), 4.30 (t, 2H, $-\text{C}(\text{O})\text{OCH}_2-$), 5.81 (dd, 1H, $-\text{CHCHC}(\text{O})-$, *trans*-position with respect to carbonyl group), 6.07-6.19 (m, 1H, $\text{CH}_2\text{CHC}(\text{O})-$), 6.37-6.43 (m, 1H, $-\text{CHCHC}(\text{O})-$, *cis*-position with respect to carbonyl group). ^{13}C NMR (100MHz, CDCl_3 , δ/ppm) 59.05 (OCH₃), 63.63(CH₂OCO), 69.14 (OCH₂CH₂OCO), 70.50 (CH₃OCH₂CH₂), 71.86 (CH₃OCH₂), 128.25 (CH=CH₂), 130.93 (CH=CH₂), 166.13 (OCO).

2.4.8.6 Synthesis of Poly(mDEGA) (PmDEGA)

mDEGA (1045 mg, 6 mmol), MBTTCP (25 mg, 0.1 mmol) and AIBN (0.99 mg, 0.006 mmol) were dissolved in toluene/DMA solvent mixture (3/2 vol) in a Schlenk flask. The concentration of monomer was fixed at 2 M. After four freeze-pump-thaw cycles, the flask was filled with argon, immersed in a preheated oil bath of 70°C and stirred for 2 hours. The polymerization was stopped by cooling the solution in an ice bath. After the solution was cooled down to room temperature, the polymers were precipitated in ice-cold diethyl ether/hexane (80/20). The crude polymer was dissolved in dichloromethane and precipitated again in ice-cold diethyl ether/hexane (80/20). This procedure was repeated three times. The polymer finally was dried under reduced pressure at room temperature. Conversion of the monomer was analyzed by GC with DMA as internal standard. SEC was used to evaluate number average molecular weight (M_n) and polydispersity index (Đ) of the obtained polymers. (see the kinetic data from Figure 2.7)

2.4.8.7 Synthesis of *N*-(pyridin-4-ylmethyl) acrylamide (NP4MAM)

4-aminomethyl pyridine (1.07 g, 9.85 mmol) and trimethylamine (0.99 g, 9.85 mmol) were dissolved in 20 mL dichloromethane. To this stirred solution, acryloyl chloride (0.98 g, 10.83 mmol) was added dropwise at 0°C . The reaction solution was stirred over night at room temperature. The reaction solution was washed twice with saturated aqueous NaHCO_3 solution, and three times with water. Then, the solvent (DCM) was evaporated under reduced pressure at room temperature. The crude

product was dissolved in distilled water. The pure product was extracted from the aqueous solution by ethyl acetate and then finally it was obtained by evaporation at 40 °C. (1.4 g, 87.6%) ^1H NMR (300 MHz CDCl_3 , δ/ppm): 4.55 (d, $J = 6.2$ Hz, 2H, $-\text{NHCH}_2-$), 5.73 (dd, $J = 10.2, 1.4$ Hz, 1H, $-\text{CHCHC}(\text{O})-$ trans-position with respect to carbonyl group), 6.02 (br, 1H, $-\text{NH}-$), 6.12-6.21 (m, 1H, $\text{CH}_2\text{CHC}(\text{O})-$), 6.37 (dd, $J = 17.0, 1.4$ Hz, 1H, $-\text{CHCHC}(\text{O})-$ cis-position with respect to carbonyl group), 7.21 (d, $J = 4.4$ Hz, 2H, α -pyridine proton), 8.56 (d, $J = 6.1$ Hz, 2H, β -pyridine proton).

2.4.8.8 Synthesis of Pyridine functionalized PmDEGA (Py-PmDEGA)

The solutions PmDEGA (280 mg, 0.033 mmol) in 1.5 mL DMF, $\text{NH}_2\text{NH}_2 \cdot \text{H}_2\text{O}$ (50 mg) in 0.5 mL DMF and NP4MAM (100 mg) in 0.5 mL DMF was placed into three Schlenk vials, respectively. 0.5 mL aqueous solution of sodium ascorbate (3.3 mg, 0.0165 mmol) as reducing agent was added into the PmDEGA solution. All of the three solutions were degassed four times by freeze-vacuum-thaw cycles. $\text{NH}_2\text{NH}_2 \cdot \text{H}_2\text{O}$ solution (83 μL , 0.165 mmol) was added into the PmDEGA solution under argon atmosphere. The reaction solution was stirred for 1 hour at 30 °C under argon atmosphere. During this period, the originally yellow solution became colorless. The NP4MAM solution (269 μL , 0.332 mmol) was added to the reaction mixture which was stirred at 30 °C for a further 12 hours. The polymer was recovered and purified by two repeated re-precipitation from DCM to hexane/diethyl ether (80:20 v/v) and a following PD-10 gel chromatography. The obtained end-functionalized polymer was confirmed by UV-Vis and SEC. (see the data in Figure 2.9 and 2.8)

2.5 References

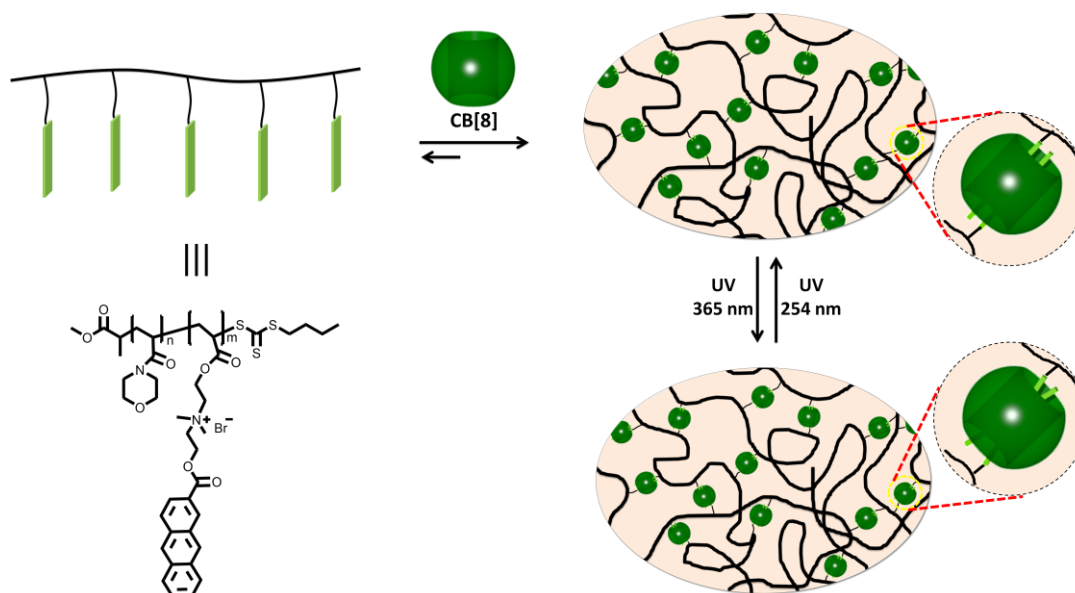
1. Ruzette, A.-V.; Leibler, L., *Nat. Mater.* **2005**, *4* (1), 19-31.
2. Rösler, A.; Vandermeulen, G. W. M.; Klok, H.-A., *Adv. Drug Delivery Rev.* **2012**, *64*, 270-279.
3. Qiu, L.; Bae, Y., *Pharm. Res.* **2006**, *23* (1), 1-30.
4. Altintas, O.; Vogt, A. P.; Barner-Kowollik, C., *et al.*, *Polym. Chem.* **2012**, *3* (1), 34-45.
5. Kempe, K.; Krieg, A.; Becer, C. R., *et al.*, *Chem. Soc. Rev.* **2012**, *41* (1), 176-91.
6. Fournier, D.; Hoogenboom, R.; Schubert, U. S., *Chem. Soc. Rev.* **2007**, *36* (8), 1369-80.
7. Higashihara, T.; Hayashi, M.; Hirao, A., *Prog. Polym. Sci.* **2011**, *36* (3), 323-375.
8. Gao, H.; Ohno, S.; Matyjaszewski, K., *J. Am. Chem. Soc.* **2006**, *128* (47), 15111-15113.
9. Jia, M.; Ren, T.; Wang, A., *et al.*, *J. Appl. Polym. Sci.* **2014**, *131* (7), n/a-n/a.
10. Gao, H.; Matyjaszewski, K., *Prog. Polym. Sci.* **2009**, *34* (4), 317-350.
11. Choi, H. K.; Nunns, A.; Sun, X. Y., *et al.*, *Adv. Mater.* **2014**, *26* (16), 2474-2479.
12. Schacher, F. H.; Rugar, P. A.; Manners, I., *Angew. Chem. Int. Ed.* **2012**, *51* (32), 7898-7921.
13. Park, M.; Harrison, C.; Chaikin, P. M., *et al.*, *Science* **1997**, *276* (5317), 1401-1404.
14. Lodge, T. P.; Rasdal, A.; Li, Z., *et al.*, *J. Am. Chem. Soc.* **2005**, *127* (50), 17608-17609.
15. Li, Z.; Kesselman, E.; Talmon, Y., *et al.*, *Science* **2004**, *306* (5693), 98-101.
16. Li, Z.; Hillmyer, M. A.; Lodge, T. P., *Langmuir* **2006**, *22* (22), 9409-9417.
17. Gao, H., *Macromol. Rapid Commun.* **2012**, *33* (9), 722-734.
18. Brunsveld, L.; Folmer, B. J. B.; Meijer, E. W., *et al.*, *Chem. Rev.* **2001**, *101* (12), 4071-4098.
19. Ma, X.; Sun, R.; Li, W., *et al.*, *Polym. Chem.* **2011**, *2* (5), 1068.
20. Mansfeld, U.; Winter, A.; Hager, M. D., *et al.*, *Polym. Chem.* **2013**, *4* (1), 113-123.
21. Stuparu, M. C.; Khan, A.; Hawker, C. J., *Polym. Chem.* **2012**, *3* (11), 3033-3044.
22. Fustin, C. A.; Guillet, P.; Schubert, U. S., *et al.*, *Adv. Mater.* **2007**, *19* (13), 1665-1673.
23. Burnworth, M.; Tang, L.; Kumpfer, J. R., *et al.*, *Nature* **2011**, *472* (7343), 334-7.
24. Binder, W. H.; Bernstorff, S.; Kluger, C., *et al.*, *Adv. Mater.* **2005**, *17* (23), 2824-2828.
25. Schmidt, B. V. K. J.; Hetzer, M.; Ritter, H., *et al.*, *Polym. Chem.* **2012**, *3* (11), 3064-3067.
26. Schmidt, B. V. K. J.; Rudolph, T.; Hetzer, M., *et al.*, *Polym. Chem.* **2012**, *3* (11), 3139.
27. Altintas, O.; Schulze-Suenninghausen, D.; Luy, B., *et al.*, *Eur. Polym. J.* **2015**, *62* (0), 409-417.
28. Altintas, O.; Tunca, U.; Barner-Kowollik, C., *Polym. Chem.* **2011**, *2* (5), 1146-1155.
29. Hoogenboom, R.; Wouters, D.; Schubert, U. S., *Macromolecules* **2003**, *36* (13), 4743-4749.
30. Yan, J.; Li, W.; Zhang, A., *Chem. Commun.* **2014**, *50* (82), 12221-12233.
31. Burattini, S.; Colquhoun, H. M.; Fox, J. D., *et al.*, *Chem. Commun.* **2009**, (44), 6717-6719.
32. Burattini, S.; Greenland, B. W.; Merino, D. H., *et al.*, *J. Am. Chem. Soc.* **2010**, *132* (34), 12051-12058.
33. Chen, M.; Ghiggino, K. P.; Launikonis, A., *et al.*, *J. Mater. Chem.* **2003**, *13* (11), 2696-2700.
34. Thévenaz, D. C.; Monnier, C. A.; Balog, S., *et al.*, *Biomacromolecules* **2014**, *15* (11), 3994-4001.
35. Gorczynski, J. L.; Chen, J.; Fraser, C. L., *J. Am. Chem. Soc.* **2005**, *127* (43), 14956-14957.
36. Bender, J. L.; Shen, Q.-D.; Fraser, C. L., *Tetrahedron* **2004**, *60* (34), 7277-7285.

37. Bender, J. L.; Corbin, P. S.; Fraser, C. L., *et al.*, *J. Am. Chem. Soc.* **2002**, *124* (29), 8526-8527.
38. Hoogenboom, R.; Moore, B. C.; Schubert, U. S., *Macromol. Rapid Commun.* **2010**, *31* (9-10), 840-845.
39. Zhang, T.; Chan, C.-F.; Lan, R., *et al.*, *Chem. Commun.* **2013**, *49* (65), 7252-7254.
40. Li, H.; Chan, C.-F.; Chan, W.-L., *et al.*, *Org. Biomol. Chem.* **2014**, *12* (31), 5876-5882.
41. Takai, A.; Chkounda, M.; Eggenspieler, A., *et al.*, *J. Am. Chem. Soc.* **2010**, *132* (12), 4477-4489.
42. Takai, A.; Gros, C. P.; Barbe, J.-M., *et al.*, *Chem. Eur. J.* **2009**, *15* (13), 3110-3122.
43. Zhang, C.; Chen, P.; Dong, H., *et al.*, *Adv. Mater.* **2015**, *27* (36), 5379-5387.
44. Satake, A.; Kobuke, Y., *Tetrahedron* **2005**, *61* (1), 13-41.
45. Chiefari, J.; Chong, Y. K.; Ercole, F., *et al.*, *Macromolecules* **1998**, *31* (16), 5559-5562.
46. Qiu, X.-P.; Winnik, F. M., *Macromol. Rapid Commun.* **2006**, *27* (19), 1648-1653.
47. Shen, W.; Qiu, Q.; Wang, Y., *et al.*, *Macromol. Rapid Commun.* **2010**, *31* (16), 1444-8.
48. Stangel, C.; Schubert, C.; Kuhri, S., *et al.*, *Nanoscale* **2015**, *7* (6), 2597-2608.
49. D'Souza, F.; Hsieh, Y.-Y.; Deviprasad, G. R., *Inorg. Chem.* **1996**, *35* (19), 5747-5749.
50. Urbani, C. N.; Monteiro, M. J., *Macromolecules* **2009**, *42* (12), 3884-3886.
51. Ellis, A.; Twyman, L. J., *Macromolecules* **2013**, *46* (17), 7055-7074.
52. Renny, J. S.; Tomasevich, L. L.; Tallmadge, E. H., *et al.*, *Angew. Chem. Int. Ed.* **2013**, *52* (46), 11998-2013.

Chapter 3 Reversible transformation from supramolecular to
covalent crosslinking of an anthracene-based hydrogel *via* UV
irradiation

Abstract:

This chapter describes a novel supramolecular hydrogel which undergoes a reversible transformation to the corresponding covalently crosslinked hydrogel upon UV-irradiation. The supramolecular hydrogel is based on the ternary host-guest interaction of two anthracene moieties and one large macrocyclic host. Two kinds of anthracene functionalized poly(*N*-acryloylmorpholine) were synthesized by post-polymerization modification of a copolymer containing *N*-acryloylmorpholine and an activated ester comonomers, with and without a charge next to the anthracene. The binding affinity of the anthracene side chains with and without an additional cationic charge were studied with two macrocyclic hosts (cucurbit[8]uril or γ -cyclodextrin) by UV-Vis titration revealing stronger binding in presence of the cationic charge due to further interactions with the macrocyclic hosts. Subsequently, the effect of the binding affinity on the hydrogelation was investigated, indicating that the stronger binding affinity facilitated the hydrogel formation at lower concentration. Finally, the reversible transformation of the supramolecular hydrogel to a chemical hydrogel by anthracene dimerization was studied by the UV irradiation at 365 nm or 254 nm. It could be demonstrated that the dynamic nature of the hydrogel that is responsible for the shear-thinning behavior was indeed lost upon UV-irradiation indicative of the formation of a covalently crosslinked hydrogel. The capabilities of the formed supramolecular hydrogel that is easily processable and able to reversibly convert to a chemical hydrogel, provides potential applications in applying mechanically robust covalently crosslinked hydrogels in complex shapes and difficult to reach locations making use of the dynamic nature of the supramolecular crosslinks.



Graphical representation of the overview of this chapter. Note that only the best performing anthracene hydrogel, including the cationic charge next to the anthracene, is shown here

3.1 Introduction

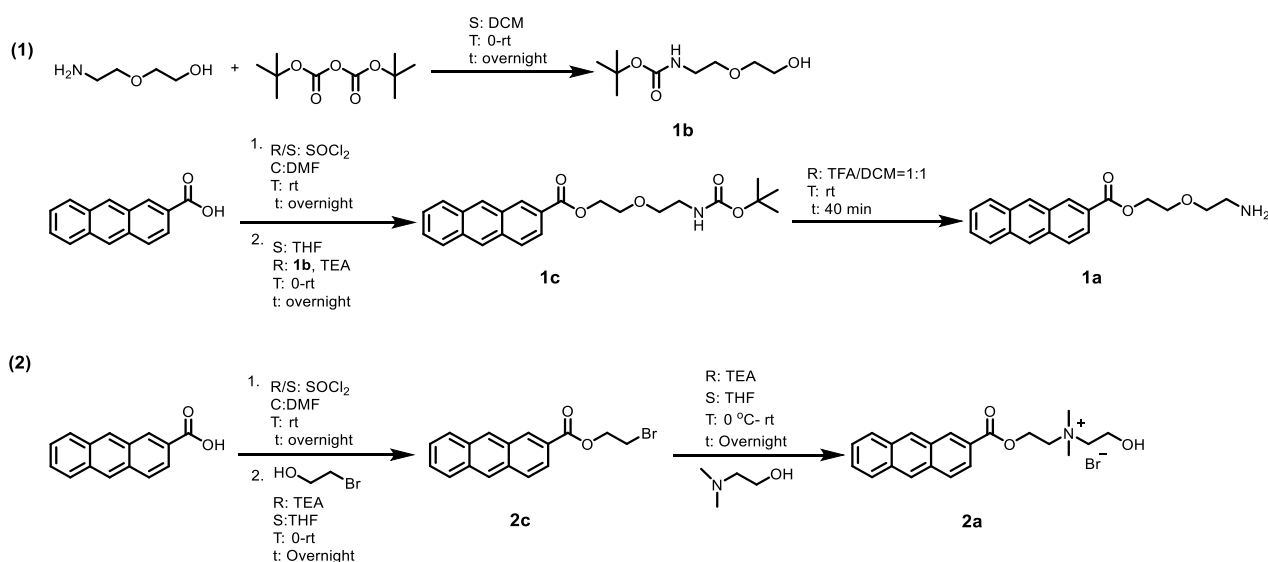
Polymeric hydrogels are water-swollen polymeric 3D networks consisting of crosslinked hydrophilic polymers. The fact that they can swell but do not dissolve in water under biological conditions makes them an ideal class of materials in biomedical applications, such as drug delivery and tissue engineering, which have attracted considerable interest of chemists during the past few decades.¹⁻² Generally, hydrogels can be categorized into chemical and physical hydrogels based on their crosslinking mechanisms. Chemically crosslinked hydrogels consist of polymer chains interconnected by permanent non-reversible covalent bonds and have been fabricated through a wide range of crosslinking chemistries.³⁻⁸ Chemical crosslinked hydrogels are stable and exhibit robust mechanical properties due to the stability of the covalent bonds, and have been commonly employed when tough and stable hydrogels are required.⁹ Furthermore, they need to be synthesized in the required shape as their shape cannot be changed once formed. However, the covalent nature of the crosslinks makes them rather brittle and unable to self-heal once the network is broken.¹⁰ In contrast, physically crosslinked hydrogels, also named supramolecular hydrogels, are formed by reversible crosslinks between polymer chains or small molecules that assemble into a fibrous network. The supramolecular crosslinks avoid the deleterious implications of chemical crosslinks (brittleness, limited reshability etc.) at the price of mechanically weaker systems, because the gelation is driven by dynamic molecular self-assembly. Moreover, the non-covalent crosslinks endow tailored viscoelasticity and a dynamic nature, which is a desirable characteristic for a variety of important applications, such as biological recapitulation and injection. However, weak non-covalent bonds are not stable against dilution followed by dissipation, which limits their application potential. In recent years, gels combining supramolecular and covalent crosslinking have been developed.¹¹⁻¹³ The resulting materials exhibited combined properties, such as mechanical properties, self-healing and shape memory behavior. However, the fact that the covalent crosslinks are presence in the hydrogel leads to irreversible damage when large ruptures occur. A system that can be switched between these two types of hydrogels could be hypothesized to combine the advantageous properties of both covalent and supramolecular hydrogels.

To date, no study regarding the conversion between supramolecular and covalent hydrogels has been reported, to the best of our knowledge. In this chapter, we designed a new hydrogel that undergoes a conversion between non-covalent and covalent crosslinking based on supramolecular assembly and dimerization of anthracene groups. Upon the addition of a large macrocyclic host, *e. g.* cucurbit[8]uril (CB[8]) or γ -cyclodextrin (γ -CD), to an anthracene functionalized polymer, a supramolecular hydrogel should be formed by host-guest interaction between the macrocyclic host and two anthracene molecules by the formation of a stable 1:2 ternary complex. Such a supramolecular hydrogel can be further converted into its corresponding covalent crosslinked hydrogel upon irradiation at *ca.* 365 nm to induce photo-dimerization of the anthracene molecules in the cavity of the host. This process should be reversible by UV irradiation at *ca.* 254 nm, which results in the photochemical cleavage of the produced anthracene dimer. The type of crosslinking

can be easily switched in order to adequately alter the properties to meet the application's requirements. The supramolecular hydrogel is dynamic and could be injected, reshaped or even heal damage, while the covalently crosslinked hydrogel provides higher strength and robustness.

3.2 Results and discussion

In most literature reports, 9-substituted anthracene derivatives have been employed for the preparation of covalently cross-linked hydrogels based on the reversible photodimerization of anthracene.¹⁴⁻¹⁷ However, 9-substituted anthracene derivatives cannot form a supramolecular complex with macrocyclic hosts due to steric effects. Thus, sterically less demanding 2-substituted anthracene derivatives were selected for the preparation of hydrogels in this chapter to enable supramolecular hydrogel formation by host-guest interactions as well as covalent hydrogels by anthracene dimerization. Compared to γ -CD, the negatively charged carbonyl portals of CB[8] result in a higher interaction strength with cationic guest, whereas γ -CD prefers to bind to neutral or anionic guests.¹⁸ Two kinds of small molecule anthracene-derivatives **1a** and **2a**, carrying no charge and a positive charge, respectively, were designed and synthesized as shown in scheme 3.1. The structures of host and guest molecules are illustrated in Figure 3.1. Commercially available 2-anthracenecarboxylic acid was selected as the precursor to prepare the desired anthracene derivatives in several straightforward synthetic steps. First, 2-anthracenecarboxylic acid was converted to the corresponding acyl chloride by reaction with thionyl chloride followed by ester formation to give **1c** or **2c** in good yield. Subsequently, The Boc group of **1c** was removed with trifluoroacetic acid (TFA) yielding the non-charged functional anthracene **1a**. The Menshutkin reaction was used to modify **2c** with dimethylethanolamine yielding the charged anthracene **2a**. The anthracene derivatives (**1a** and **2a**) were purified by column chromatography.



Scheme 3.1. The synthetic routes of **1a** and **2a**

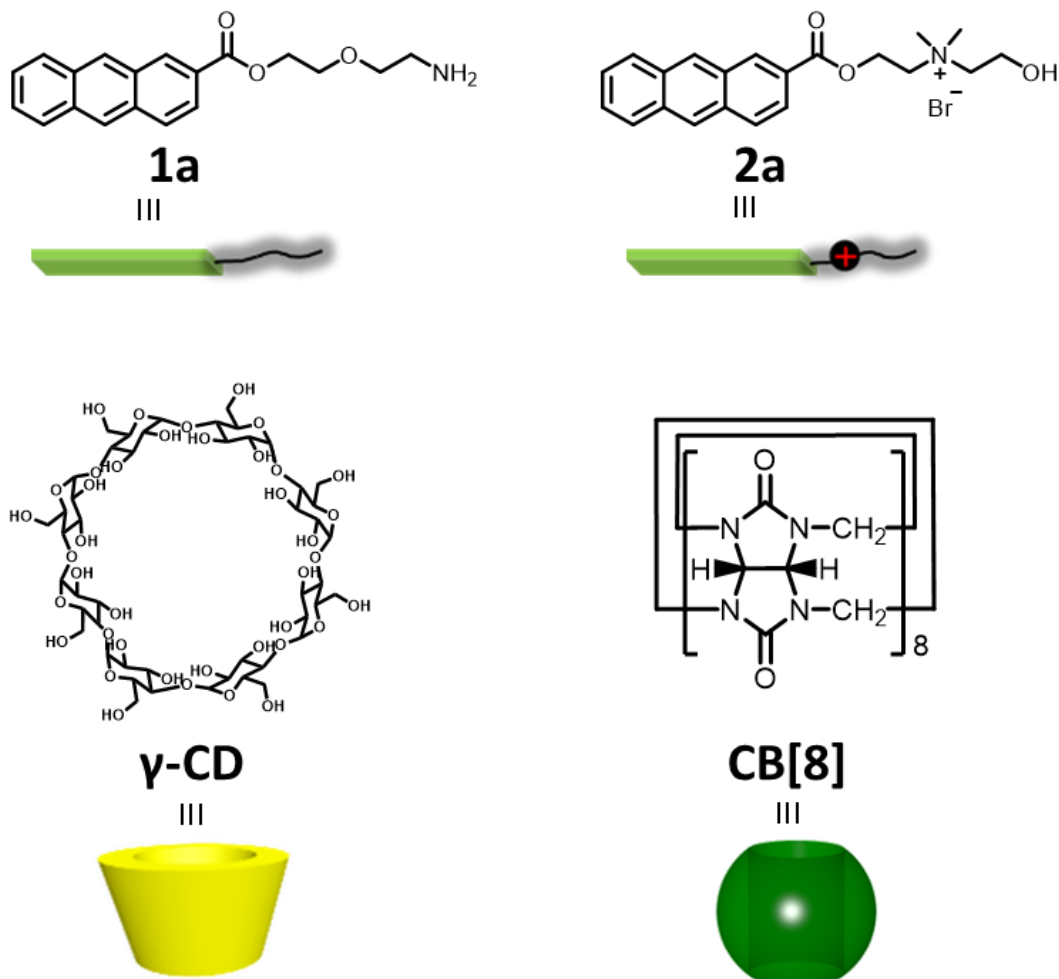


Figure 3.1. The chemical structure of anthracene derivatives and the macrocyclic host which were used in this chapter.

3.2.1 Host-guest complexation and photodimerization of small molecules anthracene **1a** and **2a**

The potential of the designed anthracene crosslinkers for hydrogel formation was assessed by investigating the host-guest complexation of the small molecule analogues and subsequent photochemical dimerization of the complexed **1a** and **2a**. The stoichiometry of the host-guest complexation of the anthracene derivatives with the macrocyclic host was determined by the continuous variation approach (Job plot) based on the change of the absorption intensity of the anthracene group upon complexation with the γ -CD or CB[8] macrocycles in water (Figure 3.2). The non-covalent binding affinity of **1a** and **2a** with γ -CD and CB[8] was studied by UV-Vis titration (Figure 3.3). The results are summarized in Table 3.1 showing that in all studied host-guest complexations, the stoichiometry is 2:1 between the anthracene derivative and the macrocyclic hosts as expected based on literature reports on related systems. In fact, many aromatic guests are efficiently and non-covalently dimerized by inclusion in a macrocycle on account of water release from the host cavity and π - π stacking interactions between the aromatic guests.¹⁹⁻²⁵ The binding affinity is generally higher with CB[8] than with γ -CD and with the charged anthracene **2a** than with the non-charged anthracene **1a**. The latter effect is stronger with CB[8] as it provides efficient carbonyl cation interactions at the rim of the CB[8].

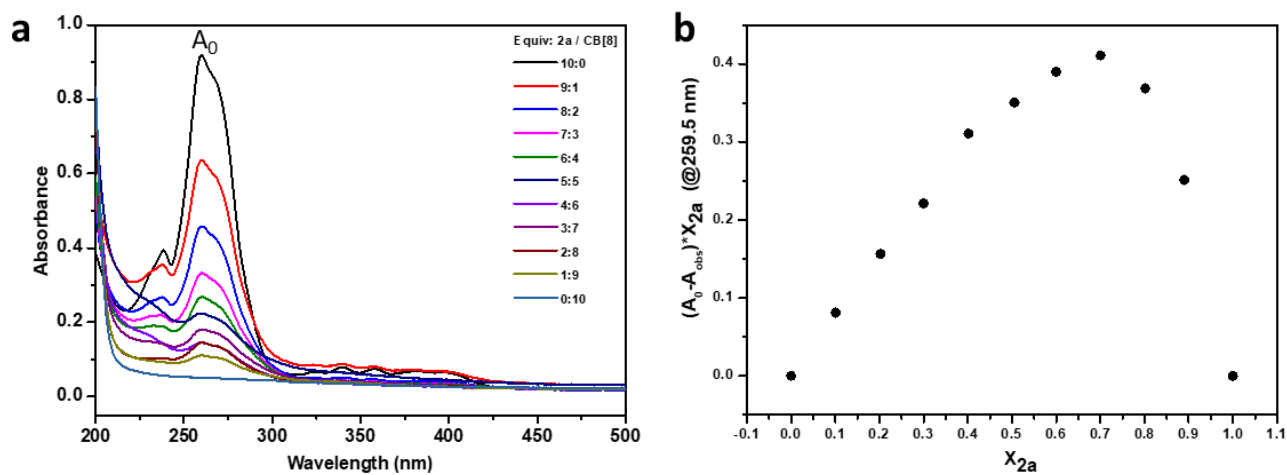


Figure 3.2. a) UV-Vis spectra of the aqueous solution of **2a** and CB[8] at different molar ratio of the two moieties at 25 °C, in which the total concentration was kept constant at 30 μ M; b) Job's plot of **2a** and CB[8], where the absorbance at 259.5 nm was plotted against the molar fraction of **2a**.

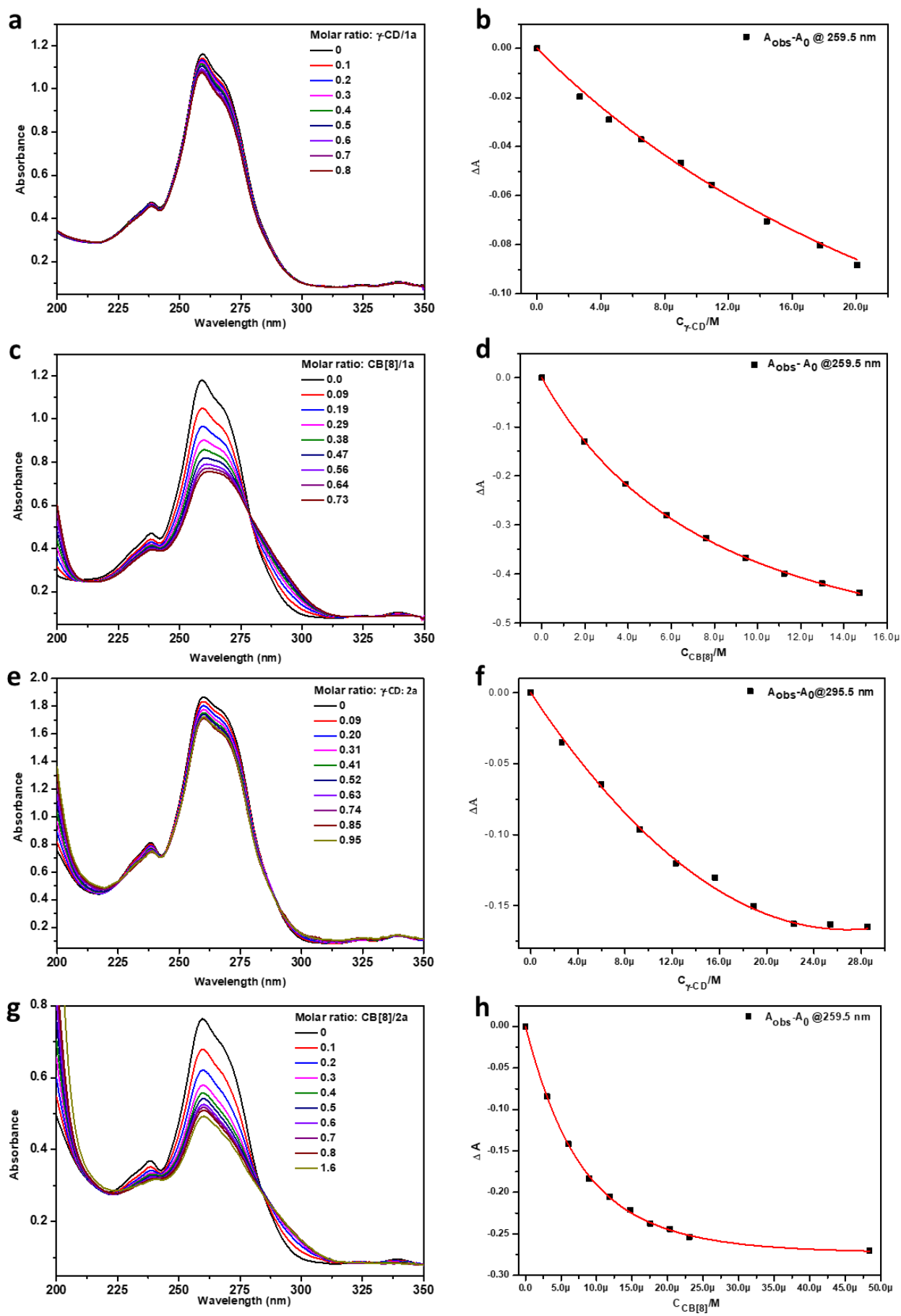


Figure 3.3 UV-Vis titration of concentrated host solution to 30 μM guest solution in Milli-Q water at 25 $^{\circ}\text{C}$: a) $\gamma\text{-CD}\rightarrow\mathbf{1a}$, c) $\text{CB}[8]\rightarrow\mathbf{1a}$, e) $\gamma\text{-CD}\rightarrow\mathbf{2a}$, g) $\text{CB}[8]\rightarrow\mathbf{2a}$; b), d), f), h) the plots of absorbance changes of anthracene group at 259.5 nm

or 259 nm upon adding host solution (left plots are corresponding to right UV-Vis spectra), the red solid lines are the binding isotherm obtained by the least-squares fit to the experimental data (all $R^2 > 0.9900$).

Table 3.1 Stoichiometry and association constant K_a between guest molecules (**1a**, **2a**) and host (γ -CD, CB[8]) from Job plot and UV-Vis titration in natural aqueous solution at 25 °C.

Guest	Host	Stoichiometry (Guest/Host)	K_a (ternary)/M ⁻²
1a	γ - CD	2:1	$(1.2 \pm 0.7) \times 10^5$
1a	CB[8]	2:1	$(7.5 \pm 1.6) \times 10^5$
2a	γ - CD	2:1	$(4.2 \pm 1.2) \times 10^6$
2a	CB[8]	2:1	$(5.1 \pm 0.3) \times 10^9$

After determining that the macrocyclic hosts (γ -CD or CB[8]) bind two anthracene units of **1a** or **2a** in its cavity, which is key for the potential formation of hydrogels, the photodimerization of the complexed anthracene molecules was investigated (Figure 3.4). To demonstrate the effect of macrocyclic host to the photodimerization of anthracene, the complexation of **1a** and CB[8] were selected as an example to compare without the presence of CB[8]. A dilute aqueous solution of **1a** (20 μ M) and 0.5 equiv. of CB[8] was irradiated with UV light at 365 nm leading to a rapid decrease in the absorbance of the bands centered around 259.5 nm with an isosbestic point at 229 nm indicating a clean transition from the anthracene monomers to the anthracene dimer, which reached full conversion within 5 min. The control experiment carried out under identical conditions in the absence of CB[8] resulted in only 50% dimerization on the same time scale and required an extra 33 min to reach full conversion. The faster anthracene photodimerization in the presence of CB[8] can be ascribed to forcing the two anthracene moieties together inside the macrocyclic host (Figure 3.4c). Moreover, the fluorescence emission intensity at 468 nm decreased upon photoirradiation revealing very similar kinetics for photodimerization as obtained by UV-vis spectroscopy (Figure 3.4d). Thus, from the combination of the two experimental observations, it can be concluded that the non-covalent association of two anthracene derivatives with CB[8] accelerates the anthracene photodimerization reaction, which is in accordance with literature.²⁶⁻²⁸

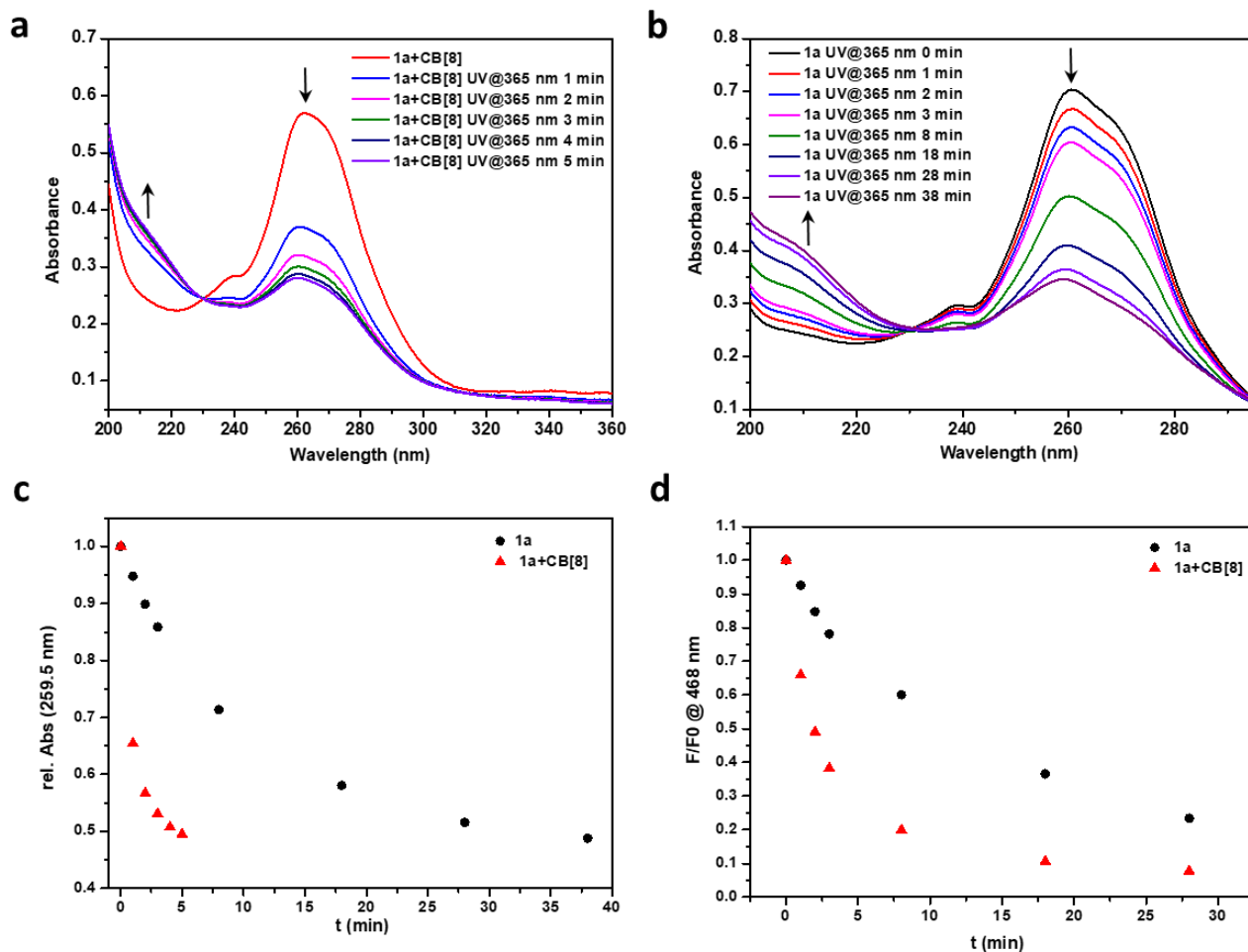
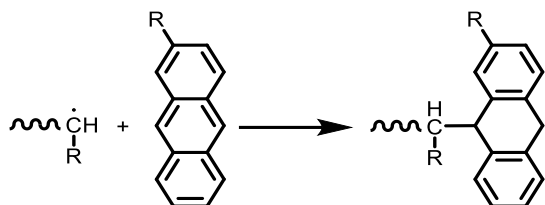


Figure 3.4 UV-Vis spectra of **1a** (20 μM) (a) in the presence of 0.5 equiv. CB[8] and (b) in the absence of CB[8] in H_2O upon photoirradiation with a 360 nm light source; (c) The normalised total intensity of the two UV-Vis spectra as function of the irradiation time; (d) the normalised intensity of fluorescence as a function of the irradiation time.

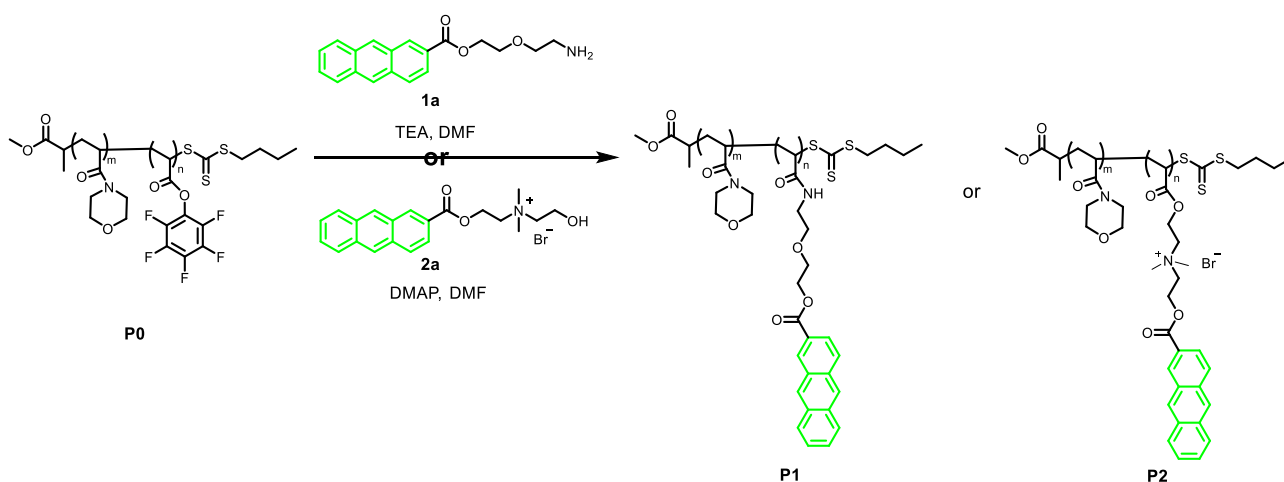
3.2.2 Synthesis and characterization of anthracene functionalized functional polymers

N-Acryloylmorpholine (NAM) is an acrylate monomer that yields hydrophilic poly(*N*-acryloylmorpholine (PNAM), which in block copolymers has shown good biocompatibility with the human body,²⁹ demonstrated promise in blood cell separation,³⁰ and as drug delivery vehicle. In this chapter, PNAM was chosen as the primary polymeric material for the preparation of hydrogels on account of its high hydrophilicity and good biocompatibility, which is an advantage for many applications. To obtain anthracene side-chain functionalized copolymers, an apparent straightforward approach was first attempted, which involved the copolymerization of NAM and an anthracene based acrylate comonomer by reversible addition-fragmentation chain transfer polymerization (RAFT). Unfortunately, the reaction did not yield the desired product, presumably due to the fact that the 2-substituted anthracene itself is an efficient radical quencher and inhibitor of radical polymerization. The propagating macroradicals are stabilized by formation of unreactive dibenzylic radicals by direct addition of anthracene to the growing polymer chain as shown in Scheme 3.2.³¹



Scheme 3.2 Schematic representation of 2-substituted anthracene as radical trap to terminate the growing polymer chain.

Therefore, to obtain the desired copolymers, a post-polymerization modification was utilized based on a reactive copolymer containing activated ester comonomers, namely poly(*N*-acryloylmorpholine-*co*-pentafluorophenyl acrylate) (PNAM-PFPA, **P0**). The activated ester containing copolymer **P0** was modified by nucleophilic substitution to incorporate the non-charged and charged anthracene derivatives (**1a** and **2a**) in presence of base (Scheme 3.3).



Scheme 3.3 Schematic representation of the nucleophilic substitution of pNAM-PFPA with anthracene derivative.

Poly(*N*-acryloylmorpholine-*co*-pentafluorophenyl acrylate) was prepared by RAFT polymerization using methyl-2-(*n*-butyltrithiocarbonyl)propanoate as chain transfer agent (CTA) and AIBN as radical initiator, at 70 °C in dioxane. After determination of the polymerization kinetics that revealed near random incorporation of the activated ester comonomer (Figure 3.5), a well-defined copolymer was prepared aiming for 90 % conversion to suppress the occurrence of chain termination reactions. The polymer was purified by precipitation in methanol (three times) and analyzed by ^1H NMR, ^{19}F NMR and FT-IR spectroscopy as well as SEC. The content of reactive ester for the polymer was determined by GC to be 3.14 % (molar fraction, spectra not included). **P0** was then used to generate the PNAM copolymers with different anthracene side chains. The polymer modification reaction was performed with excess amount of anthracene derivatives in DMF with triethylamine (TEA) or 4-dimethylaminopyridine (DMAP) as catalyst (see Scheme 3.3). In case of **P1**, a small amount of di(ethylene glycol) methyl ether acrylate (mDEGA) was added to scavenge any thiols released by the aminolysis of trithiocarbonate RAFT end groups by a thiol-Michael addition reaction. Products were isolated by extensive dialysis in water and subsequent lyophilization. The success of the reaction was confirmed by ^1H , ^{19}F NMR and FT-IR spectroscopy as well as size exclusion chromatography

(SEC). The analytical data are summarized in Table 3.2. The successful incorporation of the anthracene derivatives in **P1** and **P2** was confirmed with ^1H NMR spectroscopy by the presence of all the characteristic signals attributed to the anthracene group and the methylene protons next to ester (as assigned in Figure 3.6). However, the molar fraction of anthracene groups in copolymers, **P1** and **P2**, determined by ^1H NMR spectroscopy was found to be smaller than the theoretical incorporation of pentafluorophenyl acrylate resulting from GC conversion, which is most likely due to incomplete modification although the small signals in the ^1H NMR spectrum do not allow very accurate integration either. However, the pentafluorophenyl groups (PFP) were fully consumed after the reactions with the anthracene derivatives (**1a** and **2a**) based on the complete disappearance of the peaks originating from PFP in the ^{19}F NMR spectra (Figure 3.7). As such, the degree of anthracene modification will be around 1-3%, possibly in combination with some acrylic acid units resulting from hydrolysis of some PFP ester groups despite working under dry conditions.

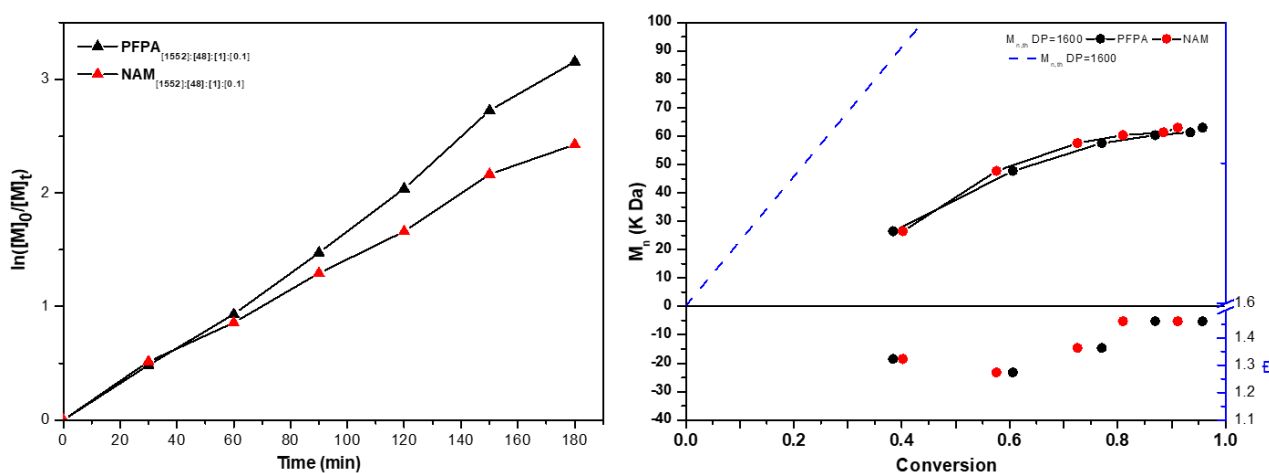


Figure 3.5 The kinetic data for the copolymerization of PNAM-PFPA.

Table 3.2 Analytical data of the synthesized copolymers

Copolymer	M_n [KDa] ^a	\bar{D} ^a	Amount of PFP [mol-%] ^b	Amount of Anthracene [mol-%] ^c
P0	72.1	1.27	3.1	/
P1	76.9	1.4	/	2.4
P2	67.7	1.4	/	1.0

^a Determined by SEC using PMMA as standards; ^b Determined by GC; ^c Determined by ^1H NMR spectroscopy

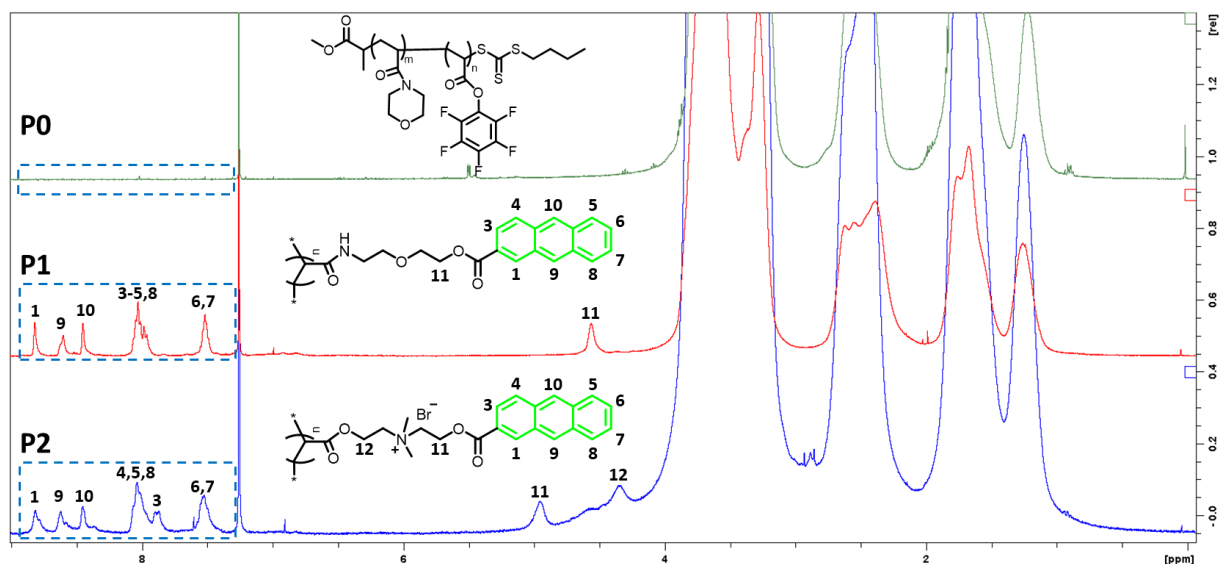


Figure 3.6 Proton NMR spectra of **P0**, **P1** and **P2** in CD_3Cl . (Note that only partial structure of **P1** and **P2** are shown here for simplicity)

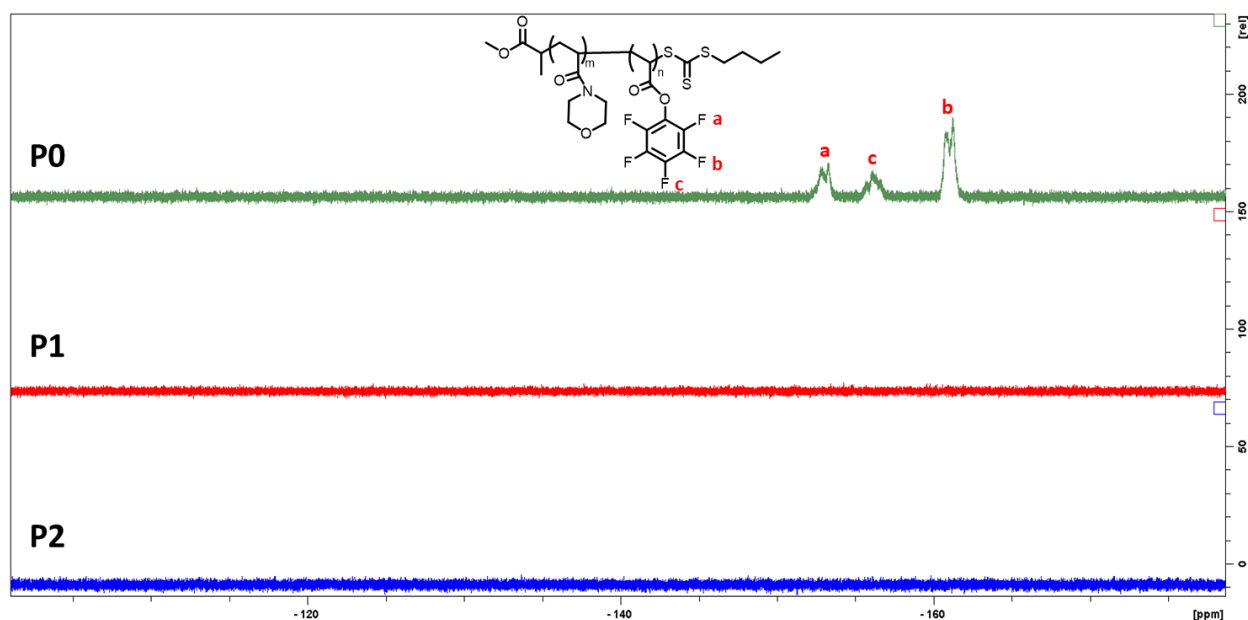


Figure 3.7 ^{19}F NMR spectra of **P0**, **P1** and **P2** in CDCl_3 .

Furthermore, FT-IR measurements were performed of these three polymers (Figure 3.8). The spectrum of **P0** showed the characteristic absorption band of the activated carbonyl group and the perfluorinated aromatic group (PFP) at 1776 and 1520 cm^{-1} , respectively. In the infrared spectrum of **P1** and **P2**, a characteristic peak at 1715 cm^{-1} appeared and this can be attributed to the $\text{C}=\text{O}$ stretching vibration of anthracene ester. The new peak at 1742 cm^{-1} in **P2** belongs to the $\text{C}=\text{O}$ of the acrylate. The appearance of the new peaks (1742 , 1715 cm^{-1}) and the disappearance of the peaks of PFP-ester at 1776 and the PFP at 1520 cm^{-1} indicate that the PFP was fully removed.

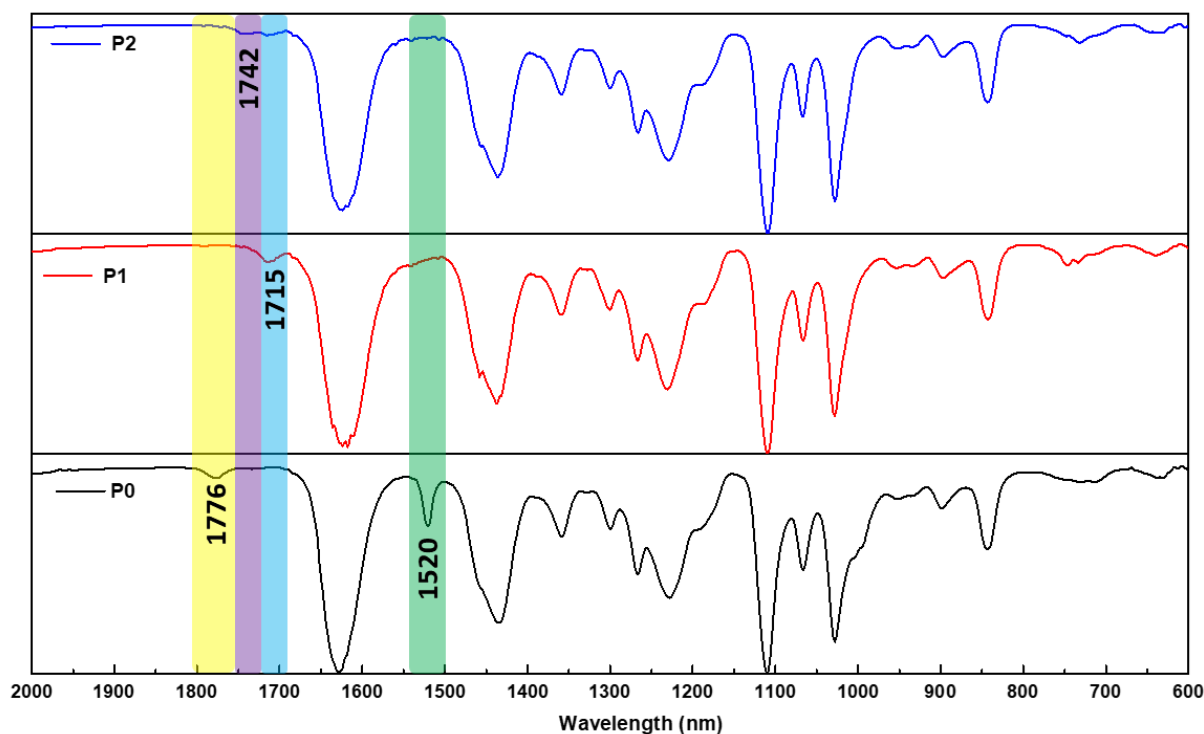


Figure 3.8 FT-IR spectra of the PNAM-PFPA precursor **P0** (bottom), the **P1** (middle) and **P2** (top).

Size exclusion chromatograms of these three copolymers are shown in Figure 3.9. The slight difference in retention time and the polydispersity indicate slight changes in the hydrodynamic diameter, which could result from the different solvation behavior of the anthracene moieties and the pentafluorophenyl group. The SEC traces detected by UV at wavelength of 400 nm, a characteristic absorption of anthracene, of these three copolymers are shown in Figure 3.9b. The appearance of SEC trace at 400 nm UV-detection proves that the anthracene group is successfully incorporated in polymers **P1** and **P2**. Additionally, the curve of **P1** did not show any shoulder toward high molar masses, suggesting that unwanted thiol-thiol coupling reactions following from aminolysis of the RAFT end groups had not occurred.

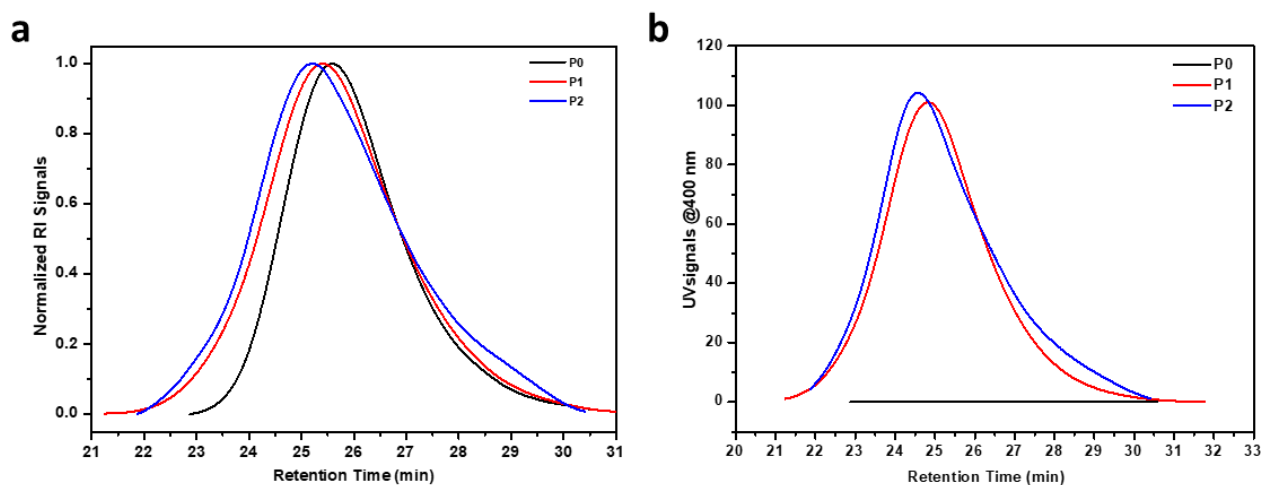


Figure 3.9 SEC traces of **P0**, **P1** and **P2** in DMA as mobile phase: a) RI detector; b) UV @400 nm detector.

3.2.3 Photochemical covalent hydrogel formation in the absence of macrocyclic host

To prove the effectiveness of the design strategy to form covalent hydrogels in absence of supramolecular host, the obtained anthracene functionalized copolymers (**P1** and **P2**) were irradiated by UV light at 360 nm for 20 min. As shown in Figure 3.10, the hydrogel was successfully formed after photoirradiation of a 5 wt % polymer solution, indicating that, on the one hand, the anthracene was successfully coupled to the polymer and, on the other hand, the content of the loaded anthracene (3.14%) is sufficient to act as covalent crosslinker to form hydrogels. In principle, if the binding affinity of host-guest is high enough the obtained copolymer should also form physical hydrogels as will be discussed in the next section.

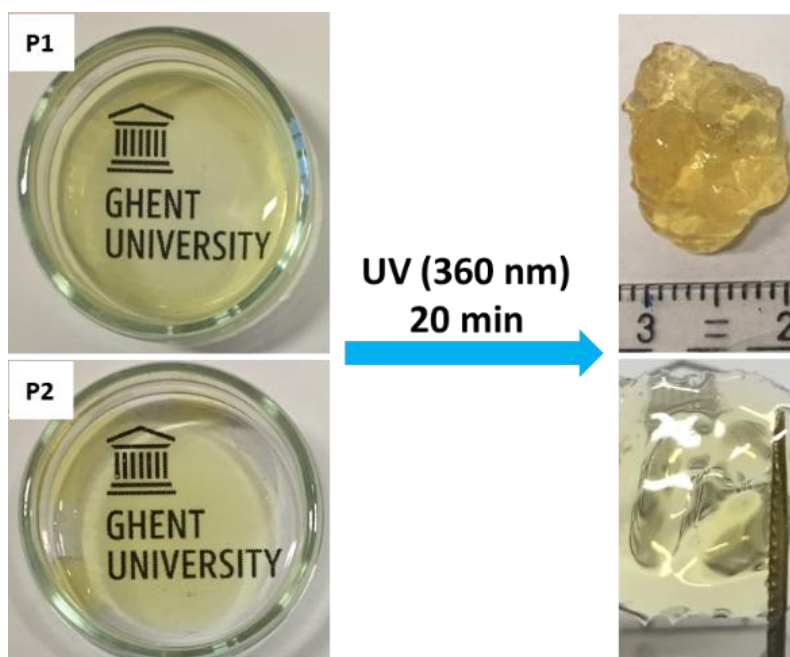


Figure 3.10 Pictures of **P1** and **P2** at 5 wt % in H₂O. Left: **P1** or **P2** prior to photoirradiation; Right: after photoirradiation at 360 nm for 20 min.

3.2.4 The formation of supramolecular hydrogels

The formation of supramolecular hydrogels is proposed to occur upon formation of the ternary host-guest inclusion complexes between one host molecule and two anthracene molecules, where the complexes act as non-covalent cross linker. The successful formation of host-guest inclusion complexes of the anthracene functionalized copolymers was confirmed by UV-Vis spectroscopy at low polymer concentration as shown in Figure 3.11 demonstrating the formation of the inclusion complex by the decrease of the intensity of the absorption peak at 260 nm.

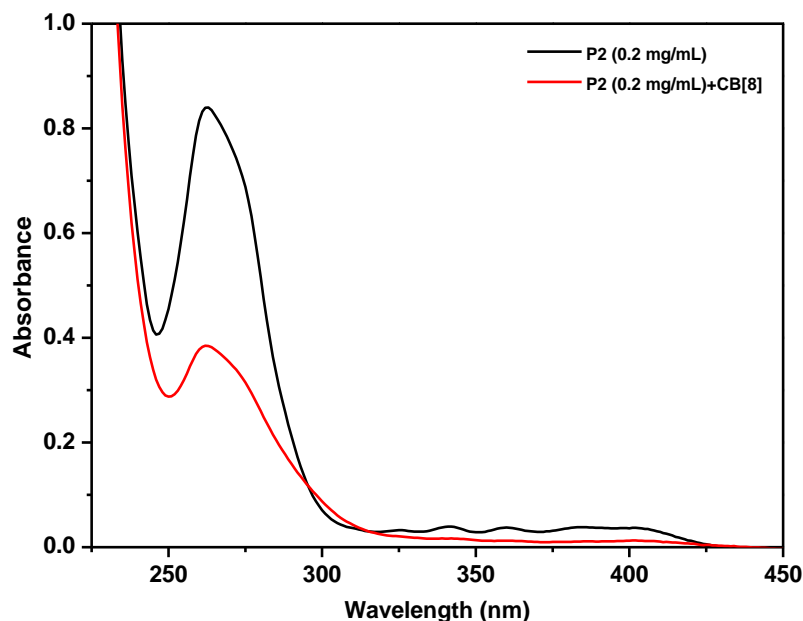


Figure 3.11 The UV-Vis spectra of 0.2 mg/mL **P2** and after the addition of 0.5 equivalents of CB[8].

After confirmation that the side-chain anthracene units can still form host-guest complexes, we continued to study whether hydrogels can be formed. The binding affinity of the host-guest inclusion complexation is a fundamental consideration in the design of the supramolecular hydrogels as too weak associating systems will require higher polymer concentration to form a sufficient number of supramolecular crosslinks. The supramolecular hydrogelation was studied by mixing the copolymers (**P1** or **P2**) with the macrocyclic hosts (CB[8] or γ -CD in a 1:0.5 molar ratio of anthracene moieties), to examine the effect of the binding affinity to the gelation. **P1** was first studied with γ -CD and CB[8] in water at different concentrations ranging from 1 to 15 wt %. The complexation of **P1** with γ -CD was found to result in hydrogels at a minimum gelation concentration of 15 wt % (Figure 3.12a). However, the complexation of **P1** with CB[8] could only be studied at a polymer concentration lower than 3 wt% due to the quite low solubility of CB[8] in water. As a result no hydrogels could be formed. The hydrogel formation of **P2** was only studied at 5 wt%, which was insufficient for hydrogel formation with γ -CD. However, the addition of CB[8] to **P2** resulted in the formation of a hydrogel already at 5 wt% due to the stronger supramolecular interaction. It should be noted that the efficient complexation of CB[8] with the charged anthracene derivative in **P2** enhanced the solubility of CB[8] enabling the study of this complexation at a higher polymer concentration than with **P1**. (Figure 3.12b). The supramolecular hydrogel formation results are summarized in Table 3.3.

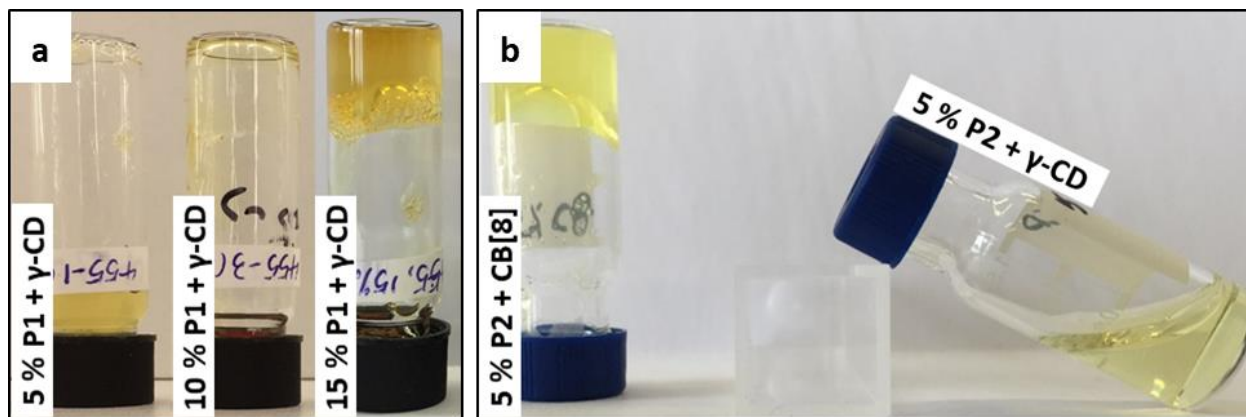


Figure 3.12 Inverted vial tests demonstrating the formation of the hydrogel from the mixture of polymer and host (0.5 eq. of anthracene group). (a) **P1** with γ -CD (**P1**/CB[8] were not given here); (b) **P2** with γ -CD and CB[8].

Table 3.3 Summary of the gelation study. (---: CB[8] is insoluble in water; /: the system was not studied)

Polymer/Host	5%	10%	15%
P1 / γ -CD	sol	sol	gel
P1 /CB[8]	---	---	---
P2 / γ -CD	sol	/	/
P2 /CB[8]	gel	/	/

Supramolecular hydrogels as a class of noncovalent cross-linked polymer materials display some basic physicochemical properties similar to covalent polymeric hydrogels, *e. g.* water-retention ability and mechanical properties. In addition, the dynamics of the crosslinked networks, that is inherent to the noncovalent nature of the crosslinks, allows the hydrogels to rapidly respond to a multitude of external stimuli, including physical (*e.g.*, temperature, dilution effect, light and magnetic field) and chemical (*e.g.*, pH, ionic strength, redox agent, glucose and competitive host/guest). In general, these external stimuli have an impact on the crosslinks leading to swelling or dissociation of the network. In this work, we examined the stimuli responsive properties of the obtained supramolecular hydrogels of **P2** with CB[8] by heating and dilution with water. As shown in Figure 3.13a, upon the addition of water the hydrogel disappeared and dissolved within 5 minutes demonstrating the dynamic nature of the crosslinks. The supramolecular hydrogels also underwent a gel-sol transition upon an increase in temperature, and subsequently the supramolecular hydrogel was reformed spontaneously when the solution was cooled down to room temperature (Figure 3.13b). This result indicated that the anthracene-CB[8] association is enthalpic in nature leading to weakening of the interaction upon increasing temperature.

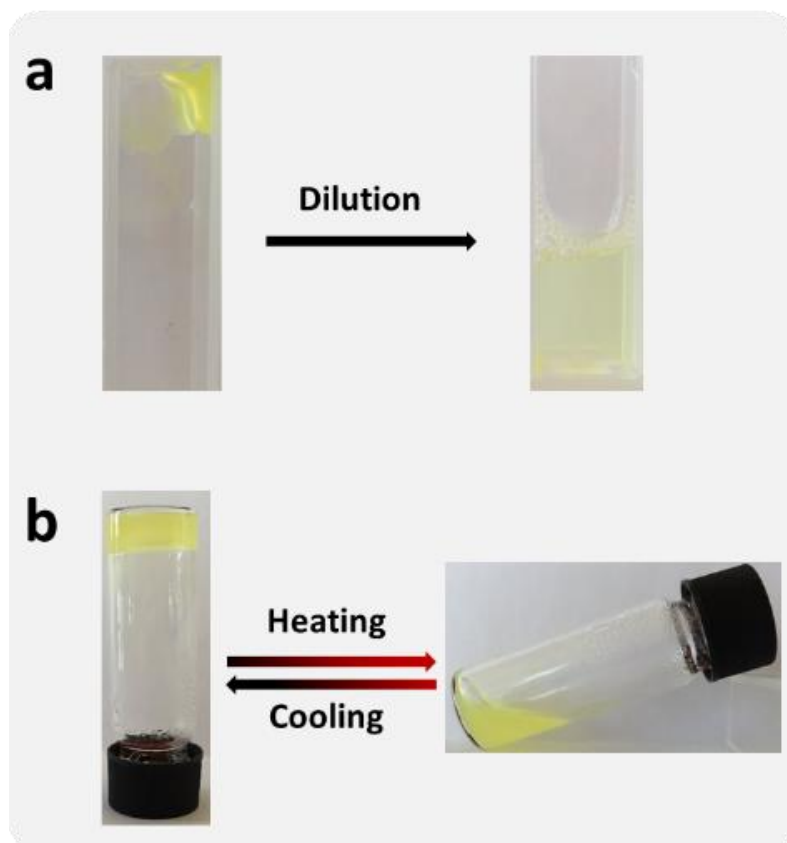


Figure 3.13 (a) Photographs of the dilution effect of the hydrogel from **P2** with CB[8] at 5 wt%; (b) photographs of the inverted vial test demonstrating thermal reversibility of the supramolecular hydrogel.

3.2.5 The reversible transformation from supramolecular hydrogel to covalent hydrogel by photoirradiation

The reversible transformation of the hydrogels from the noncovalent to covalent crosslinks upon photodimerization of the anthracene units was first studied by UV-Vis spectroscopy. As shown in Figure 3.14, **P2** displays absorption peaks at 325, 342, 360, and 385 nm, respectively, indicating the presence of the anthracene group. The addition of CB[8] to the 5 mg/mL solution of **P2** resulted in a decrease in the absorbance of the anthracene groups, indicating that they were encapsulated in the cavity of CB[8]. Upon irradiation of this solution by UV at 365 nm for 10 min, the absorbance peaks of the anthracene groups disappeared completely suggesting that a [4+4] photocyclodimerization of the anthracene groups occurred within the CB[8] cavity, which should lead to the transformation of the non-covalent supramolecular crosslinks to covalent crosslinks. Conversely, a significant increase in the absorbance of the anthracene units was observed after irradiating at 254 nm for 25 min, indicating the cycloreversion of the anthracene dimer, which leads to the transformation of the covalent hydrogel to the non-covalent supramolecular hydrogel.

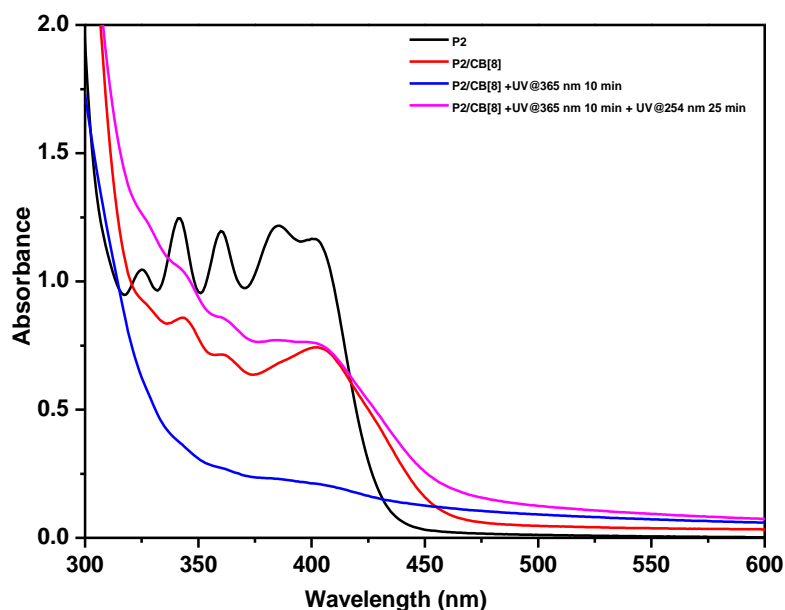


Figure 3.14 The UV-Vis spectra of **P2** (5 mg/mL), and **P2/CB[8]** (0.5 equiv. of anthracene moieties) before and after UV irradiation at 360 nm and 250 nm.

Inspired by the UV-vis spectroscopy results of the reversible transformation of the low concentration solution (5 mg/mL), the transformation of the supramolecular hydrogel to a chemically cross-linked hydrogel was carried out by UV irradiation under identical conditions. Initially, the supramolecular hydrogel from **P2/CB[8]** (5 wt% polymer) was yellow and the yellow color disappeared after UV-irradiation at 365 nm for 10 minutes (Figure 3.15a), which indicates that the transformation to anthracene dimers had taken place. The formation of the chemically cross-linked hydrogel was confirmed by heating it to 70 °C as well as by dilution with water. As shown in Figure 3.15a, the hydrogel was now resistant to heating or dilution, revealing the successful transformation of the supramolecular hydrogel to a covalently crosslinked hydrogel.

We further investigated the reversible transformation of the hydrogel. Part of the covalently crosslinked hydrogel was transferred to a quartz cuvette and UV-irradiated at 254 nm for 40 min. After irradiation the color of the hydrogel changed back to yellow, suggesting the formation of the supramolecular hydrogel. This was further evidenced by the gel-sol transition as shown in Figure 3.15b.

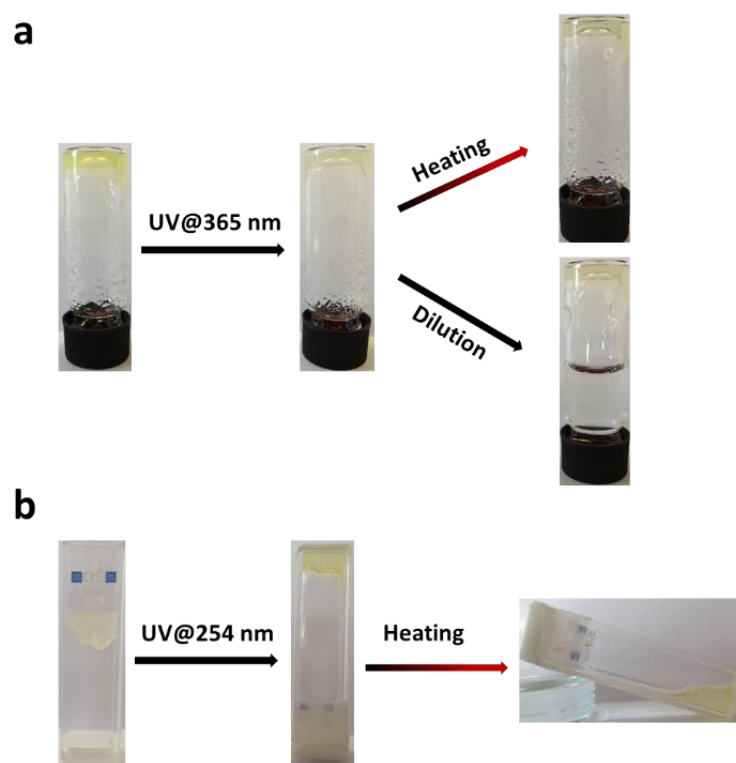


Figure 3.15 (a) Photographs of the hydrogel before and after the UV irradiation at 365 nm, and the inverted vial test demonstrating the stability of the hydrogel; (b) Photographs of the hydrogel before and after the UV irradiation at 254 nm, and the inverted vial test showing the thermal reversibility of the hydrogel.

3.3 Conclusions

In this chapter, a supramolecular hydrogel was developed based on the inclusion complexation of two anthracene moieties with a macrocyclic host as cross-linker. It was demonstrated that such a supramolecular hydrogel could undergo a reversible transformation to the corresponding covalent cross-linked hydrogel driven by the reversible photodimerization of anthracene inside the host cavity. This approach affords a strategy for the reversible transformation between supramolecular to covalently linked hydrogels providing control over the dynamics, shapability and mechanical properties of the hydrogel. Moreover, the effect of the binding affinity of the host-guest interaction to the critical hydrogelation concentration was also investigated, demonstrating the significance of the binding affinity in the construction of a supramolecular hydrogel at lower concentrations. Finally, this chapter also provided an approach of the preparation of anthracene side-chain functionalized acrylate copolymers by post-polymerization modification as the 2-substituted anthracene based acrylate monomer cannot be polymerized by RAFT polymerization since it acts as radical trap.

3.4 Experimental section

3.4.1 Materials

All chemicals and solvents were commercially available and used as received unless otherwise stated. Dichloromethane (DCM), *N,N*-dimethylacetamide (DMA), THF, methanol, CDCl_3 , hexane were obtained from Sigma Aldrich. DCM and THF was purified over aluminum oxide by means of a

solvent purification system from J.C. Meyer when it was used as reaction solvent. Milli-Q Water (18.2 MΩ/cm) was generated using a Millipore Milli-Q academic water purification system. 2-anthracenecarboxylic acid, *N*-acryloylmorpholine and γ -cyclodextrin were obtained from Tokyo Chemical Industry (TCI). 2-(2-Aminoethoxy)ethanol (98%), Di-*tert*-butyldicarbonate (99%), 2-dimethylaminoethanol, 2-bromoethanol, trifluoroacetic acid (TFA, 99%) and pentafluorophenol were purchased from Sigma-Aldrich. Azobisisobutyronitrile (AIBN, 98%, Sigma-Aldrich) was recrystallized from MeOH (2x) and stored in the freezer. Methyl-2-(*n*-butyltrithiocarbonyl)propanoate (MBTTCP) was prepared according to the established procedures.³² Cucurbit[8]urils (CB[8]) was synthesized according to a literature procedure and was kindly provided by Prof. Werner Nau.³³

3.4.2 Analytical techniques

¹H and ¹³C spectra were acquired on a Bruker Avance 400 MHz spectrometer. ¹⁹F NMR spectra were recorded on a Bruker Avance 500 MHz spectrometer. Samples were dissolved in CDCl₃ or CD₃OD. Chemical shifts are expressed in ppm by comparison with the signal of TMS used as an internal standard.

Gas chromatography (GC) was performed on a 7890A from Agilent Technologies with an Agilent J&W Advanced Capillary GC column (30 m, 0.320 mm and 0.25 μ m). Injections were performed with an Agilent Technologies 7693 auto sampler. Detection was done with a FID detector. Injector and detector temperatures were kept constant at 250 and 280 °C, respectively. The column was initially set at 50 °C, followed by two heating stages: from 50 °C to 100 °C with a rate of 20 °C/min and from 100 °C to 300 °C with a rate of 40 °C/min. and then held at this temperature for 0.5 minutes. Conversion was determined based on the integration of monomer peaks using DMA as internal standard.

Size exclusion chromatography (SEC) was performed on an Agilent 1260-series HPLC system equipped with a 1260 online degasser, a 1260 ISO-Pump, a 1260 automatic liquid sampler, a thermostatted column compartment, a 1260 diode array detector (DAD) and a 1260 refractive index detector (RID). Analyses were performed on a PPS Gram30 column in series with a PPS Gram 1000 column at 50 °C. DMA containing 50 mM of LiCl was used as an eluent at a flow rate of 0.6 mL/min. The SEC traces were analysed using the Agilent Chemstation software with the GPC add on. Molar mass and PDI values were calculated against PMMA standards.

Fluorescence measurement were carried out on a Cary Eclipse fluorescence spectrophotometer (Agilent Technologies) equipped with a Varian Cary Temperature Controller. The emission spectra resulting from excitation by a 428.5 nm laser were monitored from 500 -700 nm, and the slit width was kept at 5 nm during the measurements.

3.4.2.1 Job plots (continuous variation method)

The stoichiometry of the self-assembly was determined *via* Job's method of continuous variation.³⁴ A stock solution was prepared for each complementary recognition motif in Milli-Q water in a 5 mL round bottom flask. The appropriate amount from the stock solution was transferred to the UV-Visible cuvette or fluorescence cuvette in which the total concentration of the recognition motifs was kept constant at 50 μ M. The molar fraction of the motifs was varied between 0 and 1. The changes in absorption intensity were multiplied by the molar fraction and plotted vs. molar fraction to construct the Job plot.

3.4.2.2 UV-Vis spectrophotometric titration experiment

UV-Visible titration was performed by adding solutions containing the host (γ -CD or CB[8]) to a solution of the guest (**1a** or **2a**) in a 1 cm path quartz cuvette by using microliter syringes. In all cases the guest was present in the host solution at the same concentration as that in the cuvette to avoid dilution effects. Milli-Q water (18.2 m Ω /cm) was used as solvent for UV-Visible titration. UV-Visible scanning conditions were as follows: Scanning rate = 300 nm/min, bandwidth = 0.5 nm, response time = 0.1 s, accumulations = 1 scan.

3.4.2.3 Photochemical reactions

Photodimerization of anthracene occurred in a Metalight Classic from Primotec equipped with 12 double centered at 365 nm UV lamps of 9 W each; the cycloreversion was performed in a Metalight Classic from Primotec equipped with 12 double centered at 254 nm UV lamps of 9 W each.

3.4.3 Synthesis and characterizations

3.4.3.1 *tert*-butyl (2-(2-hydroxyethoxy) ethyl)carbamate (**1b**)

To a solution of 2-(2-aminoethoxy) ethanol (6.0 g, 56.76 mmol) in anhydrous DCM (75 mL) was added di-*tert*-butyldicarbonate (13.6 g, 62.44 mmol) at 0 $^{\circ}$ C. The reaction solution was warmed to room temperature and stirred overnight. The reaction solution was washed with H₂O (20 mL*4) and dried with anhydrous MgSO₄, filtered. The product was given after removing solvent under vacuum as colorless oil (11.05 g, 94.9%). ¹H NMR: (400 MHz, CDCl₃) δ : 5.04 (br, 1H), 3.76-3.68 (m, 2H), 3.61-3.50 (m, 4H), 3.37-3.25 (m, 2H), 1.43 (s, 9H). ¹³C NMR: (100 MHz, CDCl₃, δ): 156.32, 79.41, 72.37, 70.37, 61.62, 40.42, 28.48. HRMS (ESI, m/z): [M+Na]⁺ calcd for C₉H₁₉NNaO₄, 228.1212; found 228.1207.

3.4.3.2 2-Anthracenecarboxyl chloride

To a solution of 2-anthracenecarboxylic acid (4 g, 18 mmol) in 60 mL SOCl₂ was added one drop of DMF. The solution was stirring 48 h under anhydrous condition at room temperature and the solvent was removed under reduced pressure. The residual amount of SOCl₂ was removed as an azeotrope with toluene (50 mL*2). Pure product was obtained as fine yellow powder in quantitative yields. ¹H

NMR: (400 MHz, CDCl₃) δ : 8.98 (s, 1H, #1), 8.65 (s, 1H, #9), 8.47 (s, 1H, #10), 8.09-8.04 (m, 3H, #4,5,8), 7.97-7.94 (m, 1H, #3), 7.62-7.54 (m, 2H, #6,7). ¹³C NMR: (100 MHz, CDCl₃, δ): 168.41, 137.18, 134.17, 133.07, 132.46, 130.26, 130.07, 129.36, 128.83, 128.40, 127.67, 126.60, 123.65.

3.4.3.3 2-[2-(tert-Butoxycarbonylamino)ethoxy]ethyl-2-anthracenecarboxylate (**1c**)

To the solution of tert-butyl (2-(2-hydroxyethoxy)ethylcarbamate (3.6 g, 17.5 mmol) and Et₃N (2.4 mL, 17.5 mmol) in dry THF (50 mL), 2-Anthracenecarboxyl chloride (2 g, 8.3 mmol) in 30 mL dry THF was added dropwise. This mixture was stirred 24 hours at room temperature. The solvent was removed under reduced pressure. The residue was dissolved with DCM, then the solution was washed with saturated NaHCO₃ aqueous solution (3x), brine (1x) and water (1x). The given solution was dried with MgSO₄ and filtered. The crude product was concentrated and purified by silica chromatography (EtOAc:DCM=1:10 by volume). (2.8 g, 82.8%). ¹H NMR: (400 MHz, CDCl₃) δ : 8.84 (s, 1H, #1), 8.59 (s, 1H, #9), 8.47 (s, 1H, #10), 8.06-7.97 (m, 4H, #3,4,5,8), 7.57-7.49 (m, 2H, #6,7), 4.95 (br, 1H, NH), 4.56 (t, 2H, -C(O)OCH₂-), 3.87 (t, 2H, -C(O)OCH₂CH₂-), 3.64 (t, 2H, -C(O)NHCH₂CH₂-), 3.37 (t, 2H, -C(O)NHCH₂-), 1.42 (s, 9H, -C(CH₃)₃). ¹³C NMR: (100 MHz, CDCl₃, δ): 166.89, 133.27, 132.82, 132.60, 132.14, 130.48, 128.90, 128.63, 128.60, 128.32, 126.92, 126.74, 126.37, 126.04, 124.18, 73.62, 69.22, 64.38, 41.97.

3.4.3.4 2-(2-aminoethoxy)ethyl-2-anthracenecarboxylate (**1a**)

2-[2-(tert-Butoxycarbonylamino)ethoxy]ethyl-2-anthracenecarboxylate (2.7 g, 6.6 mmol) was dissolved in 30 mL of a 1:1 (vol/vol) solution of TFA in CH₂Cl₂. This mixture was stirred for 30 min at room temperature. The solvent was removed under reduced pressure. The residue was taken up by 50 mL CH₂Cl₂ followed by washing with saturated aqueous NaHCO₃ solution and water. The organic phase was dried with Na₂SO₄ and filtered. The result solution was concentrated and subjected to silica column chromatography (methanol (1 M NH₃) / EtOAc =1:20). The fraction containing the product was collected, solvents were removed under reduced pressure and the product was obtained as brown solid (1.95 g, 95.6 %). ¹H NMR: (400 MHz, CDCl₃) δ : 8.84 (s, 1H, #1), 8.59 (s, 1H, #9), 8.47 (s, 1H, #10), 8.06-7.97 (m, 4H, #3,4,5,8), 7.57-7.49 (m, 2H, #6,7), 4.58 (t, 2H, -C(O)OCH₂-), 3.88 (t, 2H, -C(O)OCH₂CH₂-), 3.61 (t, 2H, NH₂CH₂CH₂-), 2.92 (t, 2H, NH₂CH₂-). ¹³C NMR: (100 MHz, CDCl₃, δ): 166.89, 133.27, 132.82, 132.60, 132.14, 130.48, 128.90, 128.63, 128.60, 128.32, 126.92, 126.74, 126.37, 126.04, 124.18, 73.62, 69.22, 64.37, 41.97.

3.4.3.5 2-bromoethyl-2-anthracenecarboxylate (**2c**)

To the solution of 2-bromoethanol (2.04 g, 16.37 mmol) and Et₃N (1.5 mL, 10.9 mmol) in dry THF (40 mL), 2-Anthracenecarboxyl chloride (1.31 g, 5.46 mmol) in 20 mL dry THF was added dropwise. This mixture was stirred 24 hours at room temperature. The solvent was removed under reduced pressure. The residue was dissolved with DCM, then the solution was washed with saturated NaHCO₃ aqueous solution (3x), brine (1x) and water (1x). The given solution was dried with MgSO₄ and filtered. The crude product was concentrated and purified by silica chromatography

(petroleum:EtOAc=10:1 by volume). (1.5 g, 83.6%). ^1H NMR: (400 MHz, CDCl_3) δ : 8.85 (s, 1H, #1), 8.59 (s, 1H, #9), 8.46 (s, 1H, #10), 8.06-7.97 (m, 4H, #3,4,5,8), 7.57-7.49 (m, 2H, #6,7), 4.72 (t, 2H, - $\text{CH}_2\text{CH}_2\text{Br}$), 3.72 (t, 2H, - CH_2Br). ^{13}C NMR: (100 MHz, CDCl_3 , δ): 166.41, 133.37, 132.87, 132.19, 130.45, 129.01, 128.76, 128.63, 128.34, 126.84, 126.42, 126.11, 124.07, 64.53, 29.03. ESI-MS (m/z): $[\text{M}+\text{H}]^+$ calculated for $\text{C}_{17}\text{H}_{14}\text{BrO}_2^+$: 329.01; found: 329.03.

3.4.3.6 2-((anthracene-2-carbonyl)oxy)-N-(2-hydroxyethyl)-N, N-dimethylethan-1-aminium bromide (**2a**)

Mix the 2-bromoethyl-2-anthracenecarboxylate (0.5 g, 1.52 mmol) and 2-Dimethylaminoethanol (764 μL , 7.60 mmol) in 30 mL acetonitrile. The reaction mixture was heated to reflux overnight. A yellow solid was precipitated during this period. The precipitation was filtered off and washed with DCM. After drying under reduced pressure, the pure product (**2a**) was obtained as yellow powder. (yield 0.62 g, 97.6%). ^1H NMR: (400 MHz, CD_3OD , ppm) δ : 8.89 (s, 1H, #1), 8.70 (s, 1H, #9), 8.56 (s, 1H, #10), 8.16-8.08 (m, 3H, #4,5,8), 8.02-7.96 (m, 1H, #3), 7.61-7.52 (m, 2H, #6,7), 4.91 (m, 2H, - $\text{C}(\text{O})\text{OCH}_2-$), 4.12-4.06 (m, 2H, - $\text{NCH}_2\text{CH}_2\text{OH}$), 4.05-4.03 (m, 2H, - $\text{C}(\text{O})\text{OCH}_2\text{CH}_2-$), 3.72-3.69 (m, 2H, - CH_2OH), 3.38 (s, 6H, - $\text{N}(\text{CH}_3)_2$). ^{13}C NMR: (100 MHz, CD_3OD , δ): 167.21, 134.88, 134.12, 133.83, 133.67, 131.63, 130.00, 129.96, 129.50, 129.28, 127.99, 127.41, 127.27, 127.20, 124.53, 67.73, 65.23, 59.60, 56.91, 53.07. ESI-MS (m/z): $[\text{M}-\text{Br}]^+$ calculated for $\text{C}_{21}\text{H}_{24}\text{NO}_3^+$: 338.17; found: 338.10.

3.4.3.7 Pentafluorophenyl acrylate

Pentafluorophenol (9.0 g, 48.90 mmol) and triethylamine (7.5 mL, 53.79 mmol) were dissolved in 250 mL dry DCM and cooled to 0 $^\circ\text{C}$. To this solution, acryloyl chloride (4.4 mL, 53.79) in 100 mL dry DCM was added dropwise, and the mixture was stirred and let warm to room temperature overnight. The product was obtained after washing the organic phase with water (200 x 3). 9.59 g product was obtained by drying in oven (yield, 82%). ^1H NMR: (400 MHz, CDCl_3 , ppm) δ : 6.72 (dd, 1H, - $\text{CHCHC}(\text{O})-$, cis position with respect to carbonyl group), 6.37 (dd, 1H, $\text{CH}_2\text{CH}-$), 6.18 (dd, 1H, - $\text{CHCHC}(\text{O})-$, trans position with respect to carbonyl group). ^{13}C NMR: (100 MHz, CDCl_3 , ppm) δ : 161.82, 142.59, 140.95, 140.04, 139.32, 138.42, 136.85, 135.64, 125.49. ^{19}F NMR: (470 MHz, CDCl_3 , ppm) δ : -152.61 (m, 2F, ortho), -158.00 (t, 1F, para), -162.37 (m, 2F, meta). GC was measured for purification (>99%).

3.4.3.8 Poly(N-acryloylmorpholine-co-pentafluorophenyl acrylate) (PNAM-PFPA, **P0**)

Monomer NAM (8.8 mL, 70 mmol, 1552 equiv) and PFPA (0.356 mL, 2.16 mmol, 48 equiv), RAFT agent MBTTCP (11.38 mg, 0.045 mmol, 1 equiv), AIBN (0.74mg, 0.0015mmol, 0.1 equiv) and 1.5 mL DMA were dissolved in 23.539 mL dioxane. The concentration of the monomer was fixed at 2 M. After three freeze-pump-thaw cycles, the flask was filled with argon, and a t0 sample was taken using a degassed syringe. The flask was immersed in a preheated oil bath of 70 $^\circ\text{C}$ and stirred for 3 hours. The samples for kinetic study was taken every 30 minutes during reaction. The polymerization was stopped by quenching the reaction with liquid nitrogen. The polymer were precipitated in ice-cold methanol, the isolated polymer was redissolved in THF and precipitated in methanol for another 3 times. The final resulting polymer were dried under reduced pressure for 24 hours at 40 $^\circ\text{C}$ before

further analysis. SEC: Mn=67.9 KDa, Đ=1.46; ^{19}F NMR (470 MHz, CDCl_3 , ppm) δ : -152.9 (bm, 2F, ortho), -156.08 (bs, 1F, para), -160.09 (bm, 2F, meta). FT-IR: ν/cm^{-1} =1776 (C=O of PFP-ester), 1520 (aryl from PFP).

3.4.3.9 Post-polymerization modification of pNAM-PFPA by **1a** (P1)

P0 (3.6 g, PFP units, 1 equiv.) and di(ethylene glycol) methyl ether acrylate (mDEGA) (5 μL) were dissolved in DMF solvent and degassed by nitrogen bubbling for 20 min. Then anthracene derivative **1a** (350 mg, 1.5 equiv.) and catalytic amount of TEA were quickly added to the polymer solution, and the mixture was stirred at 80 $^\circ\text{C}$ overnight. The solution was transferred in to a dialysis bag (MWCO=3.5KDa) and dialyzed against water for 1 week. The product was isolated by freeze-drying as a yellowish solid. SEC (DMA): Mn=71.27 KDa, Đ=1.42. ^1H NMR (400 MHz, CDCl_3 , ppm) δ : 8.24 (bs, #1 of anthracene), 8.62 (bs, #9 of anthracene), 8.46 (bs, #10 of anthracene), 8.02 (bm, #3-5, 8 of anthracene), 7.53 (bm, #6, 7 of anthracene), 4.57 (m, $-\text{C}(\text{CO})\text{CH}_2-$), 4.00-3.08 (bs, morpholine and ethylene glycol), 2.77-2.17 (bs, back bone), 1.98-0.98 (bm, backbone). No signal was presented in ^{19}F NMR. FT-IR: ν/cm^{-1} =1715 (C=O of anthracene ester).

3.4.3.10 Post-polymerization modification of pNAM-PFPA by **2a** (P2)

P0 (1.0 g, PFP units, 1 equiv.) were dissolved in DMF solvent and degassed by nitrogen bubbling for 20 min. Then anthracene derivative **2a** (104 mg, 1.2 equiv) and catalytic amount of DMAP were quickly added to the polymer solution, and the mixture was stirred at 85 $^\circ\text{C}$ overnight. The solution was transferred in to a dialysis bag (MWCO=3.5KDa) and dialyzed against water for 1 week. The product was isolated by freeze-drying as a yellowish solid. SEC (DMA): Mn=67.72 KDa, Đ=1.46. ^1H NMR (400 MHz, CDCl_3 , ppm) δ : 8.24 (bs, #1 of anthracene), 8.62 (bs, #9 of anthracene), 8.46 (bs, #10 of anthracene), 8.02 (bm, #4, 5, 8 of anthracene), 7.92 (bm, #3 of anthracene), 7.53 (bm, #6, 7 of anthracene), 4.98 (backbone- $\text{C}(\text{O})\text{OCH}_2-$), 4.57 (m, $-\text{C}(\text{CO})\text{CH}_2-$), 4.00-3.08 (bs, morpholine and ethylene glycol), 2.77-2.17 (bs, back bone), 1.98-0.98 (bm, backbone). No signal was presented in ^{19}F NMR. FT-IR: ν/cm^{-1} =1742 (C=O of ester linked to backbone), 1715 (C=O of anthracene ester).

3.5 References

1. Schlaad, H.; Diehl, C.; Gress, A., *et al.*, *Macromol. Rapid Commun.* **2010**, *31* (6), 511-525.
2. Wang, C.-H.; Hwang, Y.-S.; Chiang, P.-R., *et al.*, *Biomacromolecules* **2012**, *13* (1), 40-48.
3. Pathak, C. P.; Sawhney, A. S.; Hubbell, J. A., *J. Am. Chem. Soc.* **1992**, *114* (21), 8311-8312.
4. Kurisawa, M.; Chung, J. E.; Yang, Y. Y., *et al.*, *Chem. Commun.* **2005**, (34), 4312-4314.
5. Rydholm, A. E.; Bowman, C. N.; Anseth, K. S., *Biomaterials* **2005**, *26* (22), 4495-4506.
6. Pritchard, C. D.; O'Shea, T. M.; Siegwart, D. J., *et al.*, *Biomaterials* **2011**, *32* (2), 587-597.
7. Zhang, H.; Qadeer, A.; Mynarcik, D., *et al.*, *Biomaterials* **2011**, *32* (3), 890-898.
8. Dargaville, T. R.; Lava, K.; Verbraeken, B., *et al.*, *Macromolecules* **2016**, *49* (13), 4774-4783.
9. Brochu, A. B. W.; Craig, S. L.; Reichert, W. M., *J. Biomed. Mater. Res. A* **2011**, *96A* (2), 492-506.
10. N. A. Peppas; Y. Huang; M. Torres-Lugo, *et al.*, *Annu. Rev. Biomed. Eng.* **2000**, *2* (1), 9-29.
11. Wei, H.; He, J.; Sun, L.-g., *et al.*, *Eur. Polym. J* **2005**, *41* (5), 948-957.
12. Nielsen, A. L.; Madsen, F.; Larsen, K. L., *Drug Delivery* **2009**, *16* (2), 92-101.
13. Miyamae, K.; Nakahata, M.; Takashima, Y., *et al.*, *Angew. Chem. Int. Ed.* **2015**, *54* (31), 8984-8987.
14. Chujo, Y.; Sada, K.; Nomura, R., *et al.*, *Macromolecules* **1993**, *26* (21), 5611-5614.
15. Zheng, Y.; Micic, M.; Mello, S. V., *et al.*, *Macromolecules* **2002**, *35* (13), 5228-5234.
16. Yokoe, M.; Yamauchi, K.; Long, T. E., *J. Polym. Sci., Part A: Polym. Chem.* **2016**, *54* (15), 2302-2311.
17. Xu, J.-F.; Chen, Y.-Z.; Wu, L.-Z., *et al.*, *Org. Lett.* **2013**, *15* (24), 6148-6151.
18. Lagona, J.; Mukhopadhyay, P.; Chakrabarti, S., *et al.*, *Angew. Chem. Int. Ed.* **2005**, *44* (31), 4844-4870.
19. Appel, E. A.; Loh, X. J.; Jones, S. T., *et al.*, *J. Am. Chem. Soc.* **2012**, *134* (28), 11767-11773.
20. Ji, Z.; Li, Y.; Ding, Y., *et al.*, *Polym. Chem.* **2015**, *6* (38), 6880-6884.
21. Ma, X.; Tian, H., *Acc. Chem. Res.* **2014**, *47* (7), 1971-1981.
22. Liu, Y.; Yu, Y.; Gao, J., *et al.*, *Angew. Chem.* **2010**, *122* (37), 6726-6729.
23. Appel, E. A.; Forster, R. A.; Koutsioubas, A., *et al.*, *Angew. Chem. Int. Ed.* **2014**, *53* (38), 10038-10043.
24. Liu, Y.; Huang, Z.; Tan, X., *et al.*, *Chem. Commun.* **2013**, *49* (51), 5766-5768.
25. Liu, Y.; Yang, H.; Wang, Z., *et al.*, *Chem. Asian J.* **2013**, *8* (8), 1626-1632.
26. Tamaki, T.; Kokubu, T., *J. Inclusion Phenom.* **1984**, *2*, 815-822.
27. Tamaki, T., *Chem. Lett.* **1984**, *13* (1), 53-56.
28. Tamaki, T.; Kokubu, T.; Ichimura, K., *Tetrahedron* **1987**, *43* (7), 1485-1494.
29. Fares, M. M.; Al - Shboul, A. M., *J. Biomed. Mater. Res. A* **2012**, *100A* (4), 863-871.
30. Natori, S. H.; Gomei, Y.; Higuchi, A., *J. Biomed. Mater. Res. B Appl. Biomater.* **2006**, *78B* (2), 318-326.
31. Štolka, M., *Macromolecules* **1975**, *8* (1), 8-9.
32. Urbani, C. N.; Monteiro, M. J., *Macromolecules* **2009**, *42* (12), 3884-3886.
33. Kim, J.; Jung, I.-S.; Kim, S.-Y., *et al.*, *J. Am. Chem. Soc.* **2000**, *122* (3), 540-541.
34. Renny, J. S.; Tomasevich, L. L.; Tallmadge, E. H., *et al.*, *Angew. Chem. Int. Ed.* **2013**, *52* (46), 11998-2013.

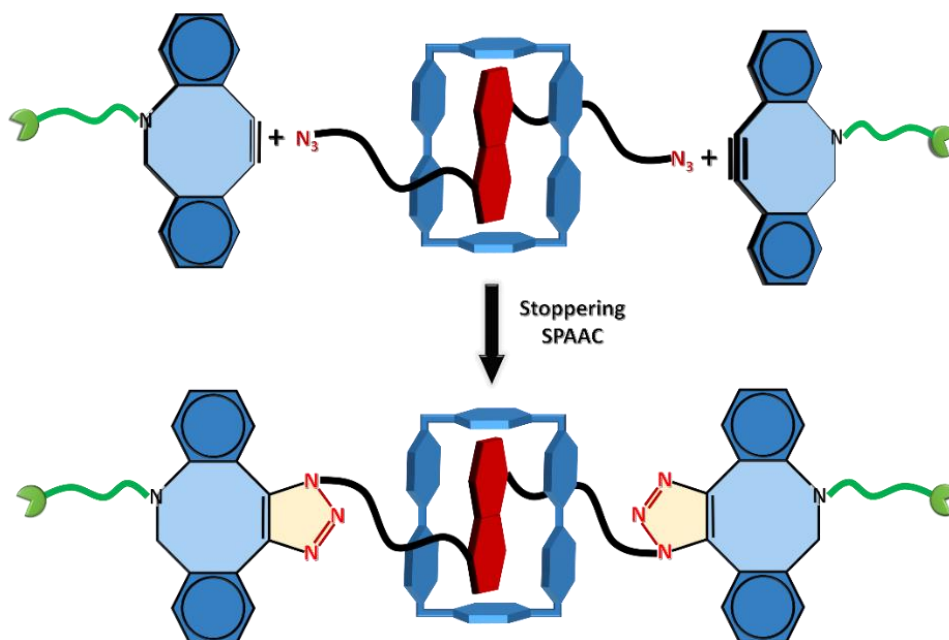
Chapter 4 A Dibenzoazacyclooctyne as a Reactive Chain Stopper for [2]rotaxanes

This chapter was published as:

Hou, Z., Yeniad, B., Van Guyse, J., Woisel, P., Mullen, K., Rutjes, F., Van Hest, J. and Hoogenboom, R., A dibenzoazacyclooctyne as a reactive chain stopper for [2]rotaxanes. *Eur. J. Org. Chem.* **2017**, 3107-3113.

My contribution includes the experiments for the formation of the rotaxanes, the interpreting of the results and the writing of the manuscript. Starting materials were provided by collaborating laboratories.

Abstract: A strained dibenzoazacyclooctyne (DIBAC) derivative was introduced for the preparation of a rotaxane by strain-promoted azide–alkyne cycloaddition (SPAAC), also referred to as a copper-free click reaction. The DIBAC can efficiently act as a bulky reactive chain stopper to transform a pseudorotaxane architecture consisting of a diazo-functionalized dialkoxynaphthalene guest and a tetracationic cyclobis(paraquat-*p*-phenylene) (CBPQT⁴⁺) host into the corresponding [2]rotaxane. Furthermore, the use of the DIBAC is demonstrated to be limited to short rigid macrocycles, as it is unable to act as stopper for a rotaxane featuring a larger crown ether macrocyclic host.



4.1 Introduction

The most recently introduced type of isomeric organic molecules¹ are mechanically interlocked molecules (MIMs) such as catenanes, rotaxanes, and knots, the inspiration for which came from various natural objects and architectures.²⁻⁵ MIMs have attracted increasing attention for over 50 years owing to their wide range of potential applications in molecular devices such as artificial machines,⁶⁻¹⁰ muscles,¹¹ elevators,¹² switches,¹³⁻¹⁴ and pumps¹⁵. It is noteworthy that the 2016 Nobel Prize was awarded for work in this area.¹⁶⁻²⁴ The rotaxane structure, as one type of mechanically interlocked molecule, has been considered as a versatile platform for the construction of functional artificial nanomachines.²⁵⁻²⁷ Therefore, the development of highly efficient synthetic strategies for the preparation of rotaxanes should facilitate the further development of this research area. The synthetic strategies for the preparation of rotaxanes range from statistical threading to directed template synthesis.²⁸⁻²⁹ In recent years, rotaxanes were mainly synthesized by either “clipping” a partially formed macrocycle around a dumbbell,^{27, 30-33} “slipping” the macrocycle over the bulky ends of the dumbbell,³⁴ or by single or double “stoppering” of a pseudorotaxane with bulky stoppers; the double-stoppering strategy employed in this work is illustrated in Figure 4.1. The stoppering approach is most widely used to make rotaxanes, especially if cyclobis(paraquat-p-phenylene) (CBPQT⁴⁺), also named blue box, is employed as the macrocyclic host to construct rotaxanes.³⁵⁻³⁸

The Cu^I-catalyzed azide–alkyne cycloaddition (CuAAC), often referred to as a click reaction,³⁹ has frequently been utilized in the stoppering strategy for the creation of rotaxanes owing to its high regioselectivity, tolerance to sensitive functional groups, and mild reaction conditions.^{35, 38, 40} However, it is commonly performed in the presence of copper ions, which increase the complexity of the workup procedure and may interfere with the pseudorotaxane formation if metal templates are involved in the assembly process. Therefore, the interest in methods involving metal-free click reactions to replace CuAAC is growing.⁴¹⁻⁴³ Rotaxanes have already been prepared by the metal-free cycloadditions of azides with bulky acetylenedicarboxylates⁴² as well as through cucurbituril-catalyzed azide–alkyne cycloaddition.⁴⁴ Several strain-promoted copper-free systems, such as oxanorbornadienes,⁴⁵⁻⁴⁶ cyclooctynes,⁴⁷⁻⁴⁹ and dibenzocyclooctynes⁵⁰⁻⁵³ have been developed for fast and selective reactions with azides, commonly referred to as strain-promoted azide–alkyne cycloaddition (SPAAC). To the best of our knowledge, there is only one previous report in which dibenzocyclooctyne was employed to construct a [2]rotaxane.⁵⁴ However, that study only utilized the dibenzocyclooctyne to evaluate a new route for the synthesis of a [2]rotaxane under solvent-free conditions without any further emphasis on its use as a stopper or the evaluation of its scope as a stopper to prepare compact [2]rotaxanes. Herein, we introduced a dibenzoazacyclooctyne (DIBAC) derivative to prepare a compact [2]rotaxane through this methodology and further addressed its scope as a stopper.

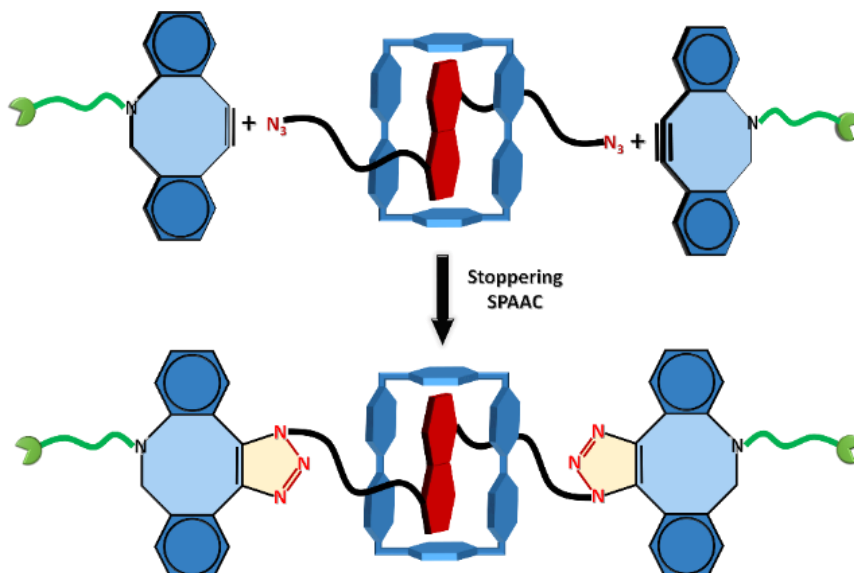


Figure 4.1 Graphical representation of the double stoppering of a pseudo-rotaxane to form a [2]rotaxane.

4.2 Results and discussion

In this chapter, we introduced a DIBAC derivative for the preparation of [2]rotaxanes, as we anticipated that it could act simultaneously as a reactive group and a bulky stopper to yield very compact [2]rotaxanes. Moreover, the commercial availability of various DIBAC derivatives further expands the applicability of such a synthetic protocol. The occurrence of the SPAAC reaction at room temperature or below is ideal for strong supramolecular binding, for example, of the CBPQT⁴⁺ ring to a variety of thread molecules with π -electron-donating nature, to form pseudorotaxanes efficiently. Strong supramolecular binding is a prerequisite for efficient rotaxane synthesis, which is often performed at room temperature or below.^{35,55} As a first step in this work, the reactivity of the DIBAC derivative in acetonitrile at 0 °C was investigated by mixing a stoichiometric ratio of the DIBAC with 1,5-dialkoxynaphthalene (DNP) derivative **1** carrying azido-terminated glycol chains. The reaction solution was stirred for 48 h and then analyzed by ESI-MS without further purification, and the results obtained by both positive and negative ionization modes revealed the high reactivity of the cyclooctyne stopper, as only the dumbbell formed through the reaction with DIBAC was detected together with a trace amount of the excess free DIBAC stopper molecules (Figure 4.2). The obtained dumbbell was then mixed with excess CBPQT⁴⁺PF₆ in acetonitrile to examine whether the stopper can effectively prevent the threading of the CBPQT⁴⁺ ring over the chain stoppers of the dumbbell molecule to form the rotaxane architecture and provide a first indication of the possible use of the DIBAC as a chain stopper. No color change was observed upon the addition of the CBPQT⁴⁺PF₆ macrocycle to the dumbbell, whereas the direct addition of the CBPQT⁴⁺PF₆ solution to a solution of DNP **1** caused the immediate appearance of a pink-purple color. These visual observations were confirmed by UV/Vis spectroscopy, which indicated the ability of the DIBAC to act as chain stopper to prevent the threading of the CBPQT⁴⁺ macrocycle over the dumbbell (Figure 4.3).

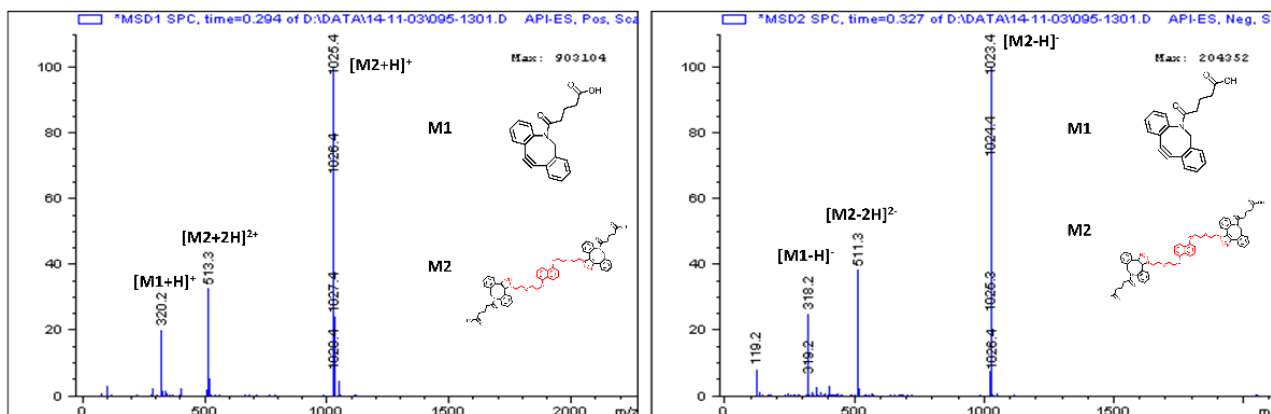


Figure 4.2 ESI-MS spectra of dumbbell molecule 4 (left: positive model, right: negative model)

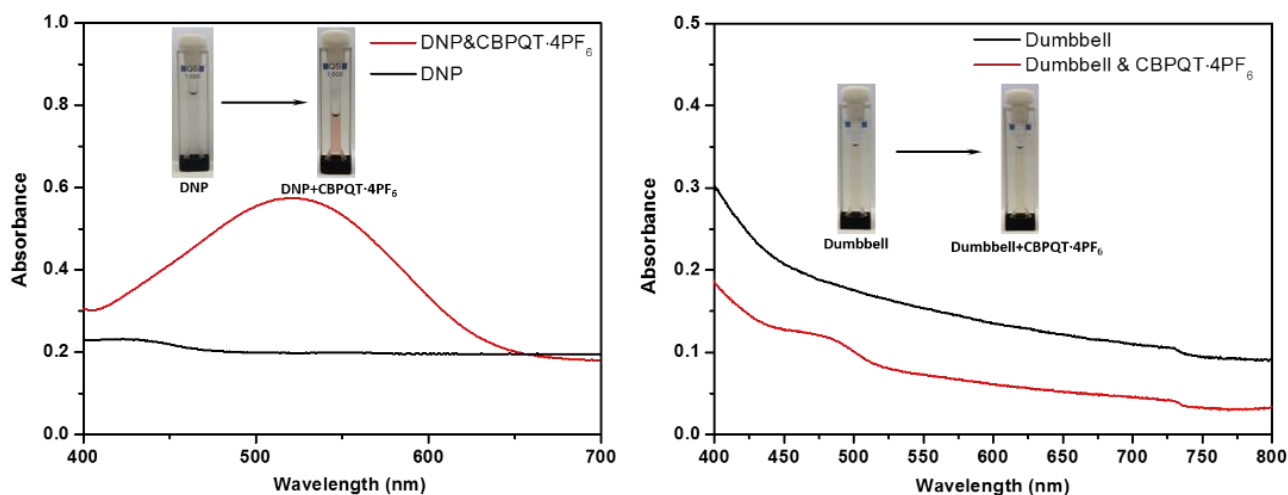
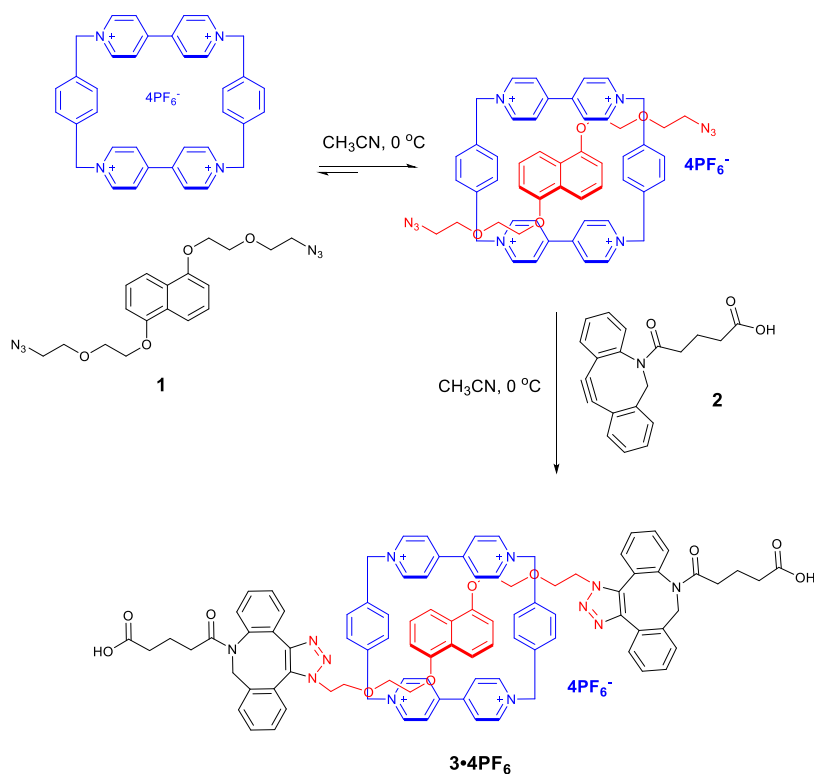


Figure 4.3 UV-Vis spectra of before (black) and after (red) the addition of CBPQT-4PF₆ to DNP (left) and dumbbell 4 (right).

Stimulated by these promising results, we synthesized the [2]rotaxane **3**·4PF₆ by the “threading-followed-by-stoppering” strategy (Figure 4.1 and Scheme 4.1). Firstly, the two recognition elements, the DNP **1** thread molecule and the CBPQT⁴⁺ macrocycle, were mixed at 0 °C to form the pseudorotaxane, as evidenced by the appearance of the characteristic purple color of the DNP-CBPQT⁴⁺ host-guest donor-acceptor complex. The rotaxane was then synthesized by the addition of the DIBAC stopper **2**, and the pure rotaxane **3**·4PF₆ could be isolated in 61 % yield by preparative TLC after the reaction mixture was stirred for 2 days at 0 °C.



Scheme 4.1 The general synthetic route to [2]rotaxane **3**·4PF₆ (Note that only one triazole isomer is shown for simplicity).

The [2]rotaxane **3**·4PF₆ was characterized by ¹H NMR spectroscopy, matrix-assisted laser-desorption/ionization time-of-flight (MALDI-TOF) mass spectrometry, and size-exclusion chromatography (SEC). Unfortunately, the rather complex structure of the obtained rotaxane, including the possible formation of different triazole isomers as well as different protonation states of the triazole and carboxylic acid groups, possibly in combination with limited mobility of certain parts of the structure led to broadened signals and a complicated ¹H NMR spectrum, which made a full assessment of the purity difficult. Nonetheless, as shown in Figure 4.4, the resonance signals of DNP shifted upfield owing to shielding by the CBPQT⁴⁺ ring, as is typical for a rotaxane containing CBPQT⁴⁺ and DNP. The shift and broadening of the resonance signals of CBPQT⁴⁺ further confirmed the formation of a CBPQT⁴⁺-DNP donor-acceptor charge-transfer complex.³⁵ The slow rotations of the bipyridinium units and *p*-phenylene rings in CBPQT⁴⁺ are reflected by the broad proton resonances at 298 K. These signals coalesce into narrower peaks at higher temperature, especially those of the β protons of the bipyridinium groups.

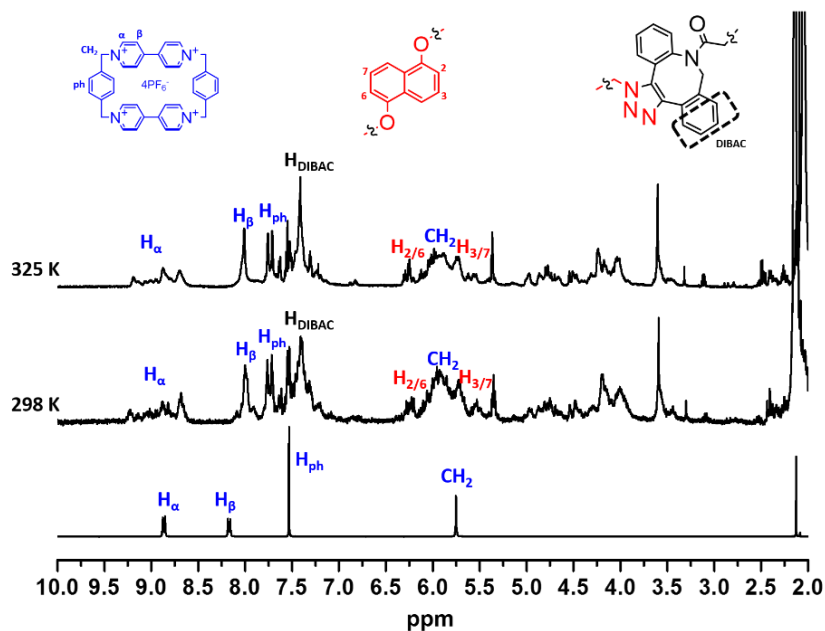


Figure 4.4 Partial ¹H NMR spectra (500 MHz, CD₃CN) of the [2]rotaxane **3**·4PF₆ at different temperatures (top: 325 K, middle: 298 K) and CBPQT·4PF₆ (bottom).

The MALDI-TOF mass spectrum of the [2]rotaxane confirmed its purity (Figure 4.5) as it only showed the peaks corresponding to the rotaxane with different numbers of PF₆⁻ counterions, that is, [M-4PF₆⁻+3e]⁺, [M-3PF₆⁻+2e]⁺, and [M-PF₆⁻+e]⁺. Furthermore, the observation of the intact rotaxane by MALDI-TOF MS indicates that the DIBAC-based stoppers are large enough to block the CBPQT⁴⁺ macrocycle on the chain. Finally, the obtained [2]rotaxane dissolved in 1,1,1,3,3,3-hexafluoroisopropanol was analyzed by SEC; the intact rotaxane eluted over the column, as detected by the UV signal at λ=520 nm (Figure 4.6), which further confirmed the stability of the obtained rotaxane.

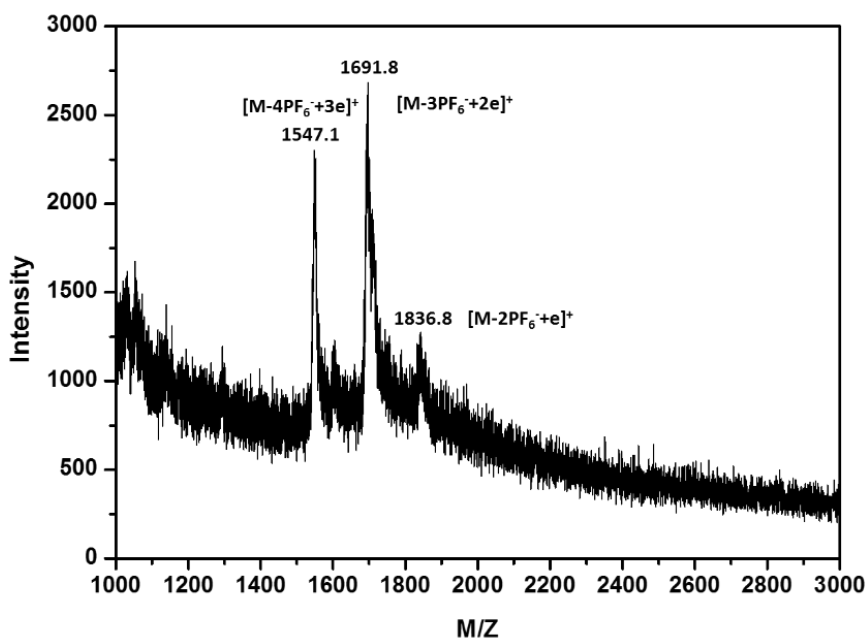


Figure 4.5 MALDI-TOF mass spectrum of the [2]rotaxane **3**·4PF₆

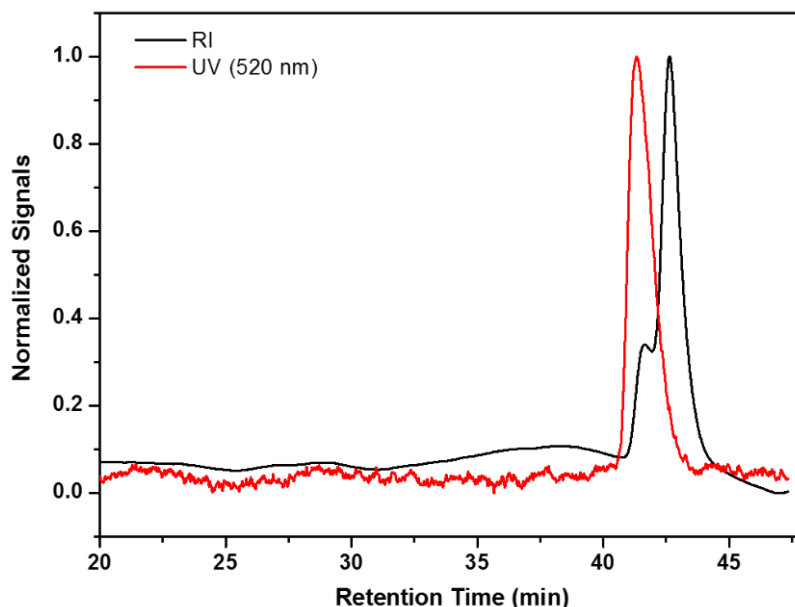


Figure 4.6 SEC trace in HFIP of the [2]rotaxane $3:4PF_6$.

To further evaluate the stability of the formed rotaxane $3:4PF_6$, the rotaxane solution was heated from 10 to 80 °C and monitored by UV/Vis spectroscopy. The temperature-dependent UV/Vis spectra are shown in Figure 4.7 and revealed that the absorption intensity of the rotaxane was constant at ca. 0.55 during the heating process. The minor decrease in absorption can be ascribed to the faster exchange between the complexed and uncomplexed forms of DNP and $CBPQT^{4+}$ resulting from the movement of $CBPQT^{4+}$ along the chain as well as a lowering of the concentration due to expansion of the solvent. In contrast, the heating of a solution of the precursor pseudorotaxane consisting of DNP **1** and $CBPQT^{4+}$ led to a strong decrease in absorption intensity upon heating indicating dethreading and loss of the pseudorotaxane structure. Thus, these comparative results indicate that rotaxane $3:4PF_6$ is stable at elevated temperatures and confirm that the DIBAC-based stopper is large enough to stabilize the rotaxane structure, even at elevated temperature. Furthermore, these results also confirmed the purity of the product and again suggested that no semi(pseudo)rotaxane is present.

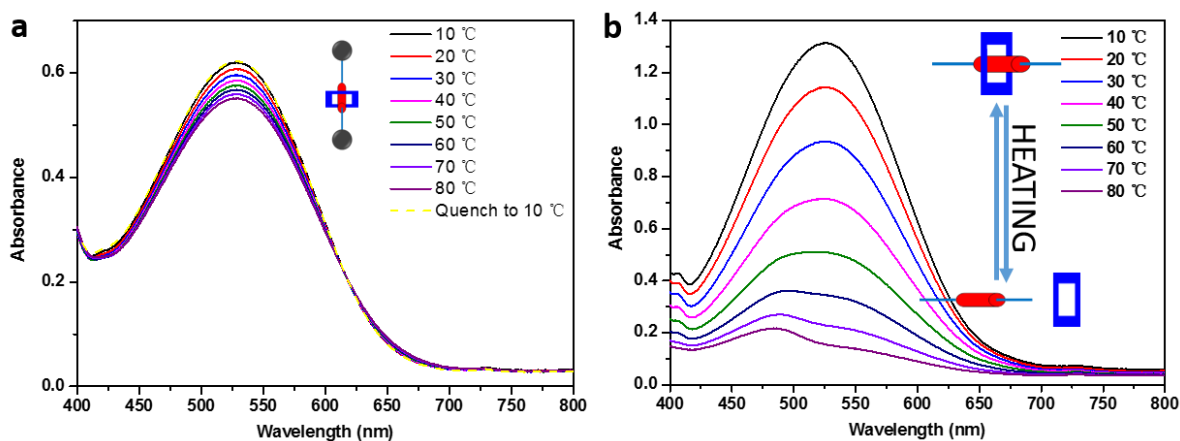


Figure 4.7 Temperature-dependent UV/Vis spectra of (a) rotaxane $3:4PF_6$ and (b) the corresponding pseudorotaxane of DNP **1** with $CBPQT^{4+}$ in acetonitrile.

In addition to its thermal stability, the stability of the rotaxane **3**·4PF₆ was also studied towards a competing guest molecule, tetrathiafulvalene (TTF), which has a much higher association constant for complexation with CBPQT⁴⁺ than that of the dialkoxynaphthalene present in the rotaxane. Moreover, the host-guest complex formed by CBPQT⁴⁺ and TTF exhibits a distinct green color, which is readily distinguishable from the purple CBPQT⁴⁺-DNP complex and allows the straightforward evaluation of the competition experiments. Upon the addition of some drops of concentrated TTF solution to a solution of rotaxane **3**·4PF₆, no clear color change was observed; therefore, no exchange was possible, and the stability of the rotaxane was confirmed (Figure 4.8). The minor change in color is most likely caused by the partial charge-transfer interaction between TTF and the CBPQT⁴⁺ ring through the complexation of TTF to the outer part of the CBPQT⁴⁺ ring. In contrast, the addition of TTF to the solution of the pseudorotaxane immediately resulted in the formation of a green solution, which is characteristic of the formation of the CBPQT⁴⁺ complex with TTF.⁵⁶ These competition experiments were also monitored by UV/Vis spectroscopy, which supported the visual observations. The UV/Vis spectra for the competition experiment with the rotaxane suggest that the naphthalene-CBPQT⁴⁺ charge-transfer absorption band, centered at $\lambda \approx 520$ nm, did not decrease upon the addition of TTF, although a new absorption band at $\lambda \approx 800$ nm most likely results from the charge-transfer interaction between TTF and the outside of the CBPQT⁴⁺ ring or trace amount of free CBPQT⁴⁺ owing to the incomplete purification. For the pseudorotaxane, the absorption band of the CBPQT⁴⁺ complex with DNP disappeared upon the addition of TTF, and a new quite strong absorption band at $\lambda = 800$ nm was ascribed to the CBPQT⁴⁺ complex with TTF. These observations demonstrate that the rotaxane is stable against the competing guest and give further evidence that the DIBAC derivative is large enough to act as stopper for the preparation of rotaxanes.

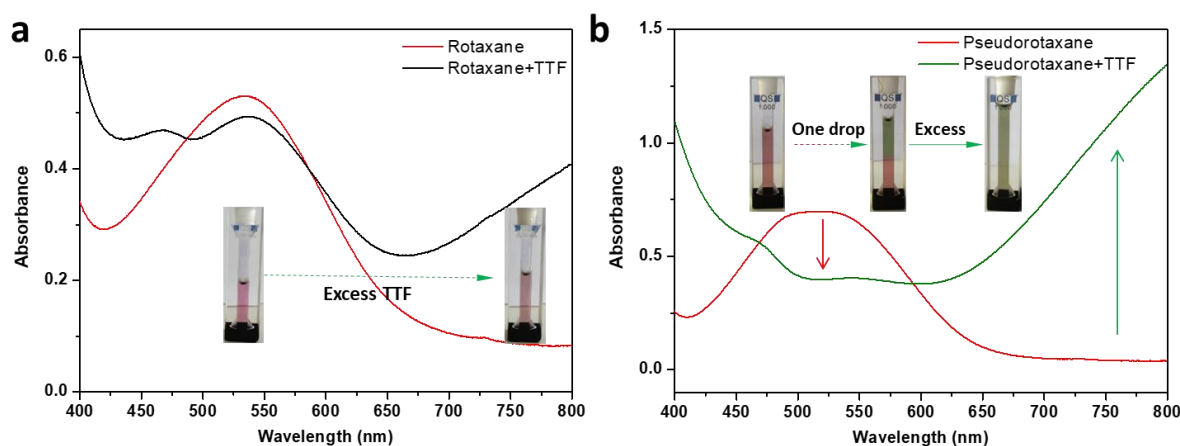
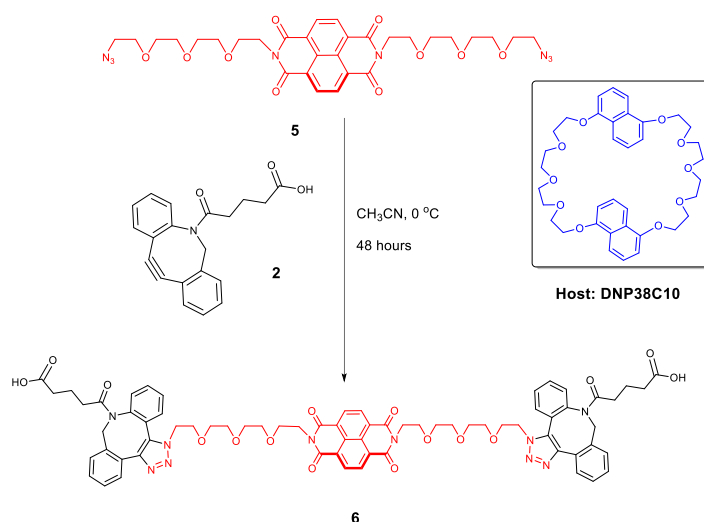


Figure 4.8 UV/Vis spectra of (a) rotaxane **3**·4PF₆ and (b) the corresponding pseudorotaxane of DNP **1** with CBPQT⁴⁺ in the absence and presence of an excess of TTF in acetone at 25°C.

To investigate the broader scope of the use of the DIBAC for the construction of macrocyclic host-based rotaxanes, it was evaluated for the preparation of a [2]rotaxane based on 1,5-dinaphtho[38]crown-10 (DNP38C10; see Scheme 4.2) as a macrocyclic host with a larger and more flexible cavity than that of CBPQT⁴⁺. Therefore, a dumbbell was prepared by reacting the 2,7-bis(2-(2-[2-(2-azidoethoxy)ethoxy]ethoxy)ethyl)benzo[1,2,3,4]phenanthroline-1,3,6,8(2H,7H)-tetraone

(5) guest molecule with DIBAC **2**. The ESI-MS results of the reaction solution (Figure 4.9) indicated the quantitative formation of the double-stoppered dumbbell, as only the dumbbell and trace amount of excess free DIBAC stopper molecules were detected. Additionally, a minor excess of DIBAC that would not interfere with the formation of the host-guest rotaxane. As depicted in Figure 4.10, the exposure of this dumbbell solution to a concentrated DNP38C10 solution in CDCl_3 revealed the immediate appearance of a pink color, which indicates the donor-acceptor host-guest complexation of DNP38C10 and the naphthodiimide unit. This observation was further confirmed by UV/Vis spectroscopy, which revealed the characteristic charge-transfer absorption band of the DNP38C10-**5** complex centered at $\lambda \approx 520$ nm. These results suggest that the cavity size of DNP38C10 is significantly larger than that of the DIBAC derivative in the dumbbell, which no longer acts as an efficient stopper. A comparison of the ^1H NMR spectrum of the bare dumbbell with that of the mixture with DNP38C10 revealed the expected partial upfield shift of the naphthodiimide proton resonances, similar to those for a mixture of DNP38C10 with **5** (Figure 4.11). These ^1H NMR spectroscopy results confirm that the DIBAC derivative cannot be used to construct rotaxanes with this larger macrocyclic ring.



Scheme 4.2 The general synthetic route to dumbbell **6**; only one triazole isomer is shown for simplicity (the inset shows the structure of host macrocycle DNP38C10).

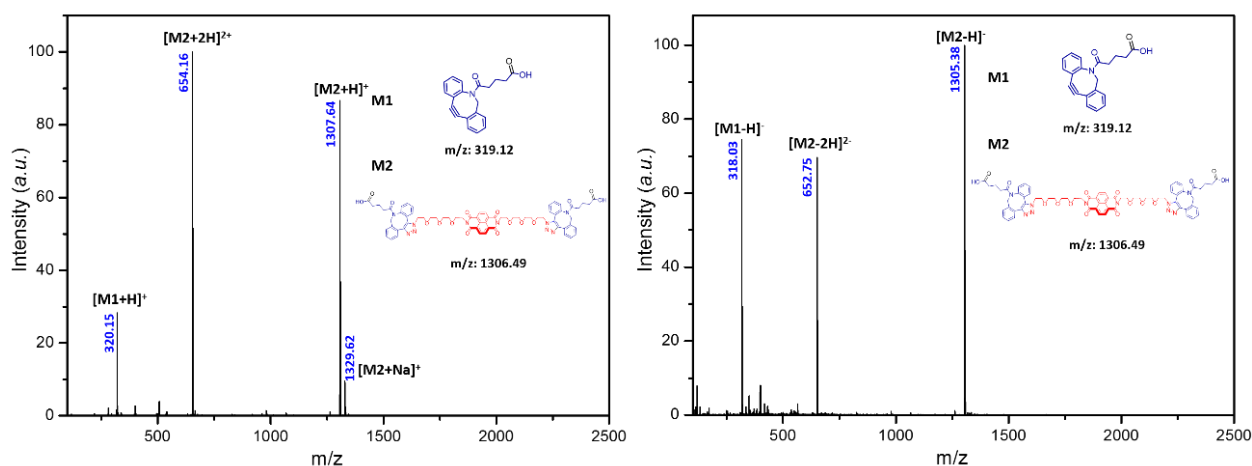


Figure 4.9 ESI-MS spectra of dumbbell molecule 6 (left: positive model, right: negative model)

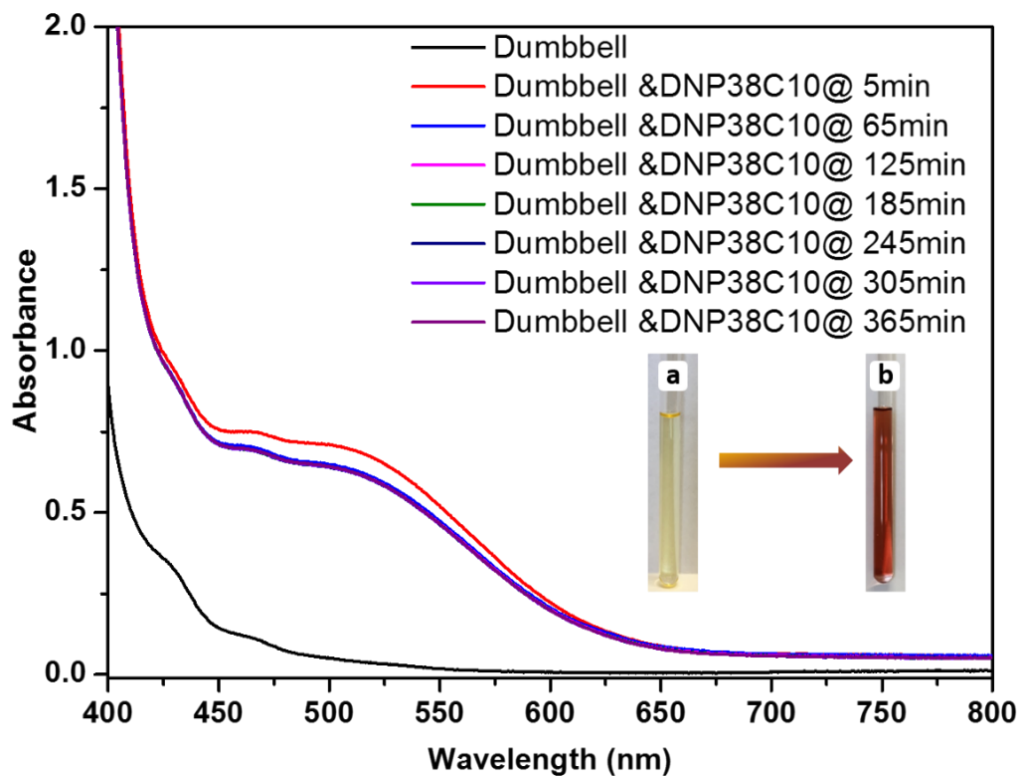


Figure 4.10 UV-Vis spectra of before and after the addition of concentrated DNP38C10 to dumbbell 6. The inset photographs showing the color change of the dumbbell solution before and after the addition of concentrated DNP38C10 solution. Recorded in $CDCl_3$ at 20 °C.

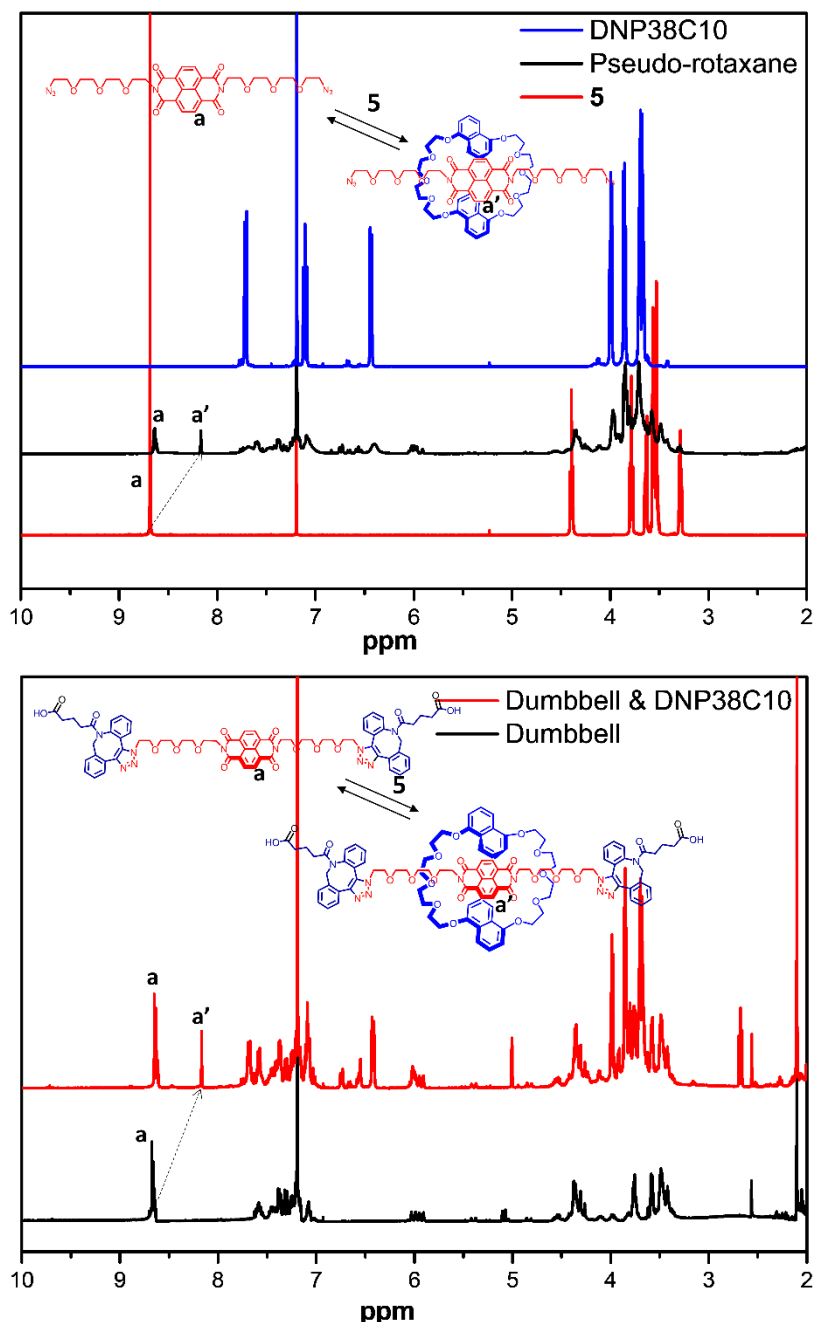


Figure 4.11 ¹H NMR comparison of the thread molecule and macrocycle with the corresponding pseudorotaxane (top), and dumbbell molecule in the presence of macrocyclic host (down).

4.3 Conclusions

A DIBAC derivative was introduced as a new reactive stopper for the preparation of small [2]rotaxanes by combining the high reactivity of DIBAC towards azides through SPAAC with a large steric bulky stopper. Several methods were employed to assess the efficiency of the stopper for the construction of a [2]rotaxane based on CBPQT⁴⁺ as a macrocyclic host, and the results clearly demonstrated that we have developed a new, highly efficient approach for the development of rotaxanes. The DIBAC was demonstrated to be limited to small rigid hosts as it was insufficient as a stopper for a rotaxane based on the larger and more flexible DNP38C10 macrocyclic host. Nonetheless, this straightforward synthetic strategy provides the opportunity to prepare

mechanically interlocked molecules efficiently. Last but not least, the commercial availability of various DIBAC derivatives facilitates their use as stoppers for the construction of rotaxanes.

4.4 Experimental Section

4.4.1 General Methods

All reagents were purchased from Sigma-Aldrich and used without further purification unless otherwise noted. 1,5-Bis[2-(2-(2-(azide)ethoxy)ethoxy)ethoxy]naphthalene (**1**),^{35, 57} cyclobis(paraquat-*p*-phenylene),⁵⁸ 2,7-bis(2-(2-(2-(2-azidoethoxy)ethoxy)ethoxy)ethyl)benzo[*lmn*]-[3,8]phenanthrol-line-1,3,6,8(2*H*,7*H*)-tetraone (**5**)⁵⁹, 1,5-dinaphtho[38]crown10⁶⁰ and 5-(11,12-didehydrodibenzo[*b,f*]-azocin-5(6*H*)-yl)-5-oxopentanoic acid (**2**)⁵³ were prepared according to procedures described in literatures. Thin layer chromatography (TLC) plates were purchased from Macherey-Nagel (pre-coated TLC-plates SIL G-25 UV₂₅₄).

4.4.2 Instrumentation and Measurements

Nuclear magnetic resonance (NMR) spectra were recorded in CD₃CN, acetone-*d*₆ or CDCl₃ on a Bruker Advance 500 MHz/400 MHz spectrometer at 298 K or 325 K. Chemical shifts are reported as parts per million (ppm) downfield from the Me₄Si resonance as internal standard for both ¹H and ¹³C NMR Spectroscopies. Spectra were all processed using TOPSPIN 3.0.

UV-Vis measurements were carried out on a Varian Cary 100 Bio UV-Visible spectrophotometer equipped with a 12 cell Peltier temperature controller.

Matrix assisted laser desorption/ionization time of flight mass spectroscopy (MALDI-TOF MS) was performed on an Applied Biosystems Voyager De STR MALDI-TOF mass spectrometer equipped with 2 m linear and 3 m reflector flight tubes, and a 355 nm Blue Lion Biotech Marathon solid state laser (3.5 ns pulse). All mass spectra were obtained in reflector mode with an accelerating potential of 20 kV in positive ion mode and delay of 700 ns. 200 single shot acquisitions were summed to give the spectra and the data were analyzed using Data Explorer software. Samples were prepared by dissolving the matrix 2-(4-Hydroxyphenylazo)benzoic acid (HABA) in THF (20 mg mL⁻¹), mixing with the rotaxane solution (2 mg·mL⁻¹) and sodium iodide in THF that was used as cationizing agent.

Electrospray ionization (ESI) mass spectra were recorded on a quadrupole ion trap LC mass spectrometer (Thermo Finnigan MAT LCQ), equipped with electrospray ionization. Acetonitrile was used as mobile phase. The data were collected in both positive and negative mode at 250 °C.

The rotaxane was analyzed by size-exclusion chromatography (HFIP-SEC) using an Agilent HPLC that was equipped with a 1260 refractive index detector (RID) and a UV (520 nm) detector. The eluent was hexafluoro-2-propanol (HFIP) containing 20 mM sodium trifluoroacetate at a flow rate of 0.426 mL·min⁻¹. PMMA standards were used to calculate the molar mass values. The column set consisted of two PSS PEG 100 Å gel 5 µm mixed D column and a similar guard column (Agilent) at 35 °C in

series. The chromatograms were analyzed using the Agilent Chemstation software with the GPC module.

4.4.3 Synthesis and characterization

4.4.3.1 Dumbbell molecule 4:

Diazide DNP derivative **1** (0.93 mg, 2.4 μmol), DIBAC **2** (1.61 mg, 5.0 μmol) were dissolved in CH_3CN (4 mL) at 0 $^\circ\text{C}$. The reaction solution was stirred at 0 $^\circ\text{C}$ for 2 days. Then the reaction solution was measured by ESI-MS without further purification. ^1H NMR (500 MHz, Acetone- d_6): δ 7.96-7.91(m, 2H, ph from DIBAC), 7.88-7.81(d, 2H, DNP *p*-O), 7.61-7.55 (m, 2H, DNP, *m*-O), 6.99-6.87 (m, DNP, 2H, *o*-O), 7.77-7.70, 7.50-7.44, 7.29-7.13 (m, 14H, ph from DIBAC), 6.14-6.00 (m, 4H, ph- CH_2 -N) 4.78-4.56 (m, 4H, CH_2 -O-DNP), 4.10-3.95 (m, 4H, OCH_2CH_2 -O-DNP), 4.35-4.21 (m, 4H, OCH_2CH_2 -triazole), 3.95-3.82 (m, 4H, OCH_2CH_2 -triazole), 2.16-2.10 (m, 4H, $\text{CH}_2\text{C}(\text{O})\text{N}$), 1.95-1.75 (m, 4H, $\text{CH}_2\text{C}(\text{O})\text{OH}$), 1.68-1.56 (m, 4H, $\text{CH}_2\text{CH}_2\text{C}(\text{O})\text{OH}$). ^{13}C NMR (125 MHz, Acetone- d_6): δ 174.0, 170.6, 161.7, 155.0, 142.9, 141.4, 137.0, 135.2, 132.1, 130.8, 130.1, 128.9, 127.7, 126.1, 114.8, 106.4, 69.3, 55.3, 33.2, 20.9. ESI-MS (*m/z*), calculated for $\text{C}_{58}\text{H}_{56}\text{N}_8\text{O}_{10}$ $[\text{M}+2\text{H}]^{2+}$ 513.2, measured 513.3; $[\text{M}+\text{H}]^+$ 1025.4, measured 1025.4.

4.4.3.2 [2]rotaxane 3·4PF₆:

Diazide DNP derivative **1** (9.5 mg, 0.025 mmol), CBPQT·4PF₆ (35.21 mg, 0.032 mmol) was dissolved in CH_3CN (25 mL) at 0 $^\circ\text{C}$ yielding a pink-purple solution. A solution of DIBAC **2** (16.5 mg, 0.052 mmol) in 7 mL acetonitrile was added after the pink-purple solution was stirred 0.5 h. The reaction solution was stirred at 0 $^\circ\text{C}$ for 48 h, and then acetonitrile was removed under reduced pressure to give a purple solid. The purple solid was washed by CH_2Cl_2 to remove trace amount of free stopper **2**. Then, the crude product was dissolved in CH_3CN and then purified by preparative TLC using 1% w/v NH_4PF_6 solution in CH_3CN as mobile phase. The product was obtained by washing the silica gel with excess of eluent solution followed by concentrating the CH_3CN solution under reduced pressure and precipitation in cold water. The pure rotaxane 3·4PF₆ was isolated as purple solid. (27 mg, 61%): ^1H NMR (500 MHz, CD_3CN , 325 K): δ 9.21-8.65 (m, 8H, α -CBPQT⁴⁺), 8.01 (s, 8H, β -CBPQT⁴⁺), 7.83 (m, 8H, aryl-CBPQT⁴⁺), 7.60-7.06 (m, 16H, aryl-DIBAC), 6.34-6.19 (m, 2H, DNP *o*-O), 6.08-5.96 (m, 8H, CH_2 -CBPQT⁴⁺), 5.79-5.65 (m, 2H, DNP *m*-O), 4.985 (br s, 4H, CH_2 -N in DIBAC), 4.90-4.60 (m, 4H, alkyl-DNP), 4.59-4.38 (m, 4H, alkyl-DNP), 4.29-4.10 (m, 4H, alkyl-DNP), 4.09-3.94 (m, 4H, alkyl-DNP), 3.67-3.51 (br s, 4H, alkyl-DIBAC), 3.51-3.37 (br s, 4H, alkyl-DIBAC), 2.58-2.44 (m, 2H, DNP *p*-O), 1.70-1.50 (br s, 4H, alkyl-DIBAC); MS (MALDI-TOF): found *m/z* 1547.1 $[\text{M}-4\text{PF}_6^-+3\text{e}]^+$, 1691.8 $[\text{M}-3\text{PF}_6^-+2\text{e}]^+$, 1836.8 $[\text{M}-2\text{PF}_6^-+\text{e}]^+$.

4.4.3.3 Dumbbell molecule 6:

2,7-Bis(2-(2-(2-(2-azidoethoxy)ethoxy)ethoxy)-ethyl)benzo[*lmn*][3,8]phenanthroline 1,3,6,8(2*H*,7-*H*)tetraone **5** (1.3 mg, 1.9 μmol), DIBAC **2** (1.27 mg, 4.0 μmol) were dissolved in CH_3CN (4 mL) at 0

°C. The reaction solution was stirred at 0 °C for 2 days. Then the reaction solution was measured by ESI-MS (Figure 4.9) without further purification.

References

1. Xue, M.; Yang, Y.; Chi, X., *et al.*, *Chem. Rev.* **2015**, *115* (15), 7398-7501.
2. Frisch, H. L.; Wasserman, E., *J. Am. Chem. Soc.* **1961**, *83* (18), 3789-3795.
3. Forgan, R. S.; Sauvage, J.-P.; Stoddart, J. F., *Chem. Rev.* **2011**, *111* (9), 5434-5464.
4. Li, S.; Huang, J.; Cook, T. R., *et al.*, *J. Am. Chem. Soc.* **2013**, *135* (6), 2084-2087.
5. Li, S.; Huang, J.; Zhou, F., *et al.*, *J. Am. Chem. Soc.* **2014**, *136* (16), 5908-5911.
6. Berna, J.; Leigh, D. A.; Lubomska, M., *et al.*, *Nat. Mater.* **2005**, *4* (9), 704-710.
7. Collin, J. P.; Heitz, V.; Bonnet, S., *et al.*, *Inorg. Chem. Commun.* **2005**, *8* (12), 1063-1074.
8. Sauvage, J. P., *Chem. Commun.* **2005**, (12), 1507-1510.
9. Champin, B.; Mobian, P.; Sauvage, J.-P., *Chem. Soc. Rev.* **2007**, *36* (2), 358-366.
10. Balzani, V.; Credi, A.; Venturi, M., *Molecular Devices and Machines – A Journey into the Nano World*, Wiley-VCH Verlag GmbH & Co. KGaA: 2004.
11. Liu, Y.; Flood, A. H.; Bonvallet, P. A., *et al.*, *J. Am. Chem. Soc.* **2005**, *127* (27), 9745-9759.
12. Badjic, J. D.; Ronconi, C. M.; Stoddart, J. F., *et al.*, *J. Am. Chem. Soc.* **2006**, *128* (5), 1489-1499.
13. Zhu, K.; O'Keefe, C. A.; Vukotic, V. N., *et al.*, *Nat. Chem.* **2015**, *7* (6), 514-519.
14. Nguyen, T. D.; Tseng, H. R.; Celestre, P. C., *et al.*, *Proc Natl Acad Sci U S A* **2005**, *102* (29), 10029-34.
15. Cheng, C.; McGonigal, P. R.; Stoddart, J. F., *et al.*, *ACS Nano* **2015**, *9* (9), 8672-8688.
16. Dietrich-Buchecker, C. O.; Sauvage, J. P.; Kintzinger, J. P., *Tetrahedron Lett.* **1983**, *24* (46), 5095-5098.
17. Sauvage, J. P.; Weiss, J., *J. Am. Chem. Soc.* **1985**, *107* (21), 6108-6110.
18. Durot, S.; Reviriego, F.; Sauvage, J.-P., *Dalton Trans.* **2010**, *39* (44), 10557-10570.
19. Bissell, R. A.; Cordova, E.; Kaifer, A. E., *et al.*, *Nature* **1994**, *369* (6476), 133-137.
20. Jiménez, M. C.; Dietrich-Buchecker, C.; Sauvage, J.-P., *Angew. Chem.* **2000**, *112* (18), 3422-3425.
21. Browne, W. R.; Feringa, B. L., *Nat. Nano.* **2006**, *1* (1), 25-35.
22. Koumura, N.; Zijlstra, R. W. J.; van Delden, R. A., *et al.*, *Nature* **1999**, *401* (6749), 152-155.
23. van Delden, R. A.; ter Wiel, M. K. J.; Pollard, M. M., *et al.*, *Nature* **2005**, *437* (7063), 1337-1340.
24. Kudernac, T.; Ruangsupapichat, N.; Parschau, M., *et al.*, *Nature* **2011**, *479* (7372), 208-211.
25. Yang, W.; Li, Y.; Liu, H., *et al.*, *Small* **2012**, *8* (4), 504-516.
26. Witus, L. S.; Hartlieb, K. J.; Wang, Y., *et al.*, *Org. Biomol. Chem.* **2014**, *12* (32), 6089-6093.
27. Anelli, P. L.; Spencer, N.; Stoddart, J. F., *J. Am. Chem. Soc.* **1991**, *113* (13), 5131-5133.
28. Harrison, I. T.; Harrison, S., *J. Am. Chem. Soc.* **1967**, *89* (22), 5723-5724.
29. Amabilino, D. B.; Stoddart, J. F., *Chem. Rev.* **1995**, *95* (8), 2725-2828.
30. Guo, X.; Zhou, Y.; Feng, M., *et al.*, *Adv. Funct. Mater.* **2007**, *17* (5), 763-769.
31. Philp, D.; Stoddart, J. F., *Synlett* **1991**, *1991* (07), 445-458.
32. Philp, D.; Stoddart, J. F., *Angew. Chem. Int. Ed. Engl.* **1996**, *35* (11), 1154-1196.
33. Cooke, G.; Garety, J. F.; Mabruk, S., *et al.*, *Tetrahedron Lett.* **2006**, *47* (5), 783-786.
34. Asakawa, M.; Ashton, P. R.; Ballardini, R., *et al.*, *J. Am. Chem. Soc.* **1997**, *119* (2), 302-310.
35. Dichtel, W. R.; Miljanić, O. Š.; Spruell, J. M., *et al.*, *J. Am. Chem. Soc.* **2006**, *128* (32), 10388-10390.

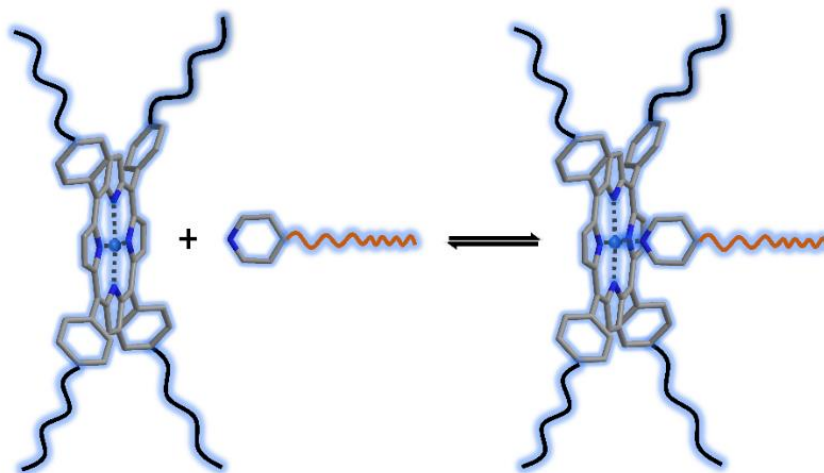
36. Spruell, J. M.; Dichtel, W. R.; Heath, J. R., *et al.*, *Chem. Eur. J.* **2008**, *14* (14), 4168-4177.
37. Aprahamian, I.; Dichtel, W. R.; Ikeda, T., *et al.*, *Org. Lett.* **2007**, *9* (7), 1287-1290.
38. Li, H.; Fahrenbach, A. C.; Dey, S. K., *et al.*, *Angew. Chem. Int. Ed.* **2010**, *49* (44), 8260-8265.
39. Kolb, H. C.; Finn, M. G.; Sharpless, K. B., *Angew. Chem. Int. Ed.* **2001**, *40* (11), 2004-2021.
40. Miljanić, O. Š.; Dichtel, W. R.; Aprahamian, I., *et al.*, *QSAR Comb. Sci.* **2007**, *26* (11-12), 1165-1174.
41. Becer, C. R.; Hoogenboom, R.; Schubert, U. S., *Angew. Chem. Int. Ed.* **2009**, *48* (27), 4900-8.
42. Cao, J.; Fyfe, M. C. T.; Stoddart, J. F., *et al.*, *J. Org. Chem.* **2000**, *65* (7), 1937-1946.
43. Bruns, C. J.; Liu, H.; Francis, M. B., *J. Am. Chem. Soc.* **2016**, *138* (47), 15307-15310.
44. Tuncel, D.; Steinke, J. H. G., *Chem. Commun.* **2002**, (5), 496-497.
45. Jirawutthiwongchai, J.; Krause, A.; Draeger, G., *et al.*, *ACS Macro Lett.* **2013**, *2* (3), 177-180.
46. van Berkel, S. S.; Dirks, A. J.; Debets, M. F., *et al.*, *ChemBioChem* **2007**, *8* (13), 1504-1508.
47. van den Bosch, S. M.; Rossin, R.; Renart Verkerk, P., *et al.*, *Nucl. Med. Biol.* **2013**, *40* (3), 415-423.
48. Chen, W.; Wang, D.; Dai, C., *et al.*, *Chem. Commun.* **2012**, *48* (12), 1736-1738.
49. Glassner, M.; Maji, S.; de la Rosa, V. R., *et al.*, *Polym. Chem.* **2015**, *6* (48), 8354-8359.
50. Jeon, J.; Kang, J. A.; Shim, H. E., *et al.*, *Bioorg. Med. Chem.* **2015**, *23* (13), 3303-3308.
51. Jewett, J. C.; Sletten, E. M.; Bertozzi, C. R., *J. Am. Chem. Soc.* **2010**, *132* (11), 3688-3690.
52. Nieves, D. J.; Azmi, N. S.; Xu, R., *et al.*, *Chem. Commun.* **2014**, *50* (86), 13157-13160.
53. Debets, M. F.; van Berkel, S. S.; Schoffelen, S., *et al.*, *Chem. Commun.* **2010**, *46* (1), 97-9.
54. Wu, K.-D.; Lin, Y.-H.; Lai, C.-C., *et al.*, *Org. Lett.* **2014**, *16* (4), 1068-1071.
55. Manoni, R.; Romano, F.; Casati, C., *et al.*, *Org. Chem. Front.* **2014**, *1* (5), 477-483.
56. Philp, D.; Slawin, A. M. Z.; Spencer, N., *et al.*, *J. Chem. Soc., Chem. Commun.* **1991**, (22), 1584-1586.
57. Rowan, S. J.; Stoddart, J. F., *Org. Lett.* **1999**, *1* (12), 1913-1916.
58. Masumi Asakawa; Wim Dehaen; L'abbe, G., *et al.*, *J. Org. Chem.* **1996**, *61*, 9591-9595.
59. Mullen, K. M.; Gunter, M. J., *J. Org. Chem.* **2008**, *73* (9), 3336-3350.
60. Hamilton, D. G.; Davies, J. E.; Prodi, L., *et al.*, *Chem. Eur. J.* **1998**, *4* (4), 608-620.

Chapter 5 General conclusions and outlook

Supramolecular chemistry has emerged as a significant tool in contemporary polymer science and nanoscience. The employment of supramolecular interactions such as hydrogen bonding, metal-ligand interactions, and host-guest interactions, has afforded a wide range of polymeric materials or molecular machines with outstanding dynamic properties and promising applications in material science and nanotechnology. The advanced organic synthesis and polymerization techniques play an important role in polymer science and nanoscience as well, which provide the opportunities for designing and preparing complex supramolecular structures. The combination of the two concepts leading to supramolecular interaction driven polymeric materials and mechanically interlocked molecules is a greatly important, fundamental science research topic providing a basis for the development of next generation advanced materials as well as providing deeper understanding of complex dynamic systems.

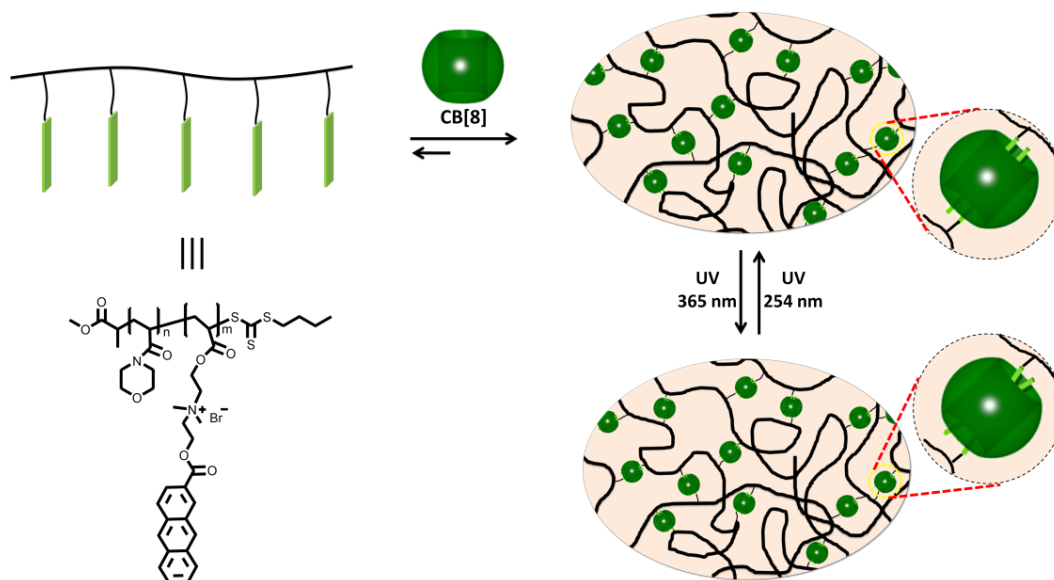
In this thesis, different non-covalent interactions were employed in polymeric materials and mechanically interlocked molecules. **Chapter 1** provided a general introduction to the concepts that are used and studied in this thesis. Recent developments in the focus research areas, namely supramolecular star polymers, supramolecular hydrogels and rotaxanes were discussed as well.

Chapter 2 described a novel strategy to construct supramolecular miktoarm star polymers through metal-ligand interactions between zinc porphyrin with pyridine. To achieve that goal, two building blocks, namely a four-arm star polymer with zinc porphyrin as core and a pyridine end-functionalized polymer, were prepared. The formation of the supramolecular mikto-arm star polymer was investigated by mixing these two components in water and was confirmed *via* a combination of UV-vis spectrophotometric titration, ITC and DOSY NMR spectroscopy. The results indicated that the strength of the metal-ligand interaction of zinc porphyrin with pyridine is not affected by the presence of the polymers and is strong enough as driving forces to form the supramolecular star polymer. These results provide future opportunities to prepare dynamic mikto-arm star polymers with different binding strength and dynamics by simply changing the metal ion of the metalloporphyrin. Furthermore, more complex dynamic macromolecular architectures can be prepared in future work by introducing polymers with multiple pyridine groups or alternative metalloporphyrin that bind pyridine on both sides leading to larger assemblies. From the point of view of applications, the assembled structures from multiple pyridine groups functionalized polymers and metalloporphyrin based polymers which bind pyridine on both sides lead to the formation of dynamic supramolecular hydrogels. The versatile properties owing to the tunable branched polymers make them good candidates as viscosity modifiers.



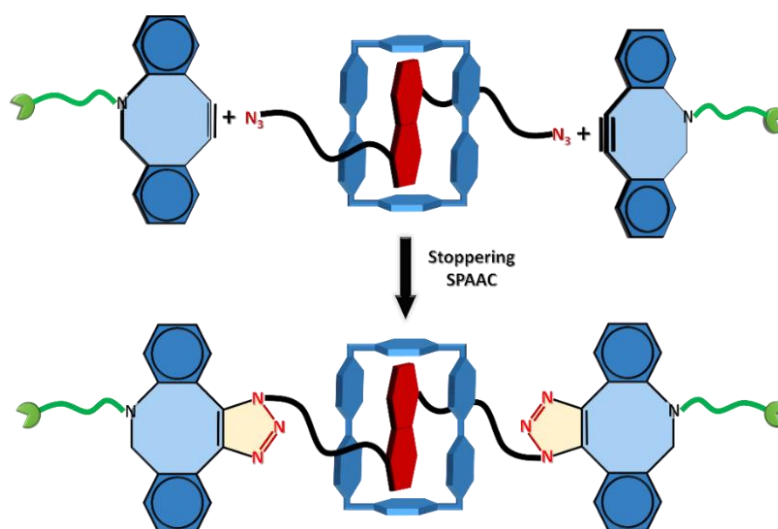
The graphical representation of the formation of a supramolecular miktoarm star polymer in **Chapter 2**

Anthracene has attracted increasing attention in recent years, because it can form ternary inclusion complexes with large macrocyclic hosts and can undergo a reversible photodimerization reaction upon UV irradiation. Taking advantage of both these properties of anthracene, **Chapter 3** described novel hydrogels in which the crosslinks could undergo a reversible transformation from supramolecular to covalent upon UV irradiation. The supramolecular hydrogel is formed based on the host-guest interaction of anthracene moieties and macrocyclic host to form ternary complexes as supramolecular crosslinks. The further photodimerization of two anthracene molecules inside the host cavity converted these supramolecular crosslinked hydrogels to covalent crosslinked hydrogels. Two kinds of anthracene functionalized poly(*N*-acryloylmorpholine) polymers were synthesized by post-polymerization modification of a copolymer containing *N*-acryloylmorpholine and an activated pentafluorophenyl ester comonomer. The main difference between the two polymers is that one polymer had a neutral side anthracene side chain while the other contained a positive charge in the linker to couple the anthracene as the cationic charge has been reported to enhance the binding constant for association with cucurbit[*n*]uril (CB[*n*]) as macrocyclic host. Importantly, attempts to prepare anthracene functionalized copolymers by copolymerization of an anthracene functionalized monomer failed since it acts as radical trap. The formation of supramolecular hydrogels and its conversion to a covalent hydrogel were investigated. The polymer with the neutral anthracene side chain was found to form supramolecular hydrogels with gamma-cyclodextrin only at high polymer concentration (15 wt%) while the polymer with the charged anthracene side chain formed supramolecular hydrogels with CB[8] already at 5 wt% representing the difference in association constants. Furthermore, it was demonstrated that the latter hydrogel underwent a reversible transformation between supramolecular to covalently linked hydrogels under photoirradiation providing control over the dynamics, reshapability and mechanical properties of the hydrogel. The switchable hydrogel provides potential applications in reused materials of which the complex shapes can be easily shaped and processed by transforming from the dynamic precursors, and this kind of materials can be recycled or reshaped by going back to the dynamic precursors.



The graphical representation of the overview of **Chapter 3**. Only the best performing anthracene hydrogel is shown.

Apart from polymeric materials, the non-covalent interactions are also employed in nanoscience, more specifically for the formation of mechanically interlocked molecules that can serve as basis for molecular motors and machines. In **Chapter 4**, a novel reactive chain stopper was introduced for the preparation of [2]rotaxanes consisting of CBPQT⁴⁺ and DNP driven by donor-acceptor interactions. The bulky dibenzocyclooctyne stopper bearing strained alkyne could be reacted with an azido functionalized pseudo-rotaxane under mild conditions without catalyst. The efficiency of the dibenzocyclooctyne stopper for construction of CBPQT⁴⁺-based [2]rotaxane by strain promoted azide-alkyne cycloaddition was assessed. The results demonstrated that the straightforward synthetic strategy provides the opportunity to prepare mechanically interlocked molecules efficiently, albeit being limited to rather small and rigid macrocyclic hosts as a more flexible crown-ether type ring could slide over the chain stopper. Moreover, the carboxyl group present on the stopper could be used for further functionalization resulting in more complex mechanically interlocked molecules, or to incorporate in larger polymeric structures.



The graphical representation of the double stoppering of a pseudo-rotaxane to form a [2]rotaxane in **Chapter 4**.

Nederlandse samenvatting

Supramoleculaire chemie wordt in de hedendaagse polymeerchemie en nanowetenschappen als een significant instrument gebruikt. Het gebruik van supramoleculaire interacties zoals waterstofbruggen, metaal-ligand interacties of gastheer-gast interacties, resulteert in een brede waaier van polymeermaterialen of moleculaire machines met opmerkelijke eigenschappen en veelbelovende toepassingsmogelijkheden in de materiaalwetenschappen en nanotechnologie. Bovendien spelen ook de geavanceerde organische synthese en polymerisatie technieken een belangrijke rol in de polymeerchemie en nanowetenschappen, waardoor complexe supramoleculaire structuren gecreëerd kunnen worden. De combinatie van beide concepten die leiden tot supramoleculaire polymeermaterialen en mechanisch verweven moleculen, is een uitermate belangrijk onderzoeksonderwerp voor de fundamentele wetenschap en als basis voor toekomstige volgende generatie geavanceerde materialen.

In deze thesis worden verschillende niet-covalente interacties gebruikt voor de synthese van polymeermaterialen en mechanisch verweven moleculen. **Hoofdstuk 1** geeft een algemene introductie over de gebruikte concepten in deze thesis. Verder worden ook de huidige ontwikkelingen in de vermelde onderzoeksvelden, supramoleculaire stervormige polymeren, hydrogelen en rotaxanen besproken.

Hoofdstuk 2 beschrijft een vernieuwende strategie om supramoleculaire miktoarm ster polymeren te synthetiseren *via* metaal-ligand interacties tussen zink porfyriene en pyridine. Om dit doel te bereiken werden eerst de twee bouwstenen gesynthetiseerd, namelijk een vierarmig ster polymeer met een zink porfyriene kern en een polymeer met pyridine als eindgroep. Het zink porfyriene ster polymeer werd gevormd door reactie tussen tetrakis(*p*-hydroxyfenyl)porfyriene en *p*-tolueen sulfonyl-PEGME, gevolgd door insertie van het zink ion in de porfyriene kern. Het polymeer met pyridine als eindgroep werd bereid *via* RAFT polymerisatie en opeenvolgende aminolyse en Michael additie reactie van pyridine acrylaat. Hierna werd de vorming van het supramoleculaire ster polymeer onderzocht in water en bevestigd met behulp van UV-Vis spectrofotometrische titratie, ITC en DOSY NMR spectroscopie. De resultaten lieten zien dat de sterkte van de metaal-ligand interactie gebaseerd op zink porfyriene met pyridine niet beïnvloed wordt door de polymeerketens en dat deze sterk genoeg is om een supramoleculair ster polymeer te vormen. Dit onderzoek creëert de mogelijkheid om in vervolgonderzoek de sterkte en dynamiek van het ster polymeer te variëren door eenvoudige wisseling van het metaal ion. Daarnaast kunnen meer complexe dynamische macromoleculaire structuren gevormd worden door koppeling van meerdere pyridine groepen aan een polymeer. In acht nemend dat de supramoleculaire interactie en de architectuur van het thermoresponsief polymeer reversibel ontbonden kunnen worden door gebruik te maken van verschillende stimuli, creëert dit werk de basis tot een nieuwe familie van responsieve materialen die het toepassingsgebied van de conventionele miktoarm ster polymeren verbreedt.

Onderzoek naar anthracenen ondervindt de laatste jaren steeds meer interesse door het feit dat ze ternaire inclusie complexen kunnen vormen met grote macrocyclische gastheer moleculen, en dat ze een reversibele fotodimerisatie reactie kunnen ondergaan door middel van UV irradiatie. In **Hoofdstuk 3** maken we gebruik van allebei deze voordelen van anthraceen door het ontwikkelen van hydrogelen die een omkeerbare transformatie kunnen ondergaan van supramoleculaire hydrogelen naar covalente hydrogelen. De supramoleculaire hydrogel is gebaseerd op ternaire gastheer-gast interacties tussen twee antraceen groepen en een macrocyclische gastheer resulterend in supramoleculaire crosslinks. De verdere fotodimerisatie van twee antraceen moleculen in de gastheer holte resulteert in omzetting van de supramoleculaire crosslinks naar covalente crosslinks. Twee soorten anthraceen-gefunctionaliseerd poly(*N*-acryloylmorfoline) werden gesynthetiseerd *via* een post-polymerisatie modificatie van een copolymeer bestaande uit *N*-acryloylmorfoline en een geactiveerd ester co-monomeer. Het belangrijkste verschil tussen de twee polymeren is dat de ene een neutrale anthraceen zijgroep heeft en de andere een anthraceen gekoppeld middeels een kationische linker, aangezien het bekend is dat de interactiesterkte van kationische anthracenen met cucurbit[*n*]uril (CB[*n*]) veel sterker is dan met neutrale anthracenen. Het is belangrijk te vermelden dat pogingen om anthraceen gefunctionaliseerde copolymeren te maken middels copolymerisatie van een anthraceen-functioneel monomeer niet mogelijk is aangezien het optreedt als radicalaire val. Vervolgens werden de vorming van de supramoleculaire hydrogel en de omzetting naar de covalente hydrogel onderzocht. Het polymeer met de neutrale anthraceen zijketens vormde alleen supramoleculaire hydrogelen met gamma-cyclodextrine bij hoge polymeerconcentraties (15 wt%), terwijl het polymeer met de kationische anthraceen zijgroepen hydrogelen vormde met CB[8] bij 5 wt%, in overeenstemming met de hogere associatieconstante. Verder is het aangetoond dat de laatste hydrogel een reversibele transitie onderging tussen een supramoleculaire hydrogel en een covalente hydrogel onder fotobestraling wat controle biedt over de dynamiek, vormgeving en mechanische eigenschappen van de hydrogel.

Naast polymeermaterialen worden niet-covalente interacties ook gebruikt in de nanowetenschappen, meer specifiek voor de vorming van mechanisch verstrengelde moleculen die als basis kunnen dienen voor moleculaire motoren en machines. In **Hoofdstuk 4** werd een nieuwe stopper geïntroduceerd voor de synthese van een [2]rotaxaan bestaande uit CBPQT⁴⁺ en DNP, gedreven door donor-acceptor gastheer-gast interacties. De relatief grote dibenzocyclooctyn stopper met gespannen alkyn functionaliteit reageerde met een azido-gefunctionaliseerde gast in een pseudorotaxaan onder milde condities zonder katalysator. De efficiëntie van de stopper voor de opbouw van een CBPQT⁴⁺-gebaseerde [2]rotaxaan werd bepaald, waaruit bleek dat deze eenvoudige synthese strategie een opportuniteit biedt voor de efficiënte bereiding van mechanisch verstrengelde moleculen. Echter, deze strategie werkt alleen met vrij kleine en rigide macrocyclische structuren aangezien een grotere kroonether gebaseerde macrocyclische gastheer over de stopper heen kon schuiven. In toekomstig onderzoek kan de carboxyl-groep op de stopper gebruikt worden voor verdere functionalisatie, wat resulteert in meer complexe mechanisch verstrengelde moleculen.

Acknowledgements

Now, I am so excited standing on the finishing line to express my thanks to all those people who have contributed to my thesis and supported me during my PhD. The first person is of course my promoter Richard Hoogenboom. I could not finish my thesis without you, thank you for always being supportive and patient. Your constant and enormous enthusiasm for research is absolutely a perfect role model. You are always available to provide tips or suggestion on my research. Richard, thank you very much!! It's my pleasure working with you.

Further, I also would like to thank my master advisor Professor Wei Wang, who introduced me into the world of supramolecular chemistry.

I truly thank my current and former colleagues in supra-group for creating a pleasant environment to work in and for the fruitful academic discussion. They are Dr. Qilu Zhang, Dr. Lenny Voorhaar, Dr. Gertjan Vancoillie, Dr. Dingying Zhang, Dr. Bahar Yeniad, Dr. Maarten Mees, Dr. Bryn Monnery, Dr. Mathias Glassner, Dr. Maji, Kanykei, Dr. Victor R. de la Rosa, Dr. Valentin Victor Jerca, Dr. Martin Purino, Dr. Debaditya Bera, Dr. Michal Ceglowski, Dr. Ondrej Sedlacek, Bart, Maarten (V.), Glenn, Joachim, Lieselot, Ali, Jente, Xiaowen, Ronald..... Special thanks go to Annelore and Wouter for their contribution to my work although not included in the thesis.

I would like to acknowledge all my collaborators, especially Professor Wim Dehaen from KULeuven, Professor Patrice Woisel and Professor Joel Lyskawa from Université Lille1.

I would also like to thank my colleagues from our department, especially Jos, Tim, Veerle.....for their kind help over the last four years.

My parents and parents-in-law are the persons who deserve all of my acknowledgements. Without your continuous love, support and encouragement this thesis would not exist. A very special thanks go to my sister-in-law Xiaoping and brother-in-law Qiuya for their guidance and constant support, and for providing me a home and relieving my homesickness.

Much love and thanks to my wife Huiying for her support and encouragement through my life and research work, I am so happy to be with you. Thank my new-born son, Danny, for coming into my life.

Here, I would like to express my sincere gratitude to the members of the reading and examination committee for providing valuable suggestions to improve my thesis.

I would like to appreciate the China Scholarship Council (CSC) and Ghent University (BOF co-funding) for the financial support.

Zhanyao

Ghent, Belgium

May 2018

Scientific publications

Peer-reviewed publications resulting from this PhD work:

1. **Z. Hou**, W. Dehaen, J. Lyskawa, P. Woisel, R. Hoogenboom,* A supramolecular miktoarm star polymer based on porphyrin metal complexation in water, *Chem. Commun.*, 2017,53, 8423 - 8426.
2. **Z. Hou**, B. Yeniad, J. van Guyse, P. Woisel, K. M. Mullen, F. P. J. T. Rutjes, J. C. M. van Hest, R. Hoogenboom,* A Dibenzoazacyclooctyne as a reactive chain stopper for [2]rotaxanes, *Eur. J. Org. Chem.*, 2017, 3107 - 3113.
3. **Z. Hou**, P. Woisel, B. G. De Geest, R. Hoogenboom,* Thermoresponsive polymer coated gold nanoparticles *via* supramolecular interaction: toward novel temperature nanosensor, *in preparation*.
4. **Z. Hou**, K. I. Assaf, W. M. Nau, R. Hoogenboom,* Reversible transformation from supramolecular to covalent crosslinking of an anthracene-based hydrogel *via* UV irradiation, *in preparation*.
5. Q. Zhang, **Z. Hou**, B. Louage, D. Zhou, N. Vanparijs, B. G. De Geest, R. Hoogenboom,* Acid-labile thermoresponsive copolymers that combine fast pH-triggered hydrolysis and high stability under neutral conditions, *Angew. Chem. Int. Ed.*, 2015, 54, 10879 - 10883
6. C. M. B. Neves, J. P. C. Tome, **Z. Hou**, W. Dehaen, R. Hoogenboom, M. G. P. M. S. Neves,* M. M. Q. Simoes,* Oxidation of monoterpenes catalysed by a water-soluble Mn(III) PEG-porphyrin in a biphasic medium, *ChemCatChem*, 10.1002/cctc.201800239.

Other peer-reviewed publications

7. **Z. Hou**, M. Hu, W. Wang*, Synthesis and Self-Assembled Structure of A Cluster-Cluster Hybrid Molecule Composed of POM and POSS Clusters. *Acta Chim. Sinica*, 2014, 72, 61-68.
8. M. Hu, **Z. Hou**, W. Hao, Y. Xiao, W. Yu, C. Ma, L. Ren, P. Zheng, W. Wang*, POM-Organic-POSS cocluster: creating a dumbbell-shaped hybrid molecule for programming hierarchical supramolecular nanostructures. *Langmuir*, 2013, 29, 5714-5722.
9. Y. Xiao, D. Chen, N. Ma, **Z. Hou**, M. Hu, C. Wang*, W. Wang*, Covalent immobilization of a polyoxometalate in porous polymer matrix: a heterogeneous catalyst towards sustainability. *RSC Advances*, 2013, 3, 21544-21551.
10. M. Hu, N. Xia, W. Yu, C. Ma, J. Tang, **Z. Hou**, P. Zheng, W. Wang*, A click chemistry approach to the efficient synthesis of polyoxometalate-polymer hybrids with well-defined structures. *Polymer Chemistry*, 2012, 3, 617-620.
11. X. Wang, Y. Wang, W. Miao, M. Hu, J. Tang, W. Yu, **Z. Hou**, P. Zhang, W. Wang*, Langmuir and langmuir-blodgett films of hybrid amphiphiles with a polyoxometalate headgroup. *Langmuir*, 2013, 29, 6537-6545.

12. L. Zhang*, J. Ma, Y. Zhao*, W. Zhang, H. Song, **Z. Hou**, B. Zheng, Rapid qualitative and quantitative analyses of 1-hydroxyethylidene-1, 1-diphosphonic acid. *Chemical Reagent*, 2009, 31(5), 359-361.

Patents

1. W. Wang*, M. Hu, **Z. Hou**, Y. Xiao, The synthesis of polyoxometalates and polyhedral oligomeric silsesquioxane hybrids. China, *CN 102659851 A*.
2. W. Wang*, C. Wang*, Y. Xiao, D. Chen, **Z. Hou**, N. Ma, The synthetic method and application of macroporous resin functionalized by polyoxometalates covalently. China, *CN 102863566 A*.
3. W. Wang*, J. Tang, Y. Xiao, M. Hu, **Z. Hou**, X. Wang, The synthesis of PEGylated polyoxometalates hybrids. China, *CN 103145978 A*.
4. W. Wang*, H. Wu, M. Hu, Y. Zhang, **Z. Hou**. The synthetic method of POM-Organic-POSS hybrids. China, *CN 201410019837*.

Conference contributions

1. **Z. Hou**, K. I. Assaf, W. M. Nau, R. Hoogenboom, Anthracene-based hydrogels: From supramolecular to covalent networks via photo-irradiation. *17th Advanced polymers via macromolecular engineering (APME17)*, May 21-25, 2017, Ghent, Belgium. (Poster)
2. **Z. Hou**, W. Dehaen, J. Lyskawa, P. Woisel, R. Hoogenboom, A supramolecular miktoarm star polymer based on porphyrin metal complexation. *European Hengstberger symposium new horizons in smart materials*, March 27-29, 2017, Heidelberg, Germany. (poster)
3. **Z. Hou**, Anthracene-based Hydrogels: From Supramolecular to Covalent Conversion via Photo-irradiation. *Seminar between "supramolecular group" of UGent and "Molecular Nanofabrication (MNF) group" of UTwente*. 17th May 2017. (Oral presentation)
4. **Z. Hou**, K. I. Assaf, R. Hoogenboom, Anthracene-based hydrogels: From supramolecular to covalently cross linking via photoirradiation. *Annual scientific meeting IAP*, September 12, 2016, liege, Belgium. (Poster)
5. **Z. Hou**, K. I. Assaf, R. Hoogenboom, Anthracene-based hydrogels: From supramolecular to covalently cross linking via photoirradiation. *Warwick Polymer Conference 2016*, July 11-14, 2016, University of Warwick, United Kingdom. (Poster)
6. **Z. Hou**, B. Yeniad, P. Woisel, F. Rutjes, J. van Hest, R. Hoogenboom, Strain-promoted copper-free "click" synthesis of a donor-acceptor rotaxane. *PhD symposium 2016-UGent faculty of sciences*, March 17, 2016, UGent. Belgium. (Poster)
7. **Z. Hou**, Synthesis and characterization of supramolecular polymers based on porphyrin metal complexation. Joint symposium between "supramolecular group" of UGent and "Precision Macromolecular Chemistry" of L'Institut Charles Sadron, September 15, 2015, Strasbourg, France. (Oral presentation)

8. **Z. Hou**, W. Dehaen, R. Hoogenboom, Synthesis and characterization of supramolecular polymers based on porphyrin. *Annual scientific meeting IAP*, September 11, 2015, Hasselt, Belgium. (Poster)
9. **Z. Hou**, W. Dehaen, R. Hoogenboom, Synthesis and characterization of supramolecular polymers based on porphyrin metal complexation. *Belgium Polymer Group Annual Meeting 2015*, May 18-19, 2015, Houffalize, Belgium. (Poster)
10. **Z. Hou**, W. Dehaen, R. Hoogenboom, Synthesis and characterization of supramolecular polymers based on porphyrin. *Kick-off event of Centre of Macromolecular Chemistry*, April 17, 2015, UGent, Belgium. (Poster)



Supramolecular Chemistry Group

Department of Organic and Macromolecular Chemistry, Ghent University